University of Alberta
Department of Civil &
Environmental Engineering

Structural Engineering Report No. 236

STIFFENER TRIPPING IN STIFFENED STEEL PLATES

by
Imtiaz A. Sheikh
Gilbert Y. Grondin
and
Alaa E. Elwi

April, 2001

Stiffener Tripping in Stiffened Steel Plates

by

Imtiaz A. Sheikh

Gilbert Y. Grondin

and

Alaa E. ELwi

Structural Engineering Report 236

Department of Civil and Environmental Engineering
University of Alberta
Edmonton, Alberta, Canada

April, 2001

Abstract

The stability of stiffened steel plates with tee-shaped stiffeners under uniaxial compression and combined compression and bending was investigated using a finite element model. The emphasis of work presented in this study is to first identify the parameters that uniquely characterise the behaviour and strength of stiffened steel plates and then to conduct a parametric study aimed at identifying the conditions that may lead to failure by tripping of stiffeners.

The study was conducted using a finite element model that was validated from a comparison of predicted behaviour and strength from a series of tests on full-scale test specimens. The numerical study indicated that the behaviour of stiffened steel plates could be characterised by non-dimensional geometric, initial conditions and loading parameters.

A numerical parametric study was conducted on the geometric part of the proposed parameters set with the parameters controlling initial conditions set to the most probable values. Only two types of loading conditions were investigated. In the first, a uniaxial compression was applied to obtain the failure condition and in the other combined bending and compression were applied.

The study indicated that the stiffener tripping failure of tee-shaped stiffeners require the application of a bending moment, causing a compressive stress in the flange of the stiffener.

The numerical analysis results show inconsistent capacity predictions by current API (American Petroleum Institute) and DnV (Det norske Veritas) design guidelines.

ACKNOWLEDGEMENTS

This study was conducted with the financial assistance of Natural Sciences and Engineering Research Council (NSERC).

This report is based on the M.Sc. dissertation of the senior author.

TABLE OF CONTENTS

LIST OF TABLES

LIST OF FIGURES

LIST OF SYMBOLS

A	total cross-sectional area of stiffened plate
A_f	cross-sectional area of stiffener flange
A_p	cross-sectional area of plate in the stiffened plate
A_s	cross-sectional area of stiffener in the stiffened plate
A_w	cross-sectional area of stiffener web
b_f	stiffener flange width
b_p	width of stiffened steel plate (taken as stiffener spacing)
dA	area of differential element
E	Young's modulus of Elasticity for steel
$f_{1,2,3}$	true stress magnitude at onset of yielding, at the end of plastic range and at the ultimate strain value
f_r	magnitude of the maximum compressive residual stress in plate
f_{yp}	yield stress of plate material
f_{ys}	yield stress of stiffener material
h_w	stiffener web height
K	Regression analysis constant used by Faulkner (1975) for defining initial plate imperfection
L_u	length of stiffened plate
M_a	applied bending moment
M_p	plastic moment capacity of stiffened plate
M_y	yield moment capacity of stiffened plate
n_p	number of half-sine waves of imperfections along the length of stiffened plate
P	axial load applied along global 1-1 direction
P_c	peak load capacity of the stiffened plate
P_y	yield capacity of the stiffened plate
$r_{x, y, z}$	radius of gyration about x-x, y-y and z-z axis
r_{xe}	radius of gyration of stiffener acting with associated plating about x-x axis
T	fictitious temperature magnitude representing residual stresses

t_f	stiffener flange thickness		
t_p	plate thickness		
t_w	stiffener web thickness		
$u_{1,2,3}$	nodal displacements along global 1, 2 and 3 directions		
U_1	axial shortening of the stiffened plate		
U_c	axial shortening corresponding to peak load capacity of stiffened plate		
U_{dm}	axial shortening at the initiation of dual failure mode of stiffened plate		
U_T	displacement caused by fictitious temperature 'T'		
x, y, z	distance from reference axis along global 1, 2 and 3 directions respectively		
α_T	co-efficient of thermal expansion		
β_1	$\frac{b_p}{t_p}\sqrt{\frac{f_{yp}}{E}}$	=	plate transverse flexural slenderness
β_2	$\frac{h_w}{t_w}\sqrt{\frac{f_{ys}}{E}}$	=	stiffener web slenderness
β_3	$\frac{b_f}{t_f}\sqrt{\frac{f_{ys}}{E}}$	=	stiffener flange slenderness
β_4	$\frac{\frac{L_u}{r_z}\sqrt{\frac{f_{ys}}{E}}}{\frac{b_p}{t_p}\sqrt{\frac{f_{yp}}{E}}}$	=	ratio of stiffener torsional slenderness to plate transverse flexural slenderness
β_5	$\frac{A_s}{A_P}$	=	stiffener to plate area ratio
β_6	$kb_1^{\,2}$	=	initial plate imperfection
β_7	$\frac{L_u}{constt}$	=	initial stiffener imperfection
β_8	$\frac{f_r}{f_{yp}}$	=	residual stresses
β_9	$\frac{M_a}{M_p}$	=	applied to plastic moment ratio

β_{10}	$\frac{P_c}{P_y}$	=	peak to yield load ratio
β_{11}	$\frac{U_1}{L_u}$	=	axial shortening in stiffened plate

d_p maximum initial imperfection in plate

d_s maximum initial imperfection in stiffener

d_0 (x, y) magnitude of plate imperfection at point (x, y) on plate

$\varepsilon_{1,2,3}$ true strain value at onset of yielding, at end of plastic range and at ultimate load

η constant used by Faulkner (1975) to define the effects of residual stresses, depends on type of welding

$\phi_{1,2,3}$ nodal rotations about global 1, 2 and 3 axis

λ	$\frac{L_u}{r_x}\sqrt{\frac{f_{ys}}{E}}$	=	slenderness of stiffener
λ_0	$\frac{L_u}{r_{xe}}\sqrt{\frac{f_y}{E}}$	=	slenderness of stiffener acting with associated plating

π 3.14159.....

ν Poisson’s ratio for steel

CHAPTER 1

INTRODUCTION

1.1 GENERAL

Thin steel plates that are stabilised in one direction by stiffeners form an integral part of many structural systems such as ship decks and hulls, components of offshore structures, bridge decks, the bottom flange of box girders and many other structural systems in which a high strength-to-weight ratio is important. Flexure of the entire hull of a ship or box girder of a bridge will induce longitudinal compressive stresses in the stiffened panels that form these elements. This may be coupled with local bending moments arising from transverse loads acting directly on the stiffened panels, e.g. wheel loads acting on a bridge deck or water pressure on a ship hull. Due to the presence of the compressive axial forces and bending moments, stiffened panels are susceptible to failure by instability. Instability of stiffened plates under uniaxial compression or under combined bending and compression can take one of four forms (Murray, 1973; Bonello *et al.*, 1993; Hu, 1993; Grondin *et al*., 1999): plate induced overall buckling (PI), stiffener induced overall buckling (SI), plate buckling (PB) and stiffener tripping (ST).

Overall buckling is characterised by simultaneous buckling of the stiffener and the plate. Because this mode of failure is similar to that of an elastic column, it is sometimes referred to as an Euler type-buckling mode. If buckling occurs with the stiffener on the convex (tension) side of the plate, overall buckling is said to be plate induced (see Figure 1.1 (a)). On the other hand, if the stiffener is on the concave side of the plate, overall buckling is said to be stiffener induced (see Figure 1.1 (b)). These two modes of failure are typically characterised by a stable post-buckling response as shown in Figure 1.2. The load versus displacement responses presented in Figure 1.2 were obtained using the finite element model described in Chapter 3.

Plate buckling failure is characterised by buckling of the plate between the stiffeners, resulting in a load re-distribution from the plate into the stiffeners. This mode of failure is illustrated in Figure 1.1 (c) with a typical load versus displacement behaviour presented in Figure 1.2. The plate buckling failure mode has a lesser post-buckling strength than the overall buckling failure mode, but still shows considerable post-buckling strength.

Stiffener tripping is characterised by the rotation of the stiffener about the stiffener to plate junction (see Figure 1.1 (d)). Stiffener tripping is, therefore, a form of lateral torsional buckling, where torsion takes place about the stiffener to plate junction. As opposed to the other modes of failure, stiffener tripping generally results in the sudden drop of load carrying capacity (see Figure 1.2).

Test results (Hu *et al.*, 1997; Murray, 1973) have indicated that stiffener tripping failure mode is more critical than plate buckling or overall buckling failure modes because it is associated with a sudden loss of load carrying capacity. Although plates stiffened on one side have considerable ability to carry transverse loads that put the flange of the stiffener under tension, stiffener tripping must also be considered when the structure is such that bending will cause compression to develop in the flange of the stiffener.

The current design guidelines dealing with stiffened steel plate design are based on simplified assumptions. For example, the Det Norske Veritas (DnV) (1995) guideline uses the Perry-Robertson first-yield criterion and does not take into account any interaction between stiffener and plate for stiffener tripping failure mode. These guidelines are applicable only over a certain range of values based on the limited amount of test and analysis results. These guidelines only predict the peak strength of the stiffened panel and do not correctly predict the behaviour of stiffened panel (Rigo *et al.*, 1995).

With the current analysis tools and computing power, however, more precise modelling of stiffened steel plate panels can be achieved. Factors such as residual stresses, initial imperfections and yielding of significant parts of the cross-section can be

explicitly incorporated into numerical models. Recently, Grondin et al. (1998) have obtained excellent correlation between results of tests on full-size stiffened plate and a numerical model using finite strain four node shell element S4R from ABAQUS (Hibbit, Karlson & Sorenson Inc. (HKS), 1997a). The same finite element model was used to find the parameters that uniquely characterise the behaviour and strength and was subsequently used to perform an extensive parametric study of the behaviour and strength of the stiffened panels under uniaxial compression and combined compression and bending.

1.2 OBJECTIVES

The primary objective of the research presented here is to find the parameters that will lead to stiffener tripping failure mode. In order to reach the primary objective, the following secondary objectives were established:

- To identify parameters that dictate the behaviour and strength of stiffened steel plates failing in any of the failure modes mentioned above (Figure 1.2).
- To conduct a parametric non-linear finite element analysis study, with emphasis on the conditions that will lead to stiffener tripping failure mode.
- To study the effect of plate and stiffener interaction for stiffener tripping failure mode, especially in the post-yield range of material behaviour.
- To review and evaluate current design guidelines.

1.3 ORGANISATION OF THESIS

Chapter 2 provides a review of the previously published research on the stiffened steel plates. Summaries of both experimental and analytical investigations are presented. A brief review about two design guidelines, API Bulletin 2V (1987) and DnV (1995) Classification Notes no. 30.1, is also presented.

Chapter 3 describes the finite element model proposed by Grondin et al. (1999) for parametric study of the stiffened steel plates. This model is also evaluated the

difference between applying residual stresses in a one step procedure as compared with a two steps procedure.

Chapter 4 describes the determination of non-dimensional parameters affecting behaviour and strength of stiffened steel plates from a literature survey and verified through finite element analysis. Four types of parameters namely geometric, material properties, loading and deformation are identified in this chapter.

Chapter 5 describes the parametric study carried out using the geometric parameters identified in Chapter 4. The study is sub-divided into sections, namely, stiffened steel plates under uniaxial compression, and stiffened steel plates under combined compression and bending. The effect of geometric parameters on behaviour and strength is discussed in this chapter.

In Chapter 6 the results of the parametric study are used to evaluate two of the most commonly used design guidelines (API, 1987; DnV, 1995) with respect to behaviour and strength.

Chapter 7 presents a summary of the research and discussion of the conclusions drawn therefrom. Further research needs are also identified.

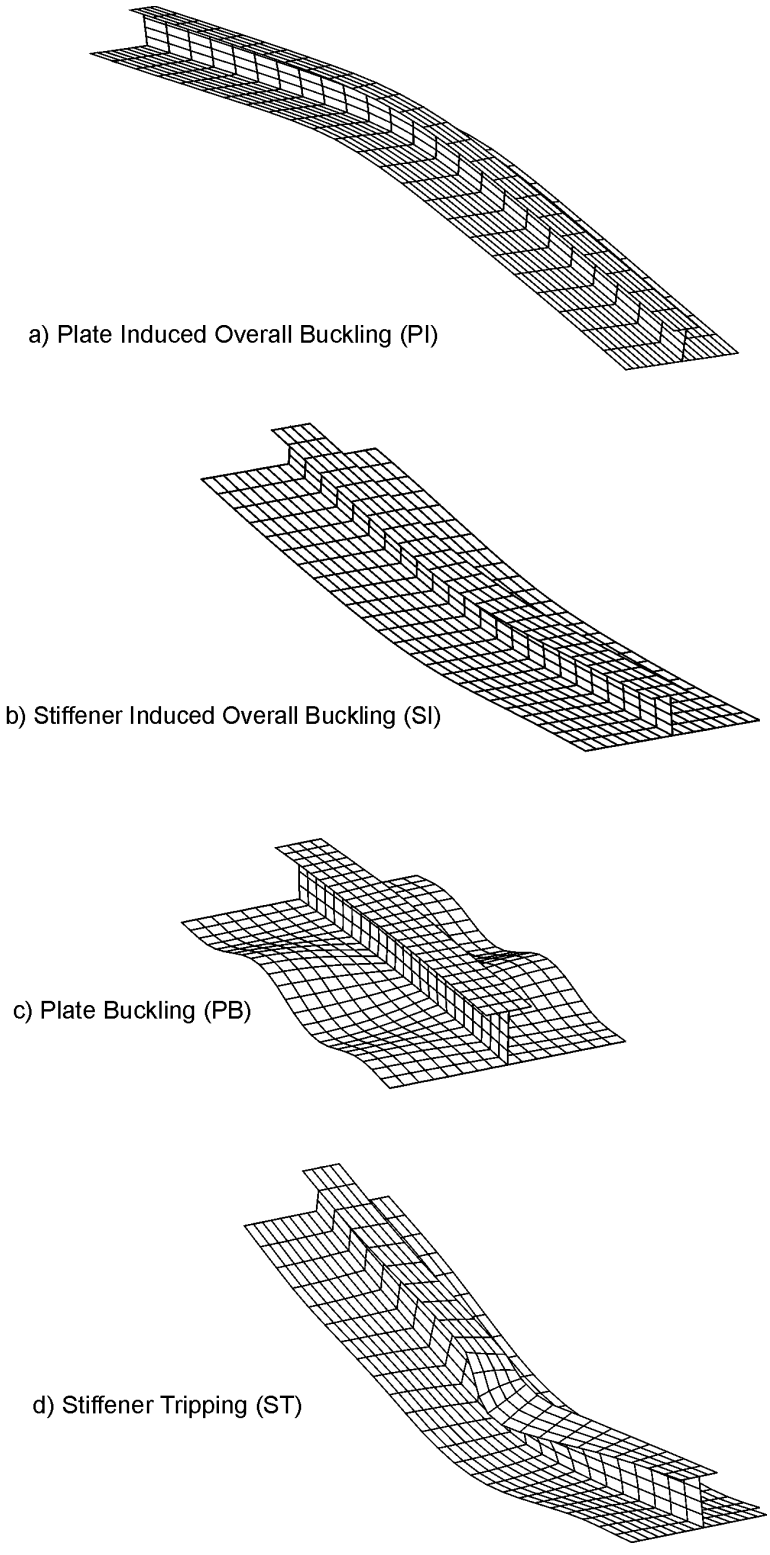

Figure 1.1 Typical buckling modes in stiffened steel plates

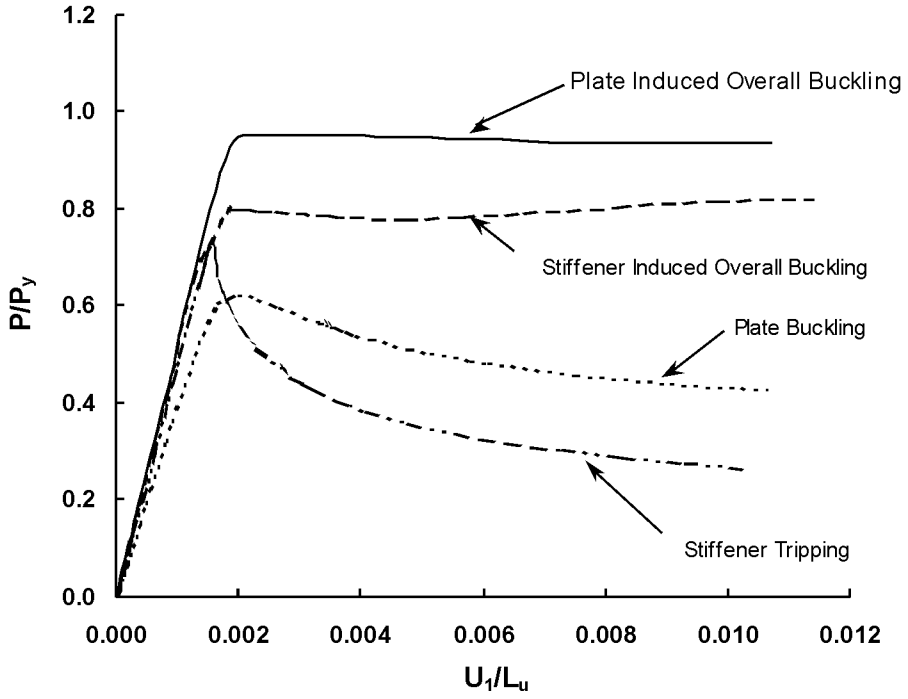

Figure 1.2 Load versus deformation responses for typical buckling modes in stiffened steel plates

CHAPTER 2

LITERATURE REVIEW

2.1 INTRODUCTION

The work on stiffened steel plates can be broadly divided into experimental, analytical and statistical work. The experimental work consists of limited number of tests carried out with idealised boundary conditions (Murray, 1973; Ghavami, 1994; Hu *et al*. 1997). The analytical work consists of various closed-form (Bleich, 1951; Timoshenko and Gere, 1961; Danielson *et al*., 1990; Bedair and Sherbourne, 1993, Hughes and Ma, 1996) and numerical parametric studies (Carlsen, 1980; Smith *et al*. 1991; Hu, 1993; Grondin *et al*. 1999). Statistical studies were performed to assess the severity of post welding distortions and residual stresses on stiffened steel plates (Faulkner, 1975; Carlsen and Czujko, 1978; Smith *et al.*, 1991) constructed under representative shipyard procedures. The experimental, analytical and statistical work resulted in the formulation of simple design equations (American Petroleum Institute, 1987; Det Norske Veritas, 1995).

This chapter summarises the experimental, analytical and statistical work performed on stiffened steel plates and discusses the American Petroleum Institute (API) and Det Norske Veritas (DnV) design guidelines for stiffened steel plates.

2.2 EXPERIMENTAL INVESTIGATION

Murray (1973) carried out full-scale tests on multiple stiffened panels, stiffened with flat bar stiffeners, under combined compression and bending loads. All the edges were simply supported in such a way as to allow longitudinal movement and restrain vertical movement. No residual stress or initial imperfection measurements were reported. Mainly, two types of failure modes were observed for all the tests: plate buckling and stiffener tripping. The peak strain observed was in the elastic range of material behaviour.

Ghavami (1994) tested seventeen stiffened panels, with different shapes (Rectangular (R), Angle (L) and T-shaped) and arrangements of stiffeners (singly and multiply stiffened in one or both directions). He studied the effect of stiffener shapes (R (Rectangular), L and T-shaped) and the effect of their spacing on the behaviour and strength of stiffened steel plates under uniaxial compression. The panels were simply supported on their edges and were tested under uniaxial compression. Initial imperfections and residual welding strains were measured. The initial imperfections were found to be within the tolerance limits specified for in-situ conditions by various standards. The plating residual stresses were found to be irregular both in distribution and magnitude as opposed to the idealised rectangular distribution of residual welding stress that is commonly assumed for analysis (Figure 2.1). He observed that the shape of stiffeners did not affect the strength of the stiffened plate, but it did affect the failure mode, e.g. the R (rectangular) and L (angle) type stiffeners failed by stiffener tripping whereas the plates stiffened with T-shaped stiffeners failed by plate buckling. He also observed that changing the plate aspect ratio did not change the collapse load, but it changed significantly the out-of-plane deflections.

Hu *et al.* (1997) carried out tests under combined compression and bending of stiffened steel plates fabricated under representative shipyard procedure. The boundary conditions used in the test program simulated those that would exist around a single stiffened panel forming part of a large stiffened plate. The unloaded edges were supported to simulate continuity in the plate and the loaded ends were pinned and restrained from warping. Ten full-scale stiffened plate panels were tested under a combination of bending and axial load. The residual stresses in a typical panel were measured and initial imperfections were measured on all the tested specimens. The residual stresses and initial imperfections were found to be within the tolerance limits specified for in-situ conditions by various standards. Two types of failure modes, namely, stiffener tripping and plate buckling were observed. Stiffener tripping was observed only in those specimens that were subjected to combined axial load and bending to place the flange of the stiffener into compression. Since all tests were conducted under displacement control, their behaviour was observed well into the post-buckling range. The peak strains were found to exceed significantly the yield strain.

Pan and Louca (1999) carried out tests to find the response of stiffened panels, stiffened with bulb flat type stiffener, under blast loading. The panel was bolted to a test frame simulating a simply supported boundary condition on all the edges. Two stiffened plate panels were tested. For the first panel the blast load was applied such as to put the stiffener's free standing end (bulb end) under flexural compression and in second it was applied to put the stiffener's free-standing end (bulb end) under flexural tension. No residual stress and initial imperfection measurements were reported. Two types of failure modes, namely, stiffener tripping and plate buckling were observed. Stiffener tripping was observed for the specimen that was subjected to the loading that caused flexural compression in the free standing end of stiffener. For the other load case, that is, blast loading applied to put the stiffeners free-standing end under flexural tension, plate buckling failure was observed. The peak strains were found to be less than the yield strain.

2.3 ANALYTICAL INVESTIGATION

Analytical work published included both closed-form solutions and numerical parametric studies.

2.3.1 Closed-Form Solutions

Theoretical attempts to treat the stiffened plates under axial compression have centered on beam and plate differential equations. Such theoretical work has been presented by Bleich (1951), Timoshenko and Gere (1961), Danielson *et al.* (1990), Bedair and Sherboune (1993) and Hughes and Ma (1996).

These closed form solutions are based on various simplifying assumptions. For example Danielson *et al*. (1990) made the following assumptions:

(1) Lateral torsional buckling of a stiffener takes place about an axis of rotation passing through the point of intersection of plate and stiffener.
(2) Stiffeners are considered as isolated element.
(3) Small strains and linear elastic material model were also assumed.

Some of these assumptions are valid only in the elastic range of material behaviour (small strains, linear elastic material model), and the others are either very conservative (considering no stiffener-plate interaction) or very restrictive (lateral torsional buckling to take place about an axis of rotation).

A review of analytical work is beyond the scope of this work. Generally, these solutions do not show good agreement with the experimental results obtained in the inelastic range of material behaviour. These analytical models, however, serve as good tools to understand the mechanics of the problem.

2.3.2 Numerical Parametric Studies

Various numerical analysis techniques were used to study the effect of various parameters defining the stiffened steel plate problems. The most commonly used numerical techniques have been the finite difference method and the finite element method. A review of these studies is presented in the following.

2.3.2.1 Finite Difference Methods

Carlsen (1980) covered a wide range of parameters in his parametric study of stiffened steel plates under uniaxial loading using a finite difference technique. The parameters considered were plate and stiffener slenderness, stiffener to plate area ratio, flange to web area ratio, effect of adjacent spans, initial imperfections and residual stresses. The buckling modes investigated were plate or stiffener induced overall buckling, stiffener tripping and plate buckling. An elasto-plastic material model was used for the analysis. The boundary conditions along the unloaded edges were considered as continuous. Two spans were modelled to find the effect of adjacent span. The investigation was restricted to the initiation of buckling and did not extend into the post-buckling range.

Stiffener and plate slenderness were found to be the governing parameters in the work of Carlsen (1980). Stiffener to plate area ratio was found to have a very small influence on the strength, whereas the effect of flange to web area ratio for a Tee-shape stiffener was found to be insignificant. The effect of initial imperfections and residual

stresses were found to be significant for stiffened plates failing by plate buckling. The effect of initial imperfections and residual stresses on the strength of the stiffened plates, failing by plate buckling failure mode, was more pronounced for slender plates than for stocky ones. The effect of initial imperfections on stiffener tripping failure mode was found to be insignificant. The adjacent span continuity only affected the out-of-plane deflection magnitudes for the plate buckling failure mode. The adjacent span continuity resulted in a larger reduction in out-of-plane stiffness for the plate buckling failure mode. The effect (out-of-plane deflection) was found to be insignificant for stiffener tripping failure mode.

Smith *et al.* (1991) used an elasto-plastic, continuous beam-column model to evaluate the buckling and post-buckling behaviour under combined compression and lateral loads. Only inelastic plate-buckling was considered. The stiffener tripping failure mode was suppressed by suitable proportioning of the stiffener. A wide range of stiffener geometries was investigated for compressive strength of the stiffened plate under different magnitudes of lateral loads. The unloaded edges were assumed to be constrained. The loaded edges were taken as pinned. Displacement-controlled large displacement analysis was carried out using Newton-Raphson's iterative procedure for finding a load corresponding to a given displacement value. The behaviour was only observed up to twice the yield strain value in the post-buckling range. The parameters investigated were: stiffener to plate area ratio, type of stiffeners (Tee and Rectangular type), yield strength of material, initial distortions, residual stress and lateral pressure for different magnitudes of plate and stiffened panels slenderness values.

The stiffener to plate area ratio was found to have little influence on strength. The type of stiffener (Tee and Rectangular) and yield stress of the material did not show any effect on the strength of the stiffened panel. The initial distortions decreased the strength with the increase in distortion magnitude. The effect was more pronounced for slender plates ($\beta > 2.0$, where $\beta = \frac{b_p}{t_p}\sqrt{\frac{f_{yp}}{E}}$, b_p is width of stiffened steel plate, t_p is plate thickness, f_{yp} is yield stress of plate material and E is Young's modulus of Elasticity for steel) than for stocky ones. Residual stresses showed a similar effect on the strength of

stiffened plates. The effect of lateral pressure on strength was more pronounced for stocky panels than for slender panels. A less stable post-buckling response was observed as the slenderness of the stiffened panel increased.

2.3.2.2 Finite Element Analysis

Hu (1993) carried out finite element analysis on stiffened steel plates to evaluate various design guidelines against stiffener tripping failure mode. He investigated various plates and stiffened panel slenderness ratios with different loading and boundary conditions. Hu (1993) used an elastic-perfectly-plastic material model with von Mises yield criterion for his large-displacement finite element analysis. Simply supported boundary conditions were employed on all four edges. "Average" magnitude of residual stresses and “average” magnitude of initial imperfections, as defined by Smith *et al.* (1991), were used in the analysis. The initial imperfection shape used for the analysis consisted of a multiple of the first buckling mode determined from a linear buckling analysis. He then analyzed different buckling modes one by one, with restraints applied to avoid the other buckling modes, for different magnitudes of plate and stiffened panels slenderness values. He concluded that the load drop in the post-buckling range for a plate-buckling failure mode is more severe as compared with the load drop in the post-buckling range for stiffener tripping failure mode.

The panel slenderness values of 0.3 and 0.6, for which the curves are plotted are either less than or equal to the limit (λ_0 = 0.6, where $\lambda_0 = \frac{L_u}{r_{xe}}\sqrt{\frac{f_y}{E}}$, L_u is length of stiffened plate, r_{xe} is radius of gyration of stiffener acting with associated plating about major axis, f_y is yield stress of steel and E is Young’s modulus of elasticity for steel) specified for yielding of specimen before buckling, by Rondal and Maquoi (1979) for the lateral-torsional buckling failure mode. Therefore, his conclusion, i.e. stiffener tripping results in lesser drop in strength than the plate buckling failure mode is expected from the range of panel slenderness that he investigated. Hu (1993) did not study the effect of interaction between plate and stiffener.

Grondin *et al.* (1999) conducted a parametric study of stiffened steel plates using a finite element model validated using the results of an experimental investigation on stiffened steel plates (Grondin *et al.*, 1998). The parameters investigated were: shape and magnitude of initial imperfections in the plate, residual stress magnitude and direction of applied uniform bending, plate slenderness ratio, plate aspect ratio, and plate to stiffener area ratio.

Grondin *et al.* (1999) showed that the magnitude and distribution of initial imperfections have a significant influence on the capacity of stiffened plates failing by plate buckling. Little influence of initial imperfections was found for stiffened plates failing by overall buckling. They also showed that residual stresses have a significant influence on the strength of stiffened plates failing by plate buckling. The stiffened plate strength was found to be reduced in direct proportion to the magnitude of the applied compressive residual stresses in the plate for plate slenderness, β , values greater than 1.7. However, when yielding sets in before buckling (for $\beta < 1.7$) the effect of compressive residual stresses gradually diminished. Out-of-plane loading was found to be necessary to change the failure mode from plate buckling to stiffener tripping. Out-of-plane loading also resulted in a decrease in stiffened plates strength. The decrease in strength resulting from out-of-plane loading was found to be more significant on the stiffener tripping failure mode than on the plate buckling failure mode. The effect of plate to stiffener area ratio was found to be insignificant. A comparison of their finite element results (Grondin *et al.*, 1999) with current design guidelines presented by American Petroleum Institute (API, 1987) and Det Norske Veritas (DnV, 1995) indicated that these design guidelines are generally conservative for 'average' (Smith *et al.*, 1991) magnitudes of plate imperfection and "average" magnitude of residual stresses. Further research for a broader range of parameters for stiffener tripping failure mode was recommended.

Pan and Louca (1999) conducted a parametric study of stiffened steel plates to find the effect of blast loading on stiffened plate. The study was conducted using a finite element model validated by experimental results on stiffened steel plates (Pan and Louca, 1999). The parameters investigated were the shape of the stiffener (bulb flat and I-beam) and the effect of boundary restraint at the unloaded edges (pinned and fixed).

Pan and Louca (1999) showed that the boundary conditions, especially in-plane restraints, significantly influences the response of stiffened plates subjected to blast loading. The effect of relative direction between blast loading and stiffener axes on the structural response (Global response, local response and force transferred to supporting system) was found to be insignificant for the investigated boundary conditions.

2.4 FIELD OBSERVATIONS OF POST-WELDING DISTORTIONS AND RESIDUAL STRESSES

The welding of stiffeners to steel plates affects both the initial distortions in stiffened plate (its magnitude and distribution) and the residual stresses (magnitude and distribution). These two parameters (initial distortions and residual stresses) can vary widely, and a statistical approach may be preferable to study their magnitude and distribution in stiffened steel plates. Faulkner (1975), Carlsen and Czujko (1978) and Smith *et al.* (1991), conducted surveys of actual structures to try to assess these parameters.

Faulkner (1975) measured maximum initial plate distortions in 300 as-built stiffened plate specimens. The observed values were then grouped statistically and relationships were proposed for maximum initial plate distortion:

$$\frac{d_p}{t_p} = Kb^2\left(\frac{t_w}{t_p}\right) \quad \text{for } t_w < t_p \text{ and } \beta < 3.0 \tag{2.1}$$

$$\frac{d_p}{t_p} = Kb^2 \quad \text{for } t_w > t_p \text{ and } \beta < 3.0 \tag{2.2}$$

where β is the plate slenderness (same as defined earlier in the chapter), t_p is plate thickness, t_w is stiffener web thickness, d_p is the maximum magnitude of plate imperfection and K is a constant that was found from the regression analysis of collected data.

Faulkner (1975) proposed values of the constant K as 0.12 for warships, 0.15 for merchant ships and 0.10 for civil engineering structures, based on root mean square values of the collected data.

Faulkner (1975) also measured residual stresses in stiffened plates, and proposed a 'tension block' in the vicinity of weld region (see Figure 2.1). He observed this 'tension block' to extend three to six times the thickness of plate on either side of the weld. He proposed the following relationship for the maximum compressive residual stress in the plate:

$$\frac{f_r}{f_{yp}} = \frac{2h}{\frac{b_p}{t_p} - 2h} \tag{2.3}$$

where f_r is the magnitude of compressive residual stress in the plate, f_{yp} is the yield strength of the plate material, b_p is the plate width, t_p is the plate thickness and h is a constant that depends on type of welding (multiple pass welding, or intermittent welding). The recommended values of h were:

6-4.5	for ship structures
4.5-3	for civil engineering structures

Carlsen and Czujko (1978) conducted a similar survey to find the maximum magnitude and distribution of post-welding distortions in stiffened steel plates. They found that the quadratic slenderness (β^2) in form of maximum magnitude, suggested by Faulkner (1975), gave conservative results for very slender plates. They proposed a formula based on conservative assumption of mean plus two times the standard deviation as a basis for predicting post-welding distortions as:

$$\frac{d_p}{t_p} = 0.016\frac{b_p}{t_p} - 0.36 \qquad \text{for } b_p/t_p > 40 \tag{2.4}$$

where b_p and t_p are the plate width and thickness, respectively, d_p is the maximum suggested value of the plate imperfection.

Carlsen and Czujko (1978) also studied the effect of distribution of post-welding distortions on the compressive strength of stiffened plates. From measurements on 196

plates, they suggested that the deformed shape of welded stiffened plates used in ship structures could be expressed by a double trigonometric series of the following form:

$$d_0\,(x,y) = \sum_{i=1}^{m}\sum_{j=1}^{n} d_p \sin\left(\frac{ipx}{L_u}\right)\sin\left(\frac{jpy}{b_p}\right) \qquad (2.5)$$

where d_0 (x,y) is the magnitude of initial imperfection at point (x,y) on the plate (where x and y are the distances along the length and width of the panel), d_p is the magnitude of maximum out-of-plane imperfection (determined from statistical analysis of collected data) in the panel, L_u is length of the panel and b_p is the width of stiffened plate.

From the field observations of typical as-built stiffened plate panels Carlsen and Czujko (1978) proposed the 'hungry horse' shape (Figure 2.2) along the length with the plate on the compression side, and a half-sine wave across the width of the panel to be the dominant distribution of initial imperfection in the stiffened panel.

Carlsen and Czujko (1978) carried out finite difference analysis to find the effect of distribution of initial imperfection on the strength of the stiffened panel. They found that the distribution of the initial imperfections, along the length, that corresponds to the governing buckling mode of the stiffened plate to be the governing parameter in determining the strength of the stiffened panel. The non-buckling components showed no weakening effect on the strength in any of the cases examined by Carlsen and Czujko (1978). The distribution of the initial imperfection across the width of the panel was found to follow a half-sine wave. So they reduced the above expression to one term of the series that is as follows:

$$d_0\,(x,y) = d_p \sin(n_p\,\pi\,x/L_u)\sin(\pi\,y/b_p) \qquad (2.6)$$

where n_p is the number of half-sine waves in the deformed shape of plate along its length.

Finite difference analyses carried on stiffened plate with different initial imperfection patterns showed that three half-sine waves along the length of the plate and one half-sine wave, across the width of the panel, gave almost the same load-deflection curve as was given by typical 'hungry horse' shape illustrated in Figure 2.2.

Smith *et al*. (1991) also studied the magnitudes of initial imperfections and residual stresses in stiffened steel plates. The level of plate distortions and compressive residual stresses in the plate were grouped into “average”, “slight” and “severe” magnitudes corresponding to mean, 3 percentile and 97 percentile values of maximum initial distortions and residual stresses measured in as-built stiffened plate structures. The maximum magnitudes for each group of imperfections and magnitude of compressive residual stresses in the plates are reproduced in Table 2.1. They also found the distortion magnitudes to be proportional to the square root of the plate transverse flexural slenderness, as opposed to the linear relationship proposed by Carlsen and Czujko (1978). The ‘hungry horse’ shape (Figure 2.2) was the dominant distribution of the observed stiffened plates. A rectangular stress distribution was proposed for the residual stress distribution (Figure 2.1).

2.5 DESIGN GUIDELINES

Two design guidelines selected for this study are Classification notes No. 30.1 by Det norske Veritas (1995) and American Petroleum Institute Bulletin RP 2V (1987). Both guidelines present a comprehensive procedure for computation of the buckling strength of stiffened steel plates whereby the stiffened plate capacity is evaluated based on the various failure modes described in Chapter 1.

DnV (1995) guidelines are based on Perry-Robertson first yield principle together with an effective plate width concept. For stiffener induced failure the yield stress in the Perry-Robertson formula is replaced by the stiffener tripping stress, found by applying Perry’s formula on the stiffener alone, to account for stiffener tripping failure.

API (1987) guidelines are based on a formulation utilizing a reduced slenderness concept. The overall buckling load for a section consisting of stiffener attached with ‘effective plate panel width’ is found. The stiffener tripping failure load is found by considering the flexural torsional strength of the section consisting of stiffener and attached with effective plating.

2.6 SUMMARY

A review of the literature indicated that the finite element method is able to predict both the behaviour and strength of stiffened steel plates accurately. There have been very few studies to find the conditions that will lead to stiffener tripping failure mode. The parametric studies carried to date on stiffened steel plates either suppressed the stiffener tripping failure mode (Smith *et al*., 1991) or were conducted in the plastic range of material behaviour (Hu, 1993). A few analytical attempts were made to study the interaction between the stiffener and plate for stiffener tripping failure mode. But these closed-form solutions were based on various simplifying assumptions and did not show good correlation with the experimental tests conducted to verify these formulation. Current design guidelines (API, 1987; DnV, 1995) for stiffener tripping failure modes do not consider any interaction between the stiffener and plate for stiffener tripping failure mode. These formulations give conservative estimates of the stiffener tripping failure load, especially in the post-yield material behaviour.

Table 2.1
Maximum plating imperfections and compressive residual stresses
(Smith *et al.,* 1991)

Level	**Maximum initial imperfection in plate** $\left(\frac{d_p}{t_p}\right)$	**Residual compressive stresses in plate** $\left(\frac{f_r}{f_{yp}}\right)$
Slight	$0.025\beta^2$	0.05
Average	$0.1\ \beta^2$	0.15
Severe	$0.3\ \beta^2$	0.3

Table 2.2

Maximum imperfections in stiffener for $\lambda_0^* > 0.6$ (Smith *et al*., 1991)

Level	**Maximum initial imperfection in stiffener** $\left(\frac{d_s}{L_u}\right)$
Slight	0.00025
Average	0.0015
Severe	0.0046

* λ_0 denotes the slenderness of the stiffener acting with associated plating

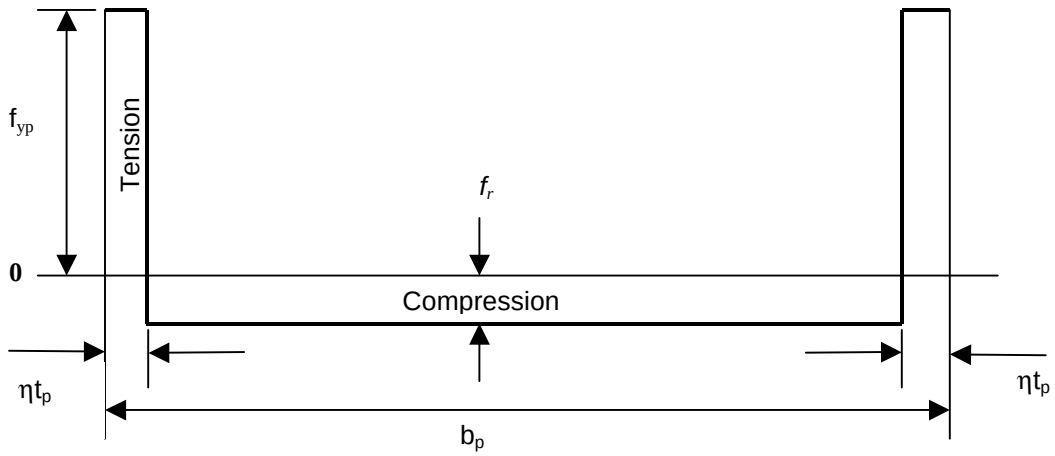

Figure 2.1 Idealised residual stress pattern in a web with edge welds (Faulkner, 1975)

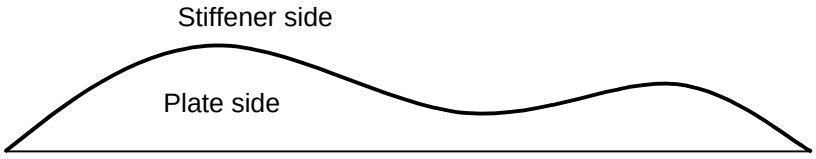

Figure 2.2 Typical 'hungry horse' shape proposed by Carlsen and Czujko, 1978

CHAPTER 3

FINITE ELEMENT ANALYSIS

3.1 INTRODUCTION

As described in Chapter 2, the finite element model proposed by Grondin *et al*. (1998) was able to predict both the behaviour and strength of as-built stiffened steel plate with excellent accuracy. The introduction of residual stresses has been performed in two steps by a number of researchers (Roman and Elwi, 1987; Chen *et al.,* 1993; Hu *et al.,* 1993; Grondin *et al.,* 1998) so that the deformations introduced by the residual stresses can be accounted for in the definition of the initial imperfections. Although this method is believed to be a more accurate method than the 1-step method to model actual residual stresses and initial imperfections, the 2-step approach represents additional modelling effort since the technique requires two separate analysis runs.

This chapter presents a description of the finite element model used to investigate the behaviour and strength of stiffened steel plates. The model is used extensively in Chapter 4 to identify the parameters that characterise the behaviour and strength of stiffened steel plates. The model is also used in Chapter 5 to conduct an extensive parametric study, seeking to delineate the values of the parameters identified in Chapter 4 that trigger stiffener tripping.

Since the work presented in Chapters 4 and 5 necessitated a few hundred separate analysis runs, preliminary analyses were conducted to compare the effect of introducing the residual stresses and initial imperfections in one run rather than in two runs. The results of this investigation are presented later in this chapter.

The stiffened steel plate problem was modelled using the commercial finite element code ABAQUS/Standard Version 5.7-1 (HKS, 1997a). This software is well suited for the solution of non-linear buckling type analysis and tracing the response well into softening post-buckling range. It provides a wide range of elements capable of

modelling thin-walled plates and allowing large displacements and finite membrane strains. All the analyses were performed on SUN UltraSparc 1 workstations at University of Alberta.

3.2 FINITE ELEMENT MODEL

A stiffened steel plate consists of a flat plate with equally spaced longitudinal stiffeners that span between bulkhead beams. A typical cross-section of a stiffened steel plate is shown in Figure 3.1. Because of the symmetry of stiffened plates, only one panel, i.e. a portion of the plate of width b_p with the stiffener centred on the plate strip, is modelled.

3.2.1 Mesh, Geometry and Boundary Conditions

A stiffened steel plate panel was developed by Grondin et al., 1998, using the finite strain shell element S4R from ABAQUS. The mesh, shown in Figure 3.2, consists of 384 S4R shell elements in the plate and 96 elements each in the flange and the stem of the stiffener. This mesh size was found to yield satisfactory convergence.

The S4R element is a four-node, doubly curved, shell element that allows for changes in the thickness as well as finite membrane strain. The element has six degrees of freedom at each node (three displacements component and three rotation components). The element is a reduced integration element with a single integration point at the centre of element. The cross-sectional behaviour of the homogeneous shell element is calculated using Simpson's rule with five integration points through the thickness of the element. (HKS, 1997b).

The initial imperfections were modelled at the time of defining the mesh. This helped in the application of known magnitude and desirable distribution of imperfections in the model. The probable distribution and magnitude of imperfections is discussed in chapter 4.

Two sets of boundary conditions were introduced, one corresponding to the loaded ends and the other to the unloaded (longitudinal) plate edges. It is expected that

the stiffeners would be welded to massive bulkheads or floor beams that are stiff in their own planes but are flexible in out-of-plane direction. This type of boundary conditions requires the ends of the specimen to rotate locally maintaining the shape of the cross-section. This effect was incorporated in the model by providing rigid frames composed of stiff three-dimensional beam elements, B31 from the ABAQUS library, aligned along the specimen ends. These beam elements used a separate set of nodes from those forming the specimen ends. The two sets of nodes were then constrained to simulate a welded connection. The loads were applied at the centroid of the rigid end frames. The stiff end frames also helped to distribute the load applied at the geometric centroid, uniformly over the cross-section. A support, at the geometric centroid of one of the two end rigid frames, was added to restrain translation along the longitudinal axis and rotation about the longitudinal (twist) and in-plane axes was used on the reaction end. A support, at the geometric centroid of the rigid frame at the loading end of the stiffened plate panel was used to prevent rotation about the longitudinal axis and translation about the other two axes. The rotation about the longitudinal axis was suppressed at all the nodes along the unloaded edges to simulate full continuity (see Figure 3.2).

3.2.2 Material Properties

An elastic-plastic material model with a von Mises yield criterion was used to model the material constitutive behaviour. Since large deformations and finite strains were developed in the model during the analysis, particularly after the formation of buckles, typical true stress versus true strain properties were used in the model. The static yield strength level of 420 MPa and modulus of elasticity of 200 GPa was used for defining the flange, web and plate materials of the stiffened plate. These levels are typical of CAN/CSA-G40.21 350W or equivalent, steel (Grondin *et al*., 1998). The actual values as well as description of the stress versus strain curve adopted for the analysis are listed in Table 3.1.

3.2.3 Residual Stresses

The only residual stresses introduced in the model were the longitudinal stresses arising in the specimen from a combination of the manufacturing process of the plate and

T-stiffener and welding of the stiffener to the plate during the fabrication of stiffened steel plate. The resulting residual stresses have been measured and reported in the literature (Grondin *et al*., 1998). The residual stresses were modelled by imposing initial strains in the form of a temperature distribution. To obtain uniaxial residual stresses, orthotropic temperature material properties that had zero thermal expansion coefficients in the two transverse directions (directions 2 and 3 in the model) was used. Changes in temperature, corresponding to the desired residual strains were applied in the first load step and an equilibrium iteration was carried out to establish equilibrium. A complication arises because of distortion in the specimen under the applied strains, thus the initial imperfection magnitude changes. This results in a geometry with unknown magnitude and distribution of initial imperfections. The manner in which this complication was dealt with is discussed in section 3.3.

3.2.4 Solution Strategy

ABAQUS uses the RIKS method (Riks, 1979) for predicting the unstable, material and geometric non-linear, collapse of structure. Since the response was desired well into unstable post-buckling range, therefore, RIKS method was used throughout to trace the load-deformation response well into the softening post-buckling range.

The RIKS procedure uses the load magnitude as an additional unknown, it solves simultaneously for loads and displacements. Therefore, another quantity must be used to measure the progress of the solution. ABAQUS uses the “arc length” along the static equilibrium path in load-displacement space to measure the progress of solution. This approach provides the solution irrespective of whether the problem is stable or unstable (Riks, 1979). A maximum magnitude of load proportionality factor or maximum displacement value at a specified degree of freedom is required to end the process.

Two loading conditions are investigated in this study, namely, uniaxial compression and combined bending and axial compression. In the uniaxial compression case the incremental RIKS procedure was used, with a maximum of 1% nominal strain value, to get the peak behaviour and strength. In the combined bending and axial compression cases, initial end moments were applied at both ends of the stiffened plate

panel using Newton-Raphson method. This initial moment was followed by uniaxial compression using RIKS procedure to observe the behaviour of the stiffened plate up to a nominal strain of 1 % in the longitudinal direction.

3.3 INFLUENCE OF RESIDUAL STRESSES AND ITS METHOD OF APPLICATION

As described above, the applied residual stresses distort the geometry of the stiffened plate. This effect of distortion has been controlled by a 2-step method (Hu, 1993; Chen *et al.*, 1993; Grondin *et al.*, 1998). The method was first proposed by Roman and Elwi (1987) to apply residual stresses in stiffened cylinders and is described as follows:

3.3.1 2- Step Method

First step can be further subdivided as:

(1) Calculate the fictitious temperature distribution (T) in the stiffened plate from the residual stress distribution as

$$T = -\frac{f_r}{\alpha_T E} \tag{3.1}$$

where f_r is the residual stress, E is the modulus of elasticity, and α_t is the coefficient of thermal expansion

(2) Select the overall distribution of residual stresses so that self equilibrium conditions

$$\int_A T dA = 0 \tag{3.2}$$

and

$$\int_A T z dA = 0 \tag{3.3}$$

are satisfied, where A is the cross-sectional area and z-coordinate is the distance of an element dA to the 2-axis (axis parallel to width of plate).

(3) Using a finite element mesh with no initial imperfections, apply a temperature change corresponding to the negative of the desired residual stresses and analyse the stiffened plate to obtain the resulting deformed mesh. The temperature change will produce residual stress f_r and displacements $-U_T$.

Add the displacements to the desired initial imperfection pattern. This will be the new input geometry for the model. It is expected that when the residual stresses are added in the first load step, the resulting displacements will be very close but of opposite sign to those that were added to the desired initial imperfections to obtain the starting mesh (i.e. $\approx + U_T$). Ideally, this procedure should proceed iteratively until the deformed shape obtained after the residual stress step corresponds to the desired initial imperfections. In practice, however, there is little to be gained by doing more than one iteration.

3.3.2 1- Step Method

In this method, residual stresses were applied in 1-step in the desired direction and the rest of the analysis was carried in a similar manner, without making any correction in the initial imperfections to account for the distortions caused by the application of residual stresses. This will result in a distorted mesh, with imperfections slightly different from the desired ones.

It can be observed from the above description that applying residual stresses in one step will result in significant saving of processing time. The 1-step can be used if the error resulting from this shorter approach is insignificant.

To find the effect of residual stresses and the method of application for all the failure modes described briefly in Chapter 1, four runs were performed with the same magnitude and distribution of residual stresses for all four failure modes. For each case the residual stresses and initial imperfections were applied using 1-step and 2-step methods described above. The data for all the four failure modes are taken from chapter 4. The results of these analyses are briefly discussed below (more details of the input data

and the definition of the parameters used for the different cases are presented in Tables 4.2, 4.3, and 4.4 of Chapter 4).

3.3.2 Discussion

The stiffened plate specimen was loaded in three steps, in 1st step the residual stresses were applied (this was applied by either 1-step or 2-step procedure), in 2nd step the end moments (20 % of plastic moment capacity of the stiffened panel) were applied and in last step an axial force was applied at the geometric centroid of the section to reach the failure condition of 1 % nominal strain value. Three different load cases were considered, for finding the effect of application of residual stress, for all the reported failure modes (Chapter 1), i.e. plate and stiffener induced overall buckling, plate buckling and stiffener tripping. They were:

i) No residual stress case

ii) Residual stress applied by 1-step procedure

iii) Residual stress applied by 2-step procedure.

For applied end moments, two load cases were considered, in 1st case the end moments were applied in such as a manner as to cause flexural compression in the flange of the stiffener (for stiffener induced overall buckling and stiffener tripping case (chapter 1)) and in the other the end moments were applied in such a way as to cause flexural tension in the stiffener flange (for plate induced and plate buckling failure mode (chapter 1)).

The load versus axial displacement curves for a stiffened plate failing by plate induced overall buckling are presented in Figure 3.3 for both the 1-step procedure and the 2-step procedure. Both curves are almost identical, which indicates that neither the strength nor the behaviour is affected by the difference that may exist between the 1-step and the 2-step procedure for this case. This means that the residual stresses can be applied either the 1-step or 2-step method for this type of failure.

Figure 3.4 presents the load versus axial deformation curves for stiffener induced overall buckling mode for both the 1-step procedure and 2-step procedure. The same observation can be made as for plate induced overall buckling failure.

Figure 3.5 presents the load versus axial deformation curves for plate buckling failure mode for both the 1-step and 2-step procedures. Since the plate buckling failure mode is sensitive to imperfections (Grondin *et al.*, 1999) so there is a different response observed for 2-step method compared with 1-step method. The residual stresses applied by 1-step method are giving a lesser peak strength and softer post-buckling response for plate-buckling failure mode. It is therefore concluded that the 1-step method would lead to more conservative results than the 2-step method.

Figure 3.6 presents the load versus axial deformation curves for stiffener tripping failure mode for both the 1-step and 2-step procedures. There is no significant difference between the response given by the 1-step method as compared with the 2-step method.

The application of residual stresses in 1-step generally results in a conservative prediction of response as compared with 2-step method. The 1-step method is, therefore, used in the rest of the study to apply the residual stresses.

Table 3.1

Material properties for finite element model

Part	f_1 (MPa)	e_1	f_2 (MPa)	e_2	f_3 (MPa)	e_3
Plate, Flange and Web	420.0	0.0021	420.825	0.0204	520.825	0.1204

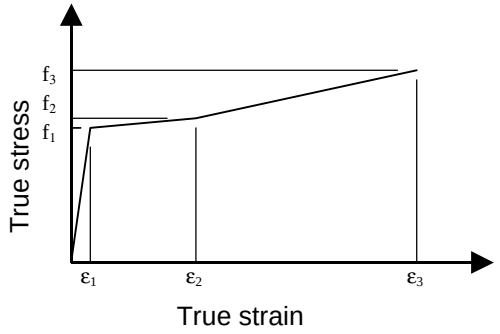

Table 3.2

Influence of residual stress and its method of application

Failure mode*	**SI**	**PI**	**PB**	**ST**
Case / Model name**	**bp_SI**	**tb_PI**	**tt_PB**	**bc_ST**
No residual stress (P_c/P_y)	0.800	0.955	0.624	0.732
Residual stress in 1-Step (P_c/P_y)	0.787	0.952	0.572	0.724
Residual stress in 2-Step (P_c/P_y)	0.786	0.953	0.599	0.718
Percentage loss in strength from residual stress (considering no residual case as base case)				
Residual stress in 1-Step	1.68%	0.29%	8.31%	1.20%
Residual stress in 2-Step	1.78%	0.20%	3.89%	1.91%
Percentage loss in accuracy (considering 2-Step method as base case)				
	-0.103%	0.088%	4.606%	-0.720%

*
SI – Stiffener Induced Overall Buckling
PI - Plate Induced Overall Buckling
PB- Plate Buckling Failure Mode
ST- Stiffener Tripping Failure Mode

**For model data refer Table 4.2 - Table 4.4

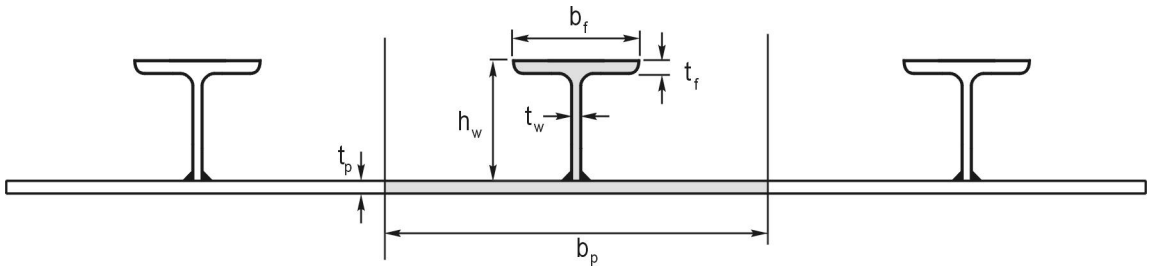

Figure 3.1 Typical stiffened steel plate panel

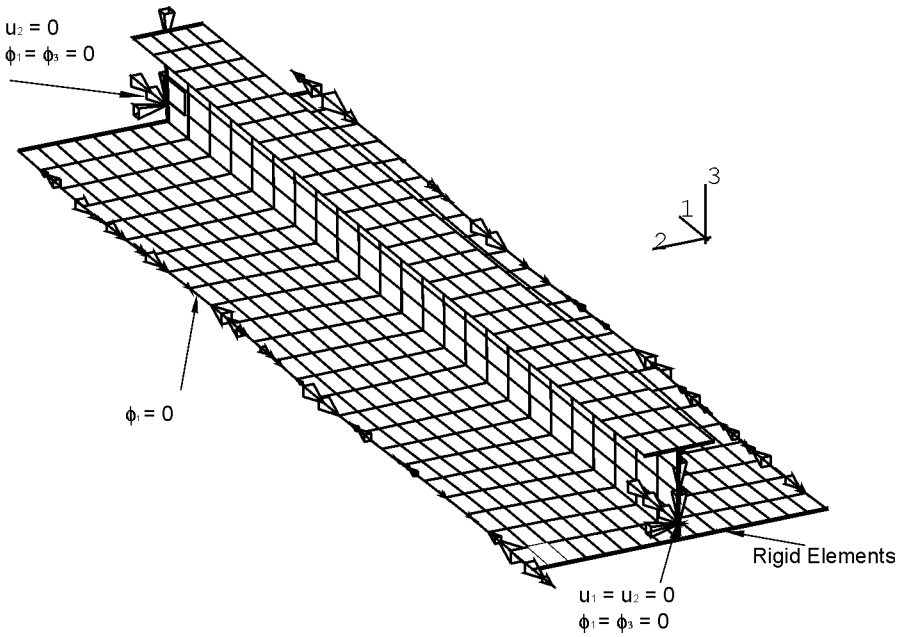

Figure 3.2 Finite element mesh with kinematic boundary conditions

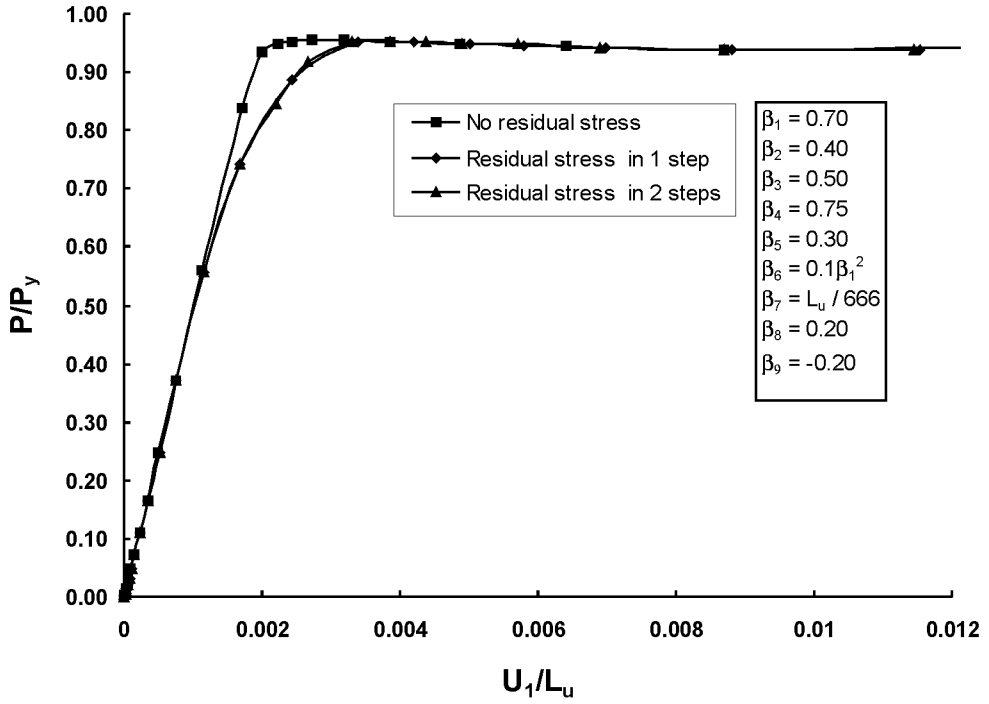

Figure 3.3 Effect of residual stresses on behaviour of plates failing by plate induced overall buckling

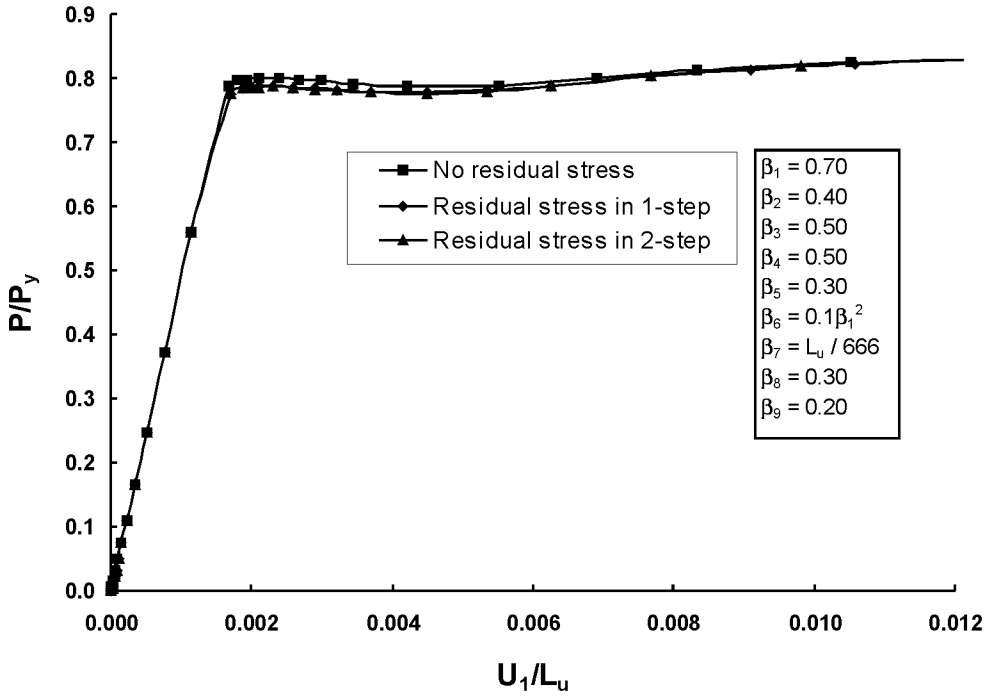

Figure 3.4 Effect of residual stresses on behaviour of plates failing by stiffener induced overall buckling

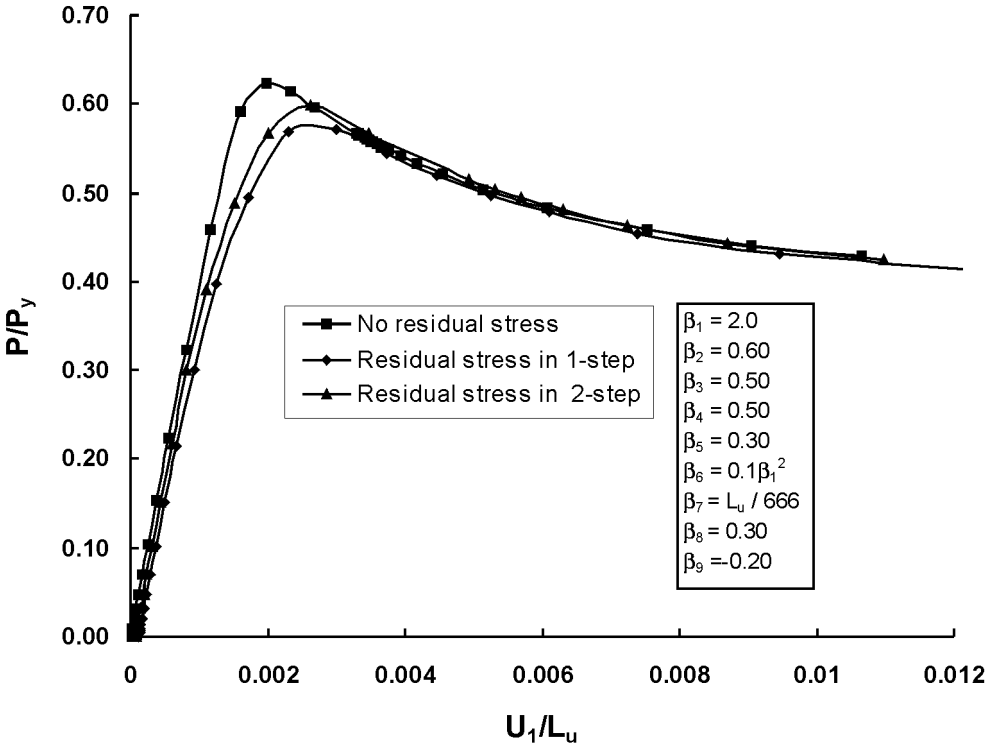

Figure 3.5 Effect of residual stresses on behaviour of plates failing by plate buckling

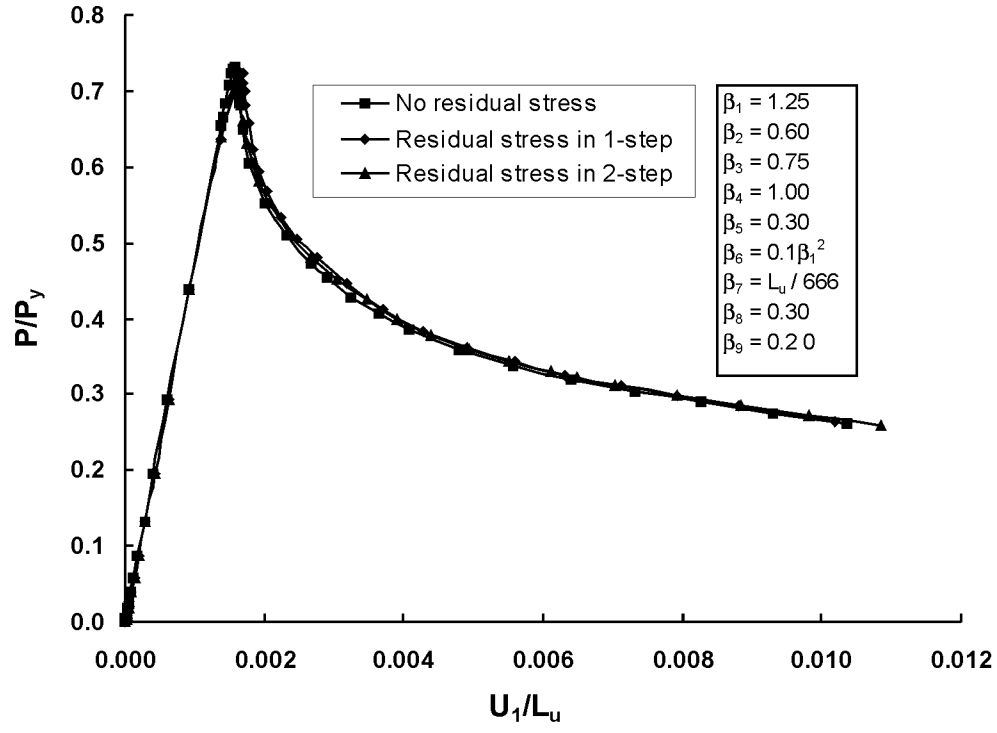

Figure 3.6 Effect of residual stresses on behaviour of plates failing by stiffener tripping

CHAPTER 4

PARAMETERS CHARACTERISING STIFFENED STEEL PLATES BEHAVIOUR AND STRENGTH

4.1 INTRODUCTION

Before a parametric study of stiffened steel plates can be carried out, it is important to determine the parameters that characterise the behaviour of stiffened steel plates for all modes of instability. Ideally these parameters should be independent of any scale or material strength effects. Since these parameters may be a function of the mode of failure and the loading conditions, it is important to first determine the possible modes of failure and assess the loading conditions of interest. This is presented in the following.

Stiffened plates can be loaded under a combination of in-plane and out-of-plane loads. In-plane loads may include axial or biaxial stresses and in-plane shear. Out-of-plane loading includes lateral pressure or bending about the transverse or longitudinal axes of the stiffened plate. Although a stiffened steel plate can be loaded in a number of ways, most research has focused on two loading cases. Most commonly, tests have been conducted under uniaxial compression applied in the direction of the stiffener (Murray, 1973; Ghavami, 1994). A limited number of tests have been conducted under combined bending and axial compression (Hu *et al*. 1997). These loading conditions are common in several civil engineering, mobile and stationary offshore structures.

Instability of stiffened plates under uniaxial compression or under combined bending and compression can take one of four forms (Murray, 1973; Bonello *et al.*, 1993; Hu, 1993; Grondin *et al*., 1999): plate induced overall buckling (PI), stiffener induced overall buckling (SI), plate buckling (PB) and stiffener tripping (ST).

Overall buckling is characterised by simultaneous buckling of the stiffener and the plate. Because this mode of failure is similar to that of an elastic column, it is sometimes referred to as an Euler type-buckling mode. If buckling occurs with the

stiffener on the convex (tension) side of the plate, overall buckling is said to be plate induced (see Figure 4.1 (a)). On the other hand, if the stiffener is on the concave side of the plate, overall buckling is said to be plate induced (see Figure 4.1 (b)). These two types of failure are typically characterised by stable post-buckling response as shown in Figure 4.2. The load versus displacement responses presented in Figure 4.2 were obtained using the finite element model described in Chapter 3.

Plate buckling failure is characterised by buckling of the plate between the stiffeners, resulting in a load re-distribution from the plate into the stiffeners. This mode of failure is illustrated in Figure 4.1 (c) with a typical load versus displacement behaviour presented in Figure 4.2. The plate buckling failure mode has a lesser post buckling strength than the overall buckling failure mode, but still shows considerable post-buckling strength.

Stiffener tripping is characterised by the rotation of the stiffener about the stiffener to plate junction (see Figure 4.1 (d)). Stiffener tripping is, therefore, a form of lateral torsional buckling, where torsion takes place about the stiffener to plate junction. As opposed to the other modes of failure, this type of failure generally results in the sudden drop of load carrying capacity (see Figure 4.2).

The main goal of this chapter is to identify the various parameters that govern the strength and modes of failure of stiffened steel plates. These parameters will then be used in the following chapters to conduct a parametric study to try to identify the range of these parameters that trigger stiffener tripping.

4.2 MODEL PARAMETERS

The geometric parameters affecting behaviour and strength of stiffened steel plates consist of the cross sectional dimensions and the length of the stiffened panel. These parameters are summarised in Figure 4.3. In addition to the dimensions, the geometric parameters also include initial imperfections in stiffener and plate. The loading parameters considered in this work consist of axial load, bending moment causing in-plane bending and residual stresses. The material parameters for elastic-plastic

material used in analysis consist of elastic modulus, Poisson's ratio and yield stresses of both stiffener and plate. The parameters to be considered in the behaviour and strength of stiffened steel plates are summarised as follows:

b_p	width of stiffened steel plate (taken as the stiffener spacing)
t_p	plate thickness
h_w	stiffener web height
t_w	stiffener web thickness
b_f	stiffener flange width
t_f	stiffener flange thickness
L_u	length of stiffened plate
f_{yp}	yield stress of plate material
f_{ys}	yield stress of stiffener material
f_r	magnitude of the maximum compressive residual stress in plate
E	Young's modulus of elasticity of steel
ν	Poisson's ratio for steel
M_a	applied bending moment
d_p	maximum initial imperfection in plate
d_s	maximum initial imperfection in stiffener
P_c	peak load capacity of the stiffened plate
U_1	axial shortening of the stiffened plate

It is apparent from the above list of parameters that the number of parameters is too large to manage in a reasonable number of analyses. It is, therefore, imperative that the number of parameters be reduced to simplify the parametric study. This is achieved through a dimensional analysis. To assess whether all of the essential variables that play a role in the behaviour of stiffened plates have been selected, a preliminary investigation is carried out to check if the results are affected by changes in scale.

4.2.1 Simplification of Parametric Study – Dimensional Analysis

The purpose of using a dimensional analysis here is to limit the complexity of the parametric study by reducing the number of parameters and choosing parameters that are

scale independent and dimensionless. Dimensional consistency is ensured by first checking the dimension of all derived quantities to see that they are properly represented in terms of primary quantities and their dimensions. The next step is the identification of the proper dimensionless groups of variables, i.e. those ratios and products of the problem parameters and variables that are themselves dimensionless. In order to identify a proper set of dimensionless parameters that characterise the behaviour of stiffened steel plates, one can resort to the use of the Buckingham Pi theorem, which is stated as follows (Langhaar, 1951):

> *If an equation is dimensionally homogeneous, it can be reduced to a relationship among a complete set of dimensionless products. The number of independent dimensionless groups of variables needed to correlate the variables in a given process is equal to n-m, where n is the number of derived variables and m is the rank of dimensional matrix.*

The importance of this transformation of primary variables into a set of dimensionless parameters is that the scale effects can be controlled in numerical modelling and the number of parameters that must be considered is reduced by m, which represents significant saving of computational cost and effort.

The fundamental variables required to define the stiffened steel plate problem under the action of uniaxial compression and bending are presented in Table 4.1. Dimensional analysis uses the fundamental dimensions of mass (M), length (L) and time (T) to define the units for the variables. These are also identified in Table 4.1.

The trial dimensionless parameters are listed as follows:

$$b_1 = \frac{b_p}{t_p}\sqrt{f_{yp}/E}$$

$$b_2 = \frac{h_w}{t_w}\sqrt{f_{ys}/E}$$

$$b_3 = \frac{b_f}{t_f}\sqrt{f_{ys}/E}$$

$$b_4 = \frac{\frac{L_u}{r_z}\sqrt{f_{ys}/E}}{\frac{b_p}{t_p}\sqrt{f_{yp}/E}}$$

$$b_5 = \frac{A_s}{A_p}$$

$$b_6 = K * b_1^{\,2}$$

$$b_7 = d_s / L_u$$

$$b_8 = \frac{f_r}{f_{yp}}$$

$$b_9 = \frac{M_a}{M_p}$$

$$b_{10} = \frac{P_c}{P_y}$$

$$b_{11} = \frac{U_1}{L_u}$$

where r_z is torsional radius of gyration of stiffener about its centroid, A_s is area of stiffener, A_p is area of plate, K is a constant (depends on severity of initial imperfection magnitude in plate), M_p is plastic moment capacity of stiffened plate and P_y is yield capacity of the stiffened plate. The other variables have already been defined in this section.

The slenderness parameters β_1, β_2, β_3, and β_4 obtained from dimensional analysis are multiplied with square root of yield strain to make them material strength independent. The first nine β-parameters will be input to the finite element model, β_{10} will be the output parameter of finite element model and β_{11} will be the control parameter, used to monitor the response of stiffened plates.

The basis for the selection of the above trial parameters is explained below.

4.2.2 Justification for Proposed Parameter Set

4.2.2.1 Plate Transverse Flexural Slenderness, b_1

The plate slenderness is well known to be one of the important factors affecting the strength of a plate (Faulkner, 1975; Carlson, 1980; Smith *et al*., 1991; Grondin *et al.*, 1999). The strength of stiffened panel increases with a decrease in plate transverse flexural slenderness and vice versa.

4.2.2.2 Stiffener Web Slenderness, b_2

Experimental work by Rogers and Dwight (1976) and Panagiotopoulos (1992) showed that there exists a critical slenderness of flat bar stiffeners at which the mode of failure changes from stiffener tripping to overall buckling. Carlson (1980) made a similar observation for tee stiffeners. It is expected that an increase of stiffener web slenderness for a Tee-shape stiffener may trigger a stiffener tripping failure mode.

4.2.2.3 Stiffener Flange Slenderness, b_3

The flange of stiffener is very effective at increasing stiffener's lateral stiffness. If local buckling of the flange is prevented, for a given flange area, a slender flange will result in a relatively stable stiffener than a stockier flange.

4.2.2.4 Ratio of Torsional Slenderness of Stiffener to Plate Transverse Flexural Slenderness, b_4

Danielson *et al.* (1990) demonstrated that stiffener tripping is dependent on torsional stiffness of stiffener. More recently, Paik *et al.* (1999) and Hughes and Ma (1996) have shown, using a closed form solution, that stiffener tripping is dictated by the ratio of torsional slenderness of stiffener to plate transverse flexural slenderness.

The impact of β_4 can also be visualised by considering a stiffener attached at the base with a spring. Small spring stiffness, simulating a flexible plate to which the stiffener is attached, would promote failure by tripping. Conversely, large spring stiffness, simulating a stiff plate, would increase the stiffener tripping resistance.

Similarly, a decrease of the torsional stiffness of the stiffener while the spring stiffness is kept constant would tend to promote failure by stiffener tripping.

4.2.2.5 Stiffener to Plate Area Ratio, b_5

Stiffener to plate area ratio was studied by Grondin *et al*., (1999), Smith *et al*. (1991), Caridas and Frieze (1988) and Carlson (1980). It has been found that the stiffener to plate area ratio does not affect the strength of the stiffened panels failing in a plate buckling failure (Grondin et al., 1999; Carlson, 1980). Stiffener to plate area ratio, however, affects the strength of stiffened panels failing by stiffener tripping. An increase in strength is found with the increase in stiffener to plate area ratio (Grondin *et al*., 1999).

4.2.2.6 Initial Plate Imperfections, b_6

Welding of stiffener to plate will affect both the initial distortions in the stiffened plate (its magnitude and distribution) and the residual stresses (magnitude and distribution). The work of various researchers (Faulkner, 1975; Carlson and Czujko, 1978; Smith *et al*., 1991; Grondin *et al*., 1999) on finding the effect of magnitude and distribution of initial imperfection has been briefly summarised in chapter 2.

Based on the work of previous researchers (Faulkner, 1975; Carlson and Czujko, 1978; Smith *et al*., 1991; Grondin *et al*., 1999), the following work assumes four half sine waves (recommended by Grondin *et al*., 1999) with an “average” magnitude (as defined by Smith *et al*., 1991; Table 2.1) of imperfections in the plate. The "severe" magnitude represents plate damage, while the "average" magnitude proposed by Smith *et al.* (1991) represents an upper bound of the initial imperfections in undamaged plates. The study of damaged plates is beyond the scope of this investigation.

4.2.2.7 Initial Stiffener Imperfections, b_7

Carlson (1980) demonstrated that the initial stiffener imperfection, expressed as a fraction of length, affects the strength of stiffened plate panels. The magnitude of stiffener imperfection is, therefore, expressed as a fraction of the stiffened panel length.

An ‘average’ magnitude (Smith *et al.*, 1991, Table 2.2) of stiffener imperfection is used throughout this study.

The distribution of initial imperfections in stiffener is defined by a half sine wave along the length at stiffener flange to web junction, with a parabolic variation along the web height. The flange deformed shape is defined from the assumption that the angle between the web and the flange remains at 90 degrees and the flange portion of the stiffener remains straight.

Stiffener imperfection can, therefore, be described as follows.

For web:

$$d_2(x,z) = d_s\left(\frac{z}{h_w}\right)^2 \sin\left(p\,\frac{x}{L_u}\right) \tag{4.1}$$

where d_2(x, z) is the initial imperfection in the web at a distance x along the length and z along the height of stiffener, d_s is the maximum initial imperfection in the stiffener and L_u is the length of the stiffened panel.

The new location of web to flange junction (y_{cl} (x, h_w)), after the application of initial imperfection in the web, can be given by the following expression:

$$y_{cl}(x,h_w) = d_s \sin\left(p\,\frac{x}{L_u}\right) \tag{4.2}$$

The slope of imperfection in stiffener flange will, therefore, be a negative reciprocal of the slope of the parabola, at the web to flange junction (because flange and web are assumed to remain at 90^0 to each other). The slope of the flange, m_2, can be found by the following expression:

$$m_2 = -\left(\frac{h_w}{2}\right)\sin\left(p\,\frac{x}{L_u}\right) \tag{4.3}$$

The imperfect shape of the flange can now be found, by offsetting the co-ordinates of all the points on the surface of the flange, in the y-direction, by a distance y_{cl} and then multiplying the slope of the initial imperfections in the flange, m_2, by the distance from the centre line of the perfect mesh.

The imperfect shape of the flange is given as:

$$d_3 = -d_s m_2 \left(\frac{2y}{b_f} \right) \tag{4.4}$$

where d_3 is the imperfection measured in the global direction-3, y is the distance across the width of the flange, measured from the centre line of the flange, and b_f is the flange width.

An 'average' magnitude imperfection, as given by Smith et al. (1991) (Table 2.2), is used to define initial imperfections in the stiffener.

4.2.2.8 Residual Stresses, b_8

The presence of residual stresses in stiffened plates is mainly attributable to the welding of stiffening elements to the plate. The welding of the stiffener to plate introduce tensile residual stresses close to the yield limit of the material (Grondin *et al.,* 1999). These residual stresses are self-equilibrating stresses, so the tensile residual stresses near the weld location are balanced by compressive residual stresses away from the weld in both the stiffener and plate. The residual stress pattern adopted for the following study is illustrated in Figure 4.4.

Residual stresses generally reduce the ultimate compressive strength of stiffened panels with little, if any, impact on the post buckling strength of stiffened panels (Faulkner, 1975; Carlson, 1980; Smith *et al.*, 1991; Grondin *et al.*, 1999). Although the residual stresses are included in the models for the following investigation, their magnitude and pattern will not be considered as one of the variables.

4.2.2.9 Applied to Plastic Moment Ratio, b_9

Balaz and Murray (1992) argued that for a thin walled section, the shape factor (M_p/M_y) is close to unity. Therefore, the non-dimensionalising factor could either be the yield moment or the plastic moment. For this study, the applied moment is non-dimensionalised relative to the plastic moment capacity of the stiffened plate section, M_p.

Grondin *et al*. (1999) have shown that the applied bending moment has two distinct effects: (1) it reduces the load carrying capacity of stiffened plates and (2) it changes the failure mode from one of plate buckling to stiffener tripping when the moment is applied to increase compression the stiffener flange.

4.2.2.10 Peak to Yield Axial Load Ratio, b_{10}

The parameter, β_{10}, is the dependent variable in the study. The load versus deformation response is monitored up to a nominal axial strain, defined as the axial shortening divided by the plate length, of 1.0%. The peak load is the maximum load that a panel will take in its pre-buckling range. The applied load is non-dimensionlised relative to the yield capacity of the plate. The non-dimensional load, therefore, provides a good measure of how effectively the stiffened panel area is being used.

4.2.2.11 Axial Shortening of Stiffened Panel, b_{11}

Axial shortening of the stiffened plate is the measure of the response to the applied load. The axial shortening is non-dimensionalised relative to the length of the stiffened plate, thus giving a measure of the average strain applied on the plate. It is used as the control parameter for the analysis. Carlson (1980) restricted his parametric study to a nominal axial strain 0.2% of, Hu (1993) went to 0.25 % and Smith *et al*. (1991) restricted his analysis to nominal axial strain value of about 0.2%. In order to have a broader picture of the behaviour, i.e., finding the response well into the post-buckling region, the analysis, presented in the following, is carried up to a nominal axial strain of 1%.

4.2.2.12 Other Parameters

Carlson (1980) found that the stiffener flange to web area ratio has little influence on the strength of stiffened steel plates. Nevertheless, the distribution of area between the web and the flange must still be addressed. The slenderness parameters for the web and

the flange help define the cross section of the stiffener for a given stiffener flange to web area ratio.

To test the suitability of the suggested parameters, the scale of the model was varied while keeping the values of the input parameters constant and checking whether the strength and the response remain the same. If the behaviour and strength are within a tolerable limit, then one can conclude that these parameters truly characterise the stiffened steel plate behaviour.

4.3 SUITABILITY OF NON-DIMENSIONAL PARAMETERS

One of the requirements of the Buckingham Pi theorem is that all of the fundamental variables necessary to describe the mechanics of the problem must be included in the set of β_n parameters. For the stiffened panel these were identified as β_1 to β_{11}. To assess whether all of the essential variables that play a role in the behaviour are represented in this set, a preliminary investigation is carried out on stiffened panels having identical input β-parameters but with different scales. If the output β-parameter (P_c / P_y) comes out to be the same, then it can be concluded that all the variables required for defining the mechanics of the problem have been included. The stiffened panel behaviour is also a variable. Hence, β_1-β_9 are given values to induce overall buckling (both plate and stiffener induced), plate buckling and stiffener tripping failure modes. The analysis, therefore, needs to be repeated for all the fundamental variables involved in defining the β–parameter values and for all the four failure modes mentioned above.

Nine analyses of stiffened panels (base case, b_p, t_p, h_w, t_w, b_f, t_f, f_{yp}, f_{ys}) each having identical input β–parameter set with different scales are tested for each failure mode. Imperfections in the plate and stiffener i.e.,β_6 and β_7 in the suggested parameters set, are given “average” values (Smith *et al*, 1991; see Table 2.1 and 2.2). The value of residual stress, β_8, is kept at zero to facilitate the interpretation of the results. Applied moment to plastic moment ratio, β_9, is given a value of 0.2. This magnitude was found to be sufficient to produce each failure mode. It is applied to cause compression on the stiffener side of the plate to trigger the stiffener induced overall buckling mode and

stiffener tripping. It is applied to cause compression in the plate to trigger plate buckling and plate induced overall buckling.

The results for each of the above mentioned failure modes are presented in Tables 4.2 to 4.5. Each model in the table is designated in the form *primary variable being changed_failure mode being considered* (e.g., b_p_PI designates a model in which the plate width was changed to investigate its effect on plate induced overall buckling). Note that it was not possible to change one variable at a time because all the primary variables are inter-related through the β parameters. A base case was run, represented with bc_failure mode, (where bc stands for base case) and values of other variables involved in defining the parameter set are changed within a range of approximately +/- 20% from the set in the base case. It should also be noted that the yield stress of some of the models is not truly representative of common structural steels. The intent of varying the yield stress was to demonstrate that the effect of model scale has been controlled appropriately.

4.4 DISCUSSION

4.4.1 Presentation of Results

The results throughout the report for critical cases ispresented in, at least, two forms, namely, a load versus deformation response and representative plots of the deformed shape.

4.4.1.1 Load Versus Axial Deformation Response

The load versus deformation history of one set of analysis results (runs having same set of β–parameters) is presented in dimensionless form such as the load divided by the yield load and change in length of the plate panel divided by the initial panel length (represents an average strain over the length of the plate specimen). The maximum load in the pre-buckling range is taken as the peak load of the model. The other useful information that is extracted from the load versus deformation history plots is the post-

buckling response of the model. The peak load alone is not a sufficient measure of stiffened plate performance since the behaviour of the plate varies considerably in the post-buckling range depending on the mode of buckling.

4.4.1.2 Deformed Shape of the Stiffened Plate

In order to determine whether all kinematic boundary conditions have been implemented properly and to obtain a feeling for the overall deformational behaviour and failure mode of the stiffened plate, it is instructive to look at the overall deflected shape at various stages during loading. The stages selected are at the initiation of buckling phase, at a later stage, in the post-buckling and finally at the nominal axial strain value of 1%.

The deformed shape at the initiation of buckling is drawn to have some idea of the dominant buckling mode at the initiation of buckling. There is the possibility of shifting of the buckling mode in the post-buckling range, for example, it is possible for a plate buckling mode to evolve either into stiffener tripping or overall buckling in the post-buckling range. In order to detect such evolution of buckling in the post-buckling range, the buckle configuration was plotted at two axial deformation levels. The deformed shape at the 1% nominal strain, the maximum strain value to which the analysis is carried, is examined to provide some measure of the ultimate state of the model.

4.4.2 RESULTS

A *base case* is run for each of the failure modes and serves as a reference for the other eight cases in each failure mode. The other eight cases are obtained by changing one of the other basic variables and adjusting the other variables to obtain the desired value of the β-parameters. The results are discussed in the following for each of the observed failure modes.

4.4.2.1 Plate Induced Overall Buckling

The input parameters selected to trigger plate induced overall buckling were: $\beta_1 = 0.7$, $\beta_2 = 0.4$, $\beta_3 = 0.5$, $\beta_4 = 0.75$ and $\beta_5 = 0.3$. From the work of Grondin *et al.* (1999), Faulkner (1975) and Carlson (1980) the selected value of β_1 should

lead to yielding of the plate before buckling. Since bending in the plate was applied to create tension in the stiffener, the likelihood of getting stiffener tripping is small. Nevertheless, low values of β_2 and β_3 were selected to avoid potential stiffener tripping problems. The stiffener area used was 30% of the plate area, which was found to be sufficient to produce overall buckling (Carlson, 1980; Grondin *et al.*, 1999). The other parameters, i.e. initial imperfections, residual stresses and applied bending moment were kept equal to the values described above, i.e. "average" magnitude for plate and stiffener imperfections, zero magnitude of residual stresses and 20% of the plastic bending moment putting the plate in compression.

The results of the investigation of the scale effect on the overall buckling behaviour are presented in Table 4.2. The table presents the value of each one of the variables that were varied in the investigation of the scale effect. The last column of Table 4.2 presents the peak to yield load ratio, P_c / P_y. The mean and standard deviation of P_c / P_y, for all the analysis runs for plate induced overall buckling, is found to be 0.951 and 0.002 respectively.

The load deformation response of all the models showed stable response in the post-buckling range (see Figure 4.5). The ratio of mean post-buckling capacity (at a nominal strain value of 1%) to mean peak capacity is about 0.92. The representative deformed shape history is plotted in Figure 4.9. The final deformed shape resembles closely an Euler-type column buckling shape.

4.4.2.2 Stiffener Induced Overall Buckling

All the β parameters were kept at the same values as for plate induced overall buckling mode except for the applied moment. The superimposed bending moment was 20% of the plastic bending moment and was applied to place the plate in tension. The results of the analyses are presented in Table 4.2a. The mean and standard deviation of P_c / P_y, for all the analysis runs for stiffener induced overall buckling, is found to be 0.791 and 0.002 respectively.

The load deformation response for all the models is stable in the post-buckling range. The ratio of mean post-buckling strength (at 1% nominal strain value) to mean peak strength is found to be 0.95. The representative deformed shape history plot of a stiffener induced overall buckling mode is shown in Figure 4.10. The final deformed shape closely resembles a Euler-type column buckling shape.

4.4.2.3 Plate Buckling

The input parameters selected to trigger the plate-buckling mode were: $\beta_1 = 2.0$, $\beta_2 = 0.6$, $\beta_3 = 0.5$, $\beta_4 = 0.5$ and $\beta_5 = 0.3$. A value of 2.0 was selected for β_1 because earlier research indicated that this would lead to plate buckling (Grondin *et al.*, 1999; Faulkner, 1975; Carlson, 1980). Again to avoid stiffener tripping the web and flange slenderness parameters were kept low. A bending moment equal to 20% of the plastic moment capacity of the section was applied to create compression in the plate. Initial imperfections and residual stresses were the same as for the specimen used to investigate the scale effect for overall buckling mode.

Table 4.3 summarises the scale effect investigated for plate buckling. For all the nine models investigate the mean and standard deviation was found to be 0.623 and 0.005 respectively. The load deformation response is relatively less stable as compared with the plate and stiffened induced overall buckling modes but still a gradual loss in capacity with the increase in nominal strain value is observed (see Figure 4.7). The ratio of mean post-buckling capacity (at a nominal strain value of 1%) to mean peak capacity was found to be 0.69. The representative deformed shape history plot at various stages of interest is plotted in Figure 4.11.

4.4.2.4 Stiffener Tripping

The input parameters selected to trigger the stiffener-tripping mode were: $\beta_1 = 1.25$, $\beta_2 = 0.6$, $\beta_3 = 0.75$, $\beta_4 = 1.0$ and $\beta_5 = 0.3$. The value of $\beta_1 = 1.25$ was selected from the results of the previous research that demonstrated that such a low value of β_1 would delay buckling of the plate into the yield range (Grondin *et al.*, 1999; Faulkner, 1975; Carlson, 1980). A large value of β_2 was used since the failure by stiffener tripping

was desired. Once the value of β_1 was set, the torsional slenderness of the stiffener was adjusted to obtain a large value of β_4 so that tripping failure would be the governing failure mode. The other parameters such as initial imperfections, residual stresses and applied moment ratio were the same as for the other failure modes. The moment was applied to create flexural compression in stiffener flange.

The results of the analysis are presented in Table 4.4. As shown in the table, the mean and standard deviation of P_c/P_y ratio for all the nine cases investigated is found to be 0.733 and 0.004 respectively. This indicates that the selected β parameters are scale independent for tripping failure mode. As shown in Figure 4.7, however the stiffener tripping displays a drastic loss in capacity in the post-buckling range. The ratio of mean post buckling capacity (at a nominal strain value of 1%) to mean peak capacity is about 0.33. The representative deformed shape history plot at various stages of interest is plotted in Figure 4.12.

4.6 SUMMARY AND CONCLUSIONS

Four types of parameters, namely, geometric, elastic properties, loading, and deformation, characterising the behaviour of stiffened steel plate were identified. Specific non-dimensional parameters from each one of these categories were identified from an extensive literature survey on the work done to investigate overall buckling, plate buckling and stiffener tripping of stiffened steel plates. The validity of the parameters was then established by conducting a series of analysis where the dimensions of the specimens were changed without changing the value of the dimensionless parameters.

The selected β-parameters were found to be able to predict the behaviour and strength of stiffened steel plates, in whichever mode they are buckling, for different scales of the model. These β-parameters were also found to be independent of any material strength effects.

Table 4.1

Dimensional analysis of stiffened steel plate panel

	Symbol	**L**	**M**	**T**
Geometric Variables:				
Length of stiffened plate	L_u	1	0	0
Width of stiffened plate	b_p	1	0	0
Thickness of plate	t_p	1	0	0
Stiffener web height	h_w	1	0	0
Stiffener flange thickness	t_w	1	0	0
Stiffener flange width	b_f	1	0	0
Stiffener flange thickness	t_f	1	0	0
Loading Variables:				
Peak load	P_c	1	1	-2
Applied moment	M_a	2	1	-2
Residual stress	f_r	-1	1	-2
Material Properties:				
Young's modulus of elasticity	E	-1	1	-2
Yield stress of plate material	f_{yp}	-1	1	-2
Yield stress of stiffener material	f_{ys}	-1	1	-2
Poisson's ratio	ν	0	0	0
Deformation Variables:				
Maximum plate imperfection	d_p	1	0	0
Maximum stiffener imperfection	d_s	1	0	0
Axial shortening	U_1	1	0	0

Table 4.2a
Investigation of scale effects for plate induced overall buckling
($\beta_1 = 0.7$; $\beta_2 = 0.4$; $\beta_3 = 0.5$; $\beta_4 = 0.75$; $\beta_5 = 0.3$)

Model*	b_p	L_u	h_w	b_f	f_{yp}	f_{ys}	t_p	t_w	t_f	P_c/P_y
bc_PI	393.8	559.6	116.2	127.9	400	400	25.16	12.99	11.44	0.95
b_p_PI	500.0	694.2	147.5	162.4	420	420	32.73	16.90	14.89	0.95
t_p_PI	593.2	909.7	175.0	192.7	341	341	35.00	18.07	15.92	0.95
h_w_PI	322.0	573.4	95.0	104.6	250	250	16.27	8.40	7.40	0.95
t_w_PI	254.2	452.7	75.0	82.6	250	250	12.84	6.63	5.84	0.95
b_f_PI	230.9	411.1	68.1	75.0	250	250	11.66	6.02	5.30	0.95
t_f_PI	538.8	959.3	158.9	175.0	250	250	27.21	14.05	12.37	0.95
f_{yp}_PI	445.2	684.2	132.0	145.3	350	343	26.61	13.67	12.04	0.96
f_{ys}_PI	534.6	742.2	157.7	173.7	420	420	35.00	18.07	15.92	0.95
Mean	423.6	665.2	125.0	137.7	325.7	324.9	24.7	12.8	11.2	0.951
Std. Dev.	109.7	147.5	32.4	35.7	67.3	66.6	7.4	3.8	3.4	0.002

Table 4.2b
Investigation of scale effects for stiffener induced overall buckling
($\beta_1 = 0.7$; $\beta_2 = 0.4$; $\beta_3 = 0.5$; $\beta_4 = 0.75$; $\beta_5 = 0.3$)

Model*	b_p	L_u	h_w	b_f	f_{yp}	f_{ys}	t_p	t_w	t_f	P_c/P_y
b_c_SI	393.8	559.6	116.2	127.9	400	400	25.16	12.99	11.44	0.80
b_p_SI	500.0	694.2	147.5	162.4	420	420	32.73	16.90	14.89	0.80
t_p_SI	593.2	909.7	175.0	192.7	341	341	35.00	18.07	15.92	0.79
h_w_SI	322.0	573.4	95.0	104.6	250	250	16.27	8.40	7.40	0.79
t_w_SI	254.2	452.7	75.0	82.6	250	250	12.84	6.63	5.84	0.79
b_f_SI	230.9	411.1	68.1	75.0	250	250	11.66	6.02	5.30	0.79
t_f_SI	538.8	959.3	158.9	175.0	250	250	27.21	14.05	12.37	0.79
f_{yp}_SI	445.2	684.2	132.0	145.3	350	343	26.61	13.67	12.04	0.78
f_{ys}_SI	534.6	742.2	157.7	173.7	420	420	35.00	18.07	15.92	0.80
Mean	423.6	665.2	125.0	137.7	325.7	324.9	24.7	12.8	11.2	0.791
Std. Dev.	109.7	147.5	32.4	35.7	67.3	66.6	7.4	3.8	3.4	0.002

*The model designation follows the following format: *Primary variable investigated_Failure mode considered* "bc" is used to designate the base case

Table 4.3
Investigation of scale effects for plate buckling
($\beta_1 = 2.0$; $\beta_2 = 0.6$; $\beta_3 = 0.5$; $\beta_4 = 0.5$; $\beta_5 = 0.3$)

Model *	b_p	L_u	h_w	b_f	f_{yp}	f_{ys}	t_p	t_w	t_f	P_c/P_y
b_c_PB	500.0	896.3	106.3	95.6	412	420	11.34	8.12	8.76	0.62
b_p_PB	600.0	1075.6	127.6	114.7	412	420	13.61	9.75	10.51	0.62
t_p_PB	701.8	1264.4	150.0	134.9	420	420	16.08	11.46	12.36	0.62
h_w_PB	350.9	811.8	75.0	67.4	250	250	6.20	4.42	4.77	0.64
t_w_PB	517.2	932.6	110.0	98.9	407	415	11.66	8.35	9.01	0.62
b_f_PB	392.2	830.7	83.4	75.0	291	297	7.48	5.36	5.78	0.63
t_f_PB	784.5	1406.3	166.8	150.0	412	420	17.80	12.74	13.75	0.62
f_{yp}_PB	722.6	1442.0	155.2	139.6	350	343	15.12	10.72	11.56	0.62
f_{ys}_PB	783.6	1411.7	167.5	150.6	420	420	17.95	12.79	13.80	0.62
Mean	594.8	1119.0	126.9	114.1	374.9	378.3	13.0	9.3	10.0	0.623
Std. Dev.	137.5	232.9	29.5	26.5	51.9	54.4	3.4	2.4	2.6	0.005

Table 4.4
Investigation of scale effects for stiffener tripping
($\beta_1 = 1.25$; $\beta_2 = 0.6$; $\beta_3 = 0.75$; $\beta_4 = 1.0$; $\beta_5 = 0.3$)

Model *	b_p	L_u	h_w	b_f	f_{yp}	f_{ys}	t_p	t_w	t_f	P_c/P_y
b_c_ST	500.0	1491.7	135.2	148.9	420	420	18.33	10.32	9.10	0.73
b_p_ST	600.0	1790.1	162.2	178.6	420	420	22.00	12.39	10.91	0.73
t_p_ST	479.9	1761.9	129.1	142.1	266	271	14.00	7.93	6.98	0.74
h_w_ST	369.9	1420.6	100.0	110.1	250	250	10.46	5.89	5.19	0.73
t_w_ST	557.6	1655.3	150.0	165.2	412	420	20.24	11.46	10.09	0.74
b_f_ST	319.1	1225.6	86.3	95.0	250	250	9.03	5.08	4.48	0.73
t_f_ST	251.9	967.6	68.1	75.0	250	250	7.13	4.01	3.54	0.73
f_{yp}_ST	302.0	970.0	81.2	89.5	350	357	10.11	5.72	5.04	0.74
f_{ys}_ST	314.7	963.2	85.2	93.9	403	400	11.30	6.35	5.60	0.73
Mean	410.6	1360.7	110.8	122.0	335.7	337.6	13.6	7.7	6.8	0.733
Std. Dev.	110.1	292.5	29.6	32.6	72.6	73.2	4.5	2.5	2.2	0.004

*The model designation follows the following format: *Primary variable investigated_Failure mode considered* "bc" is used to designate the base case.

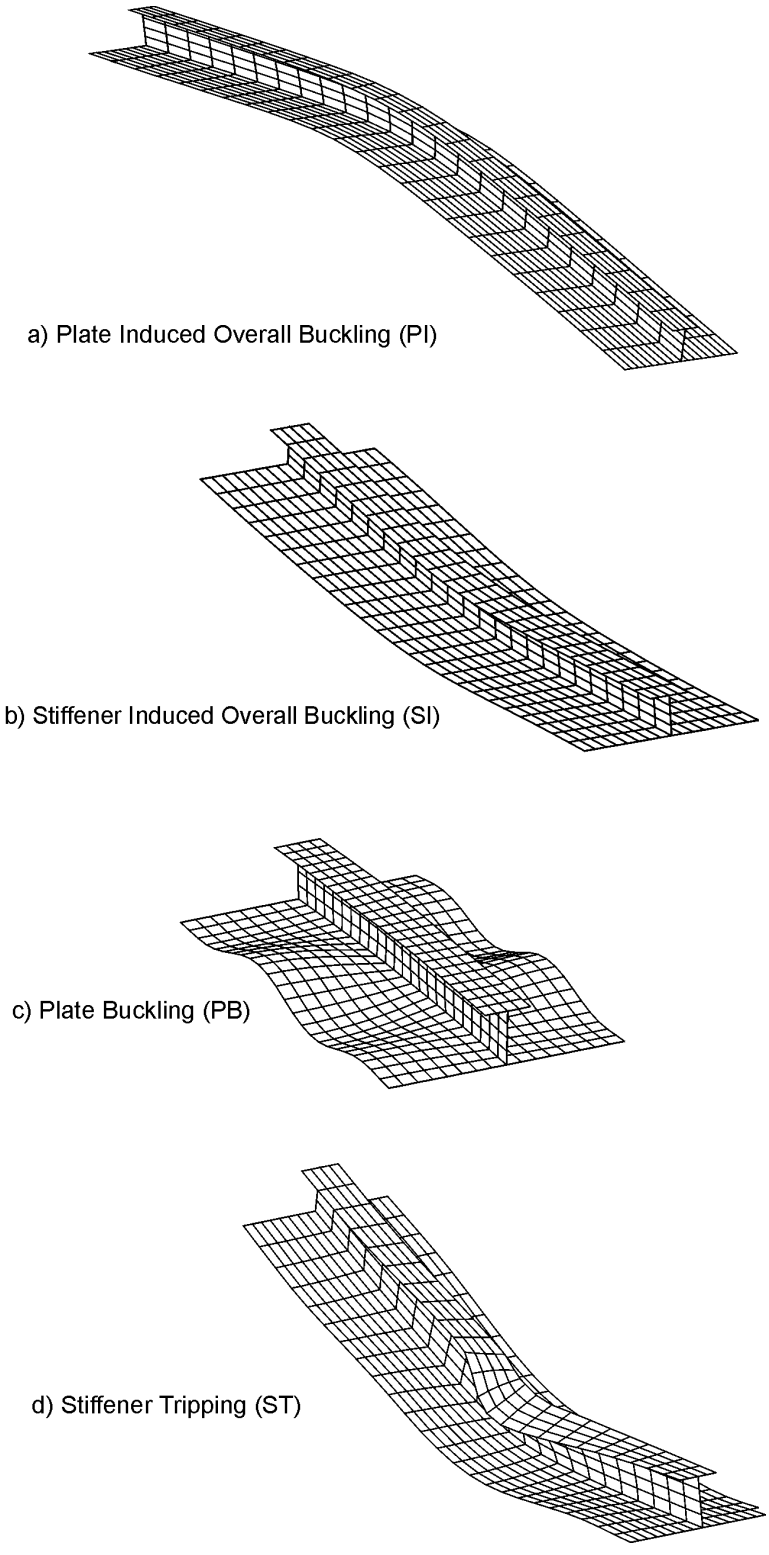

Figure 4.1 Typical buckling modes in stiffened steel plates

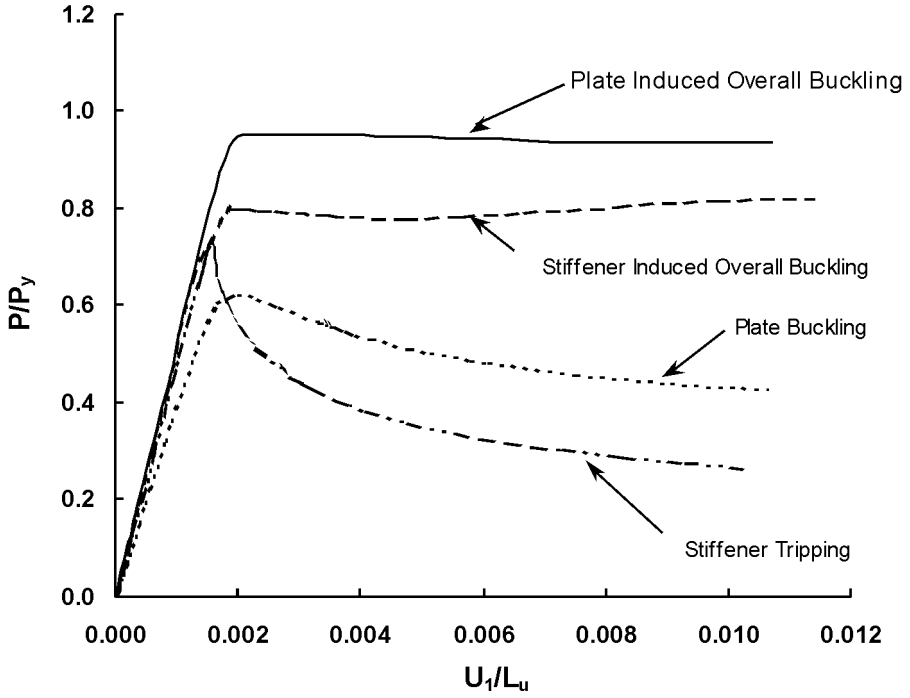

Figure 4.2 Load versus deformation responses for typical buckling modes in stiffened steel plates

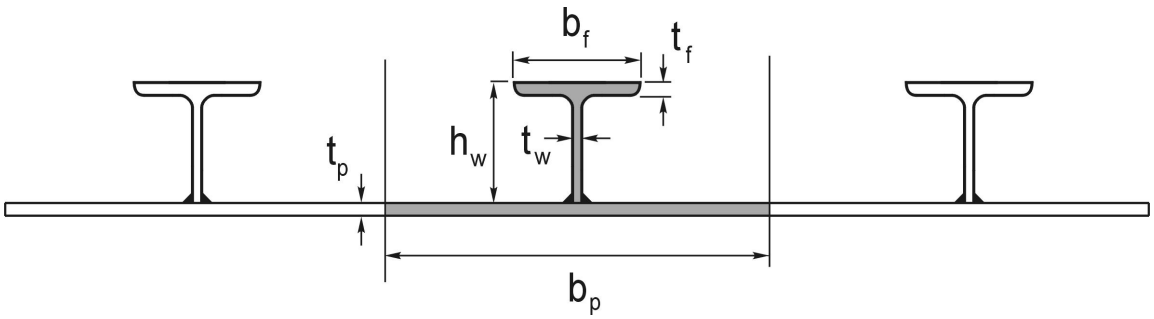

Figure 4.3 Typical stiffened steel plate panel

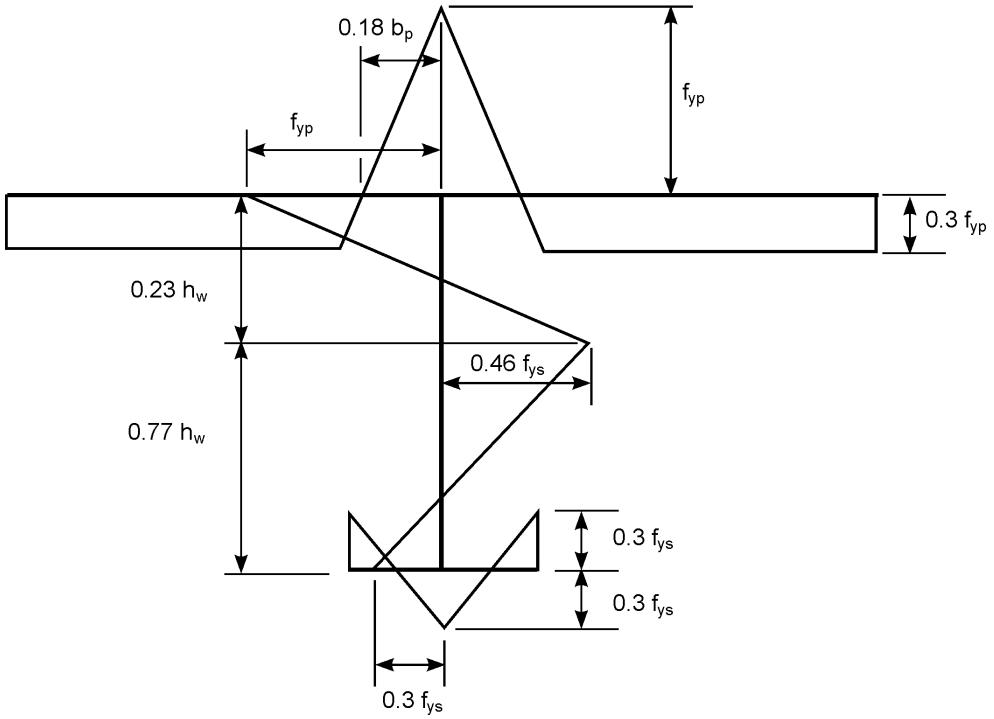

Figure 4.4 Typical residual stress pattern in stiffened plate

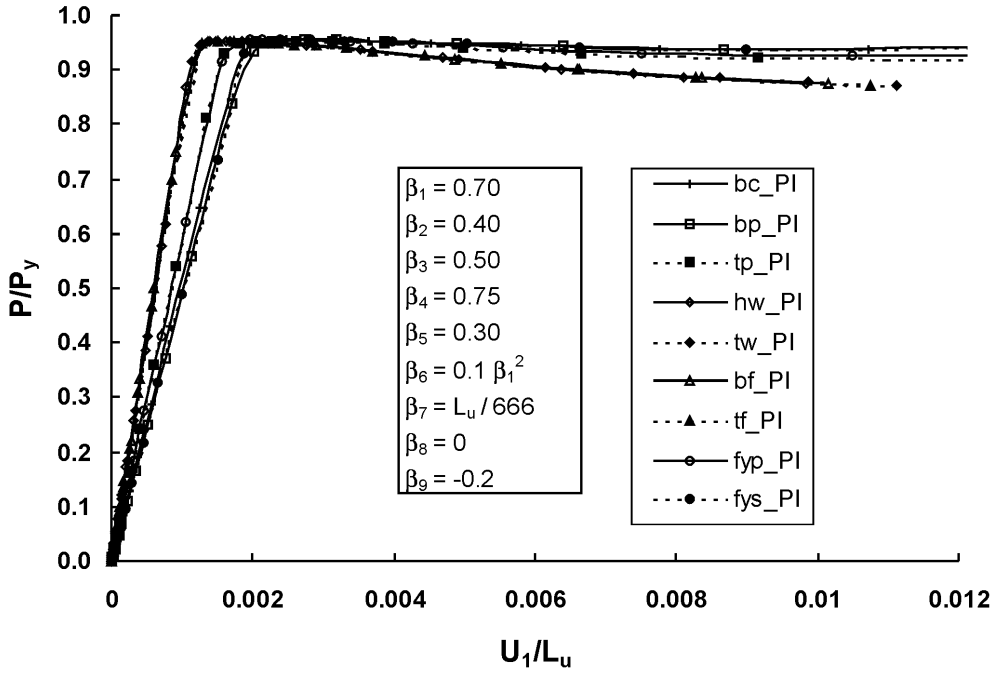

Figure 4.5 Load vs. deformation response – scale effect for plate induced overall buckling

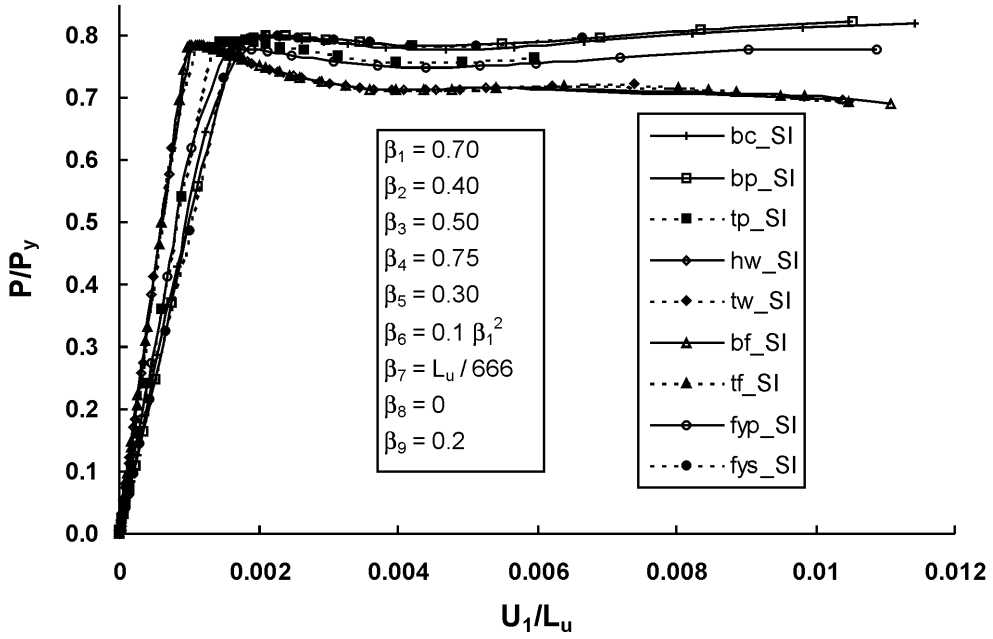

Figure 4.6 Load vs. deformation response – scale effect for stiffener induced overall buckling

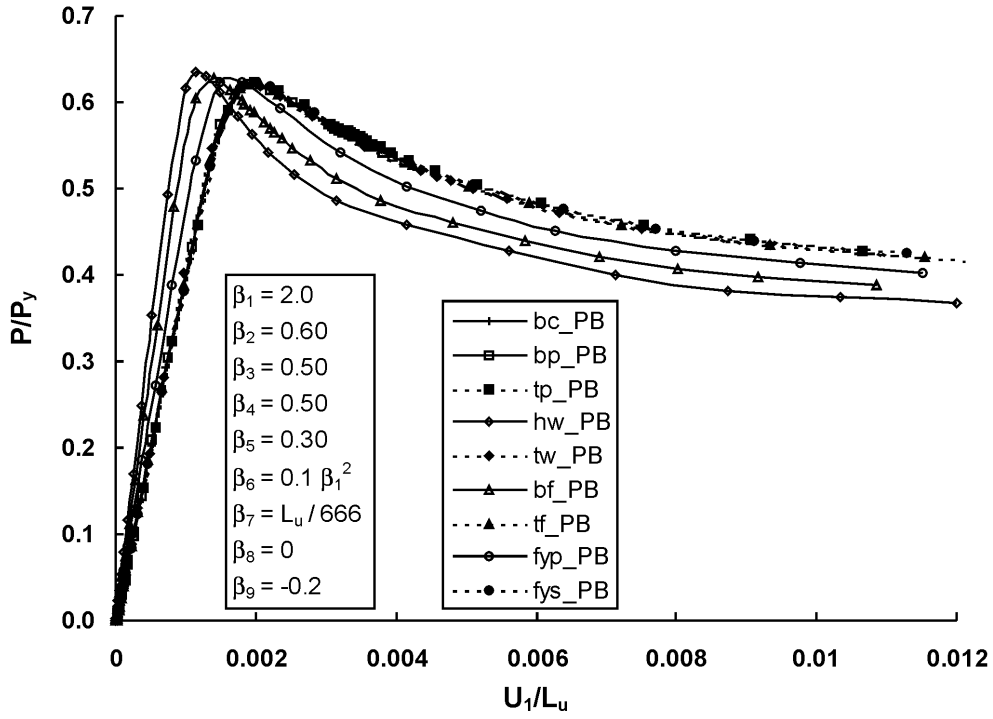

Figure 4.7 Load vs. deformation response – scale effect for plate buckling

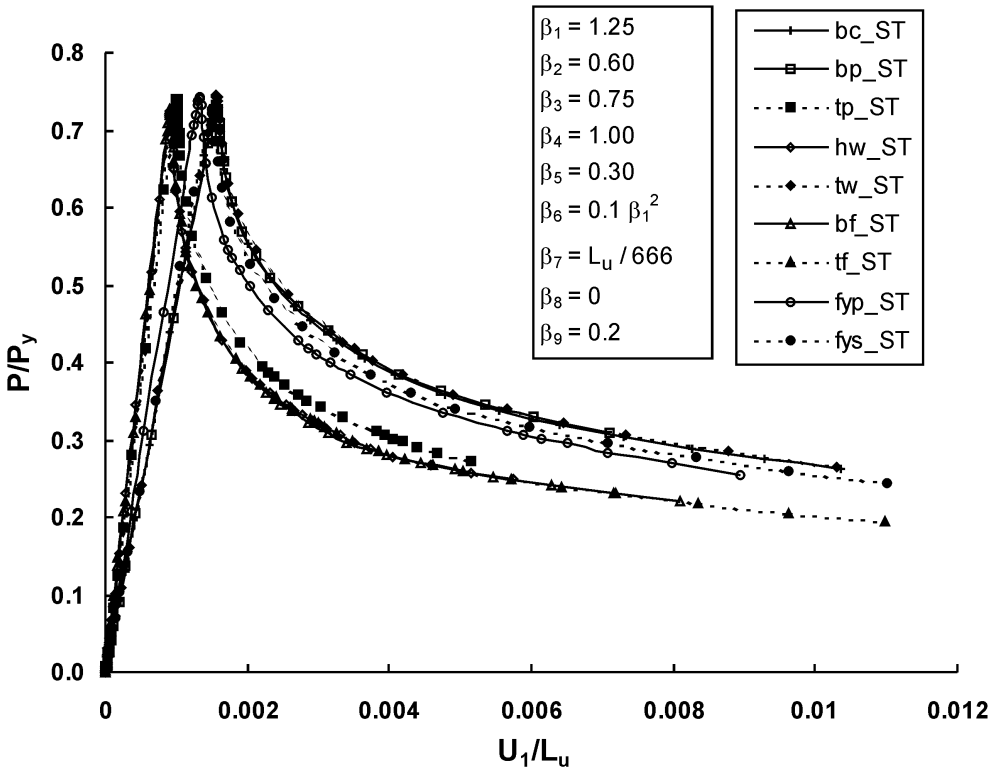

Figure 4.8 Load vs. deformation response – scale effect for stiffener tripping

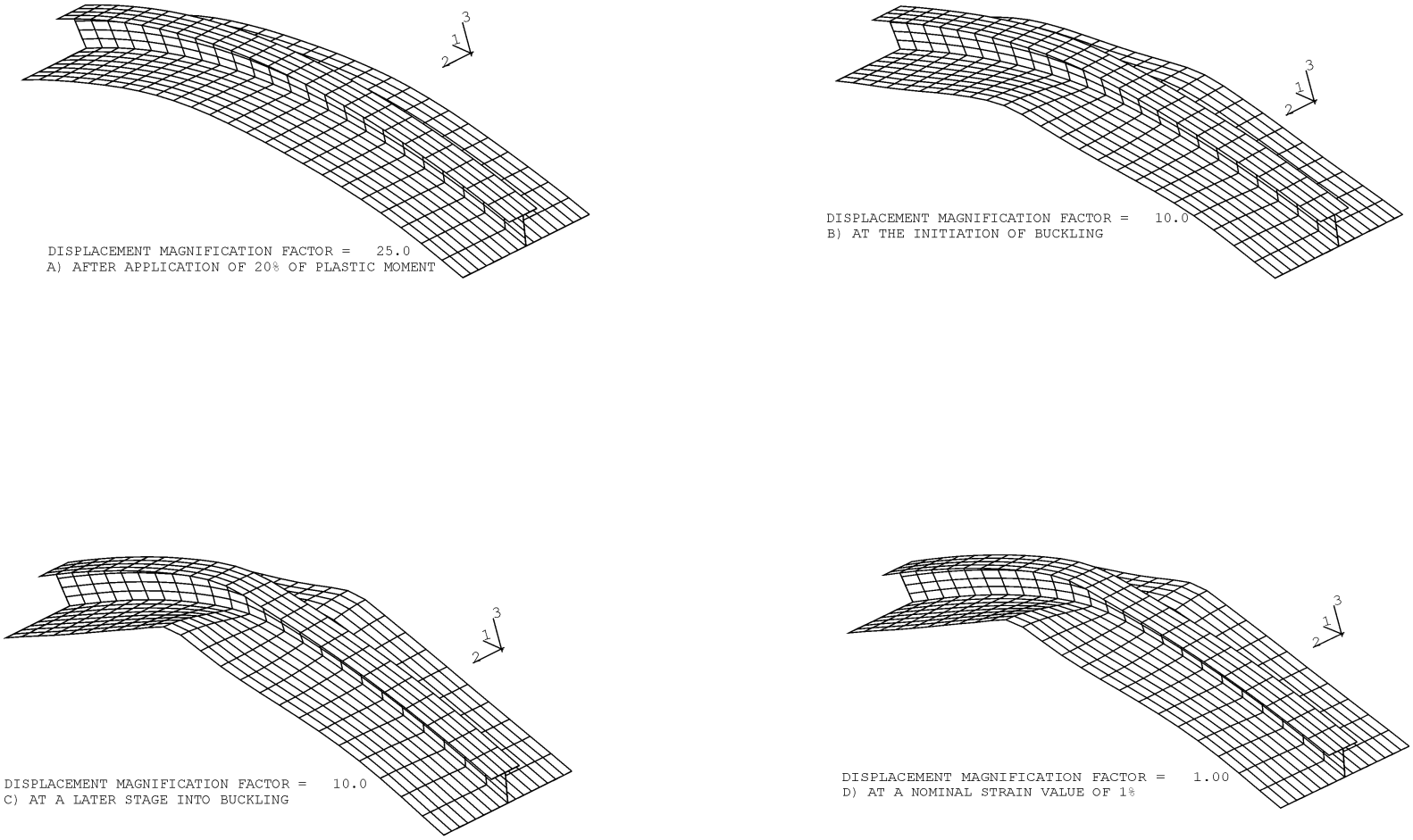

Figure 4.9 Typical deformed shape history of plate induced overall buckling mode

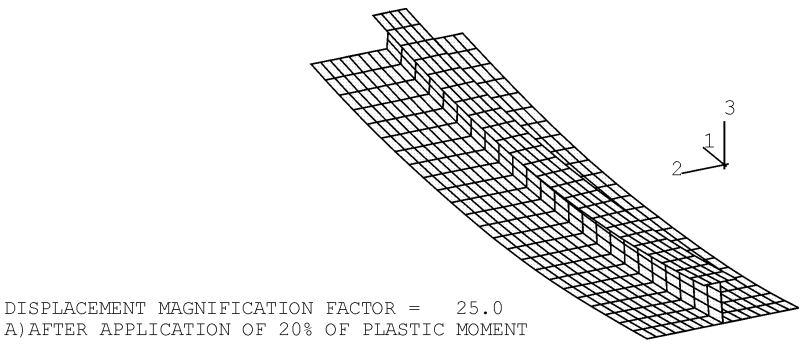

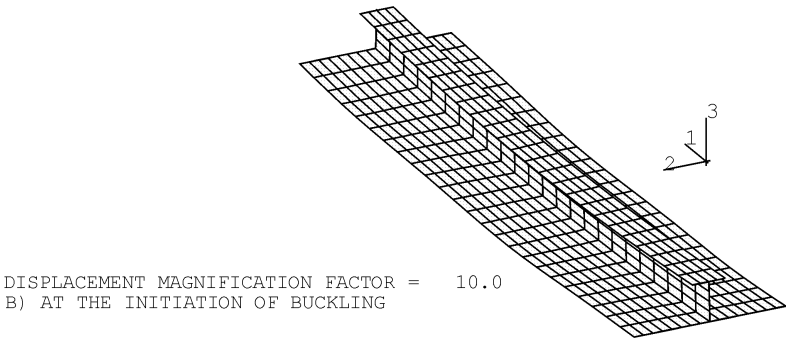

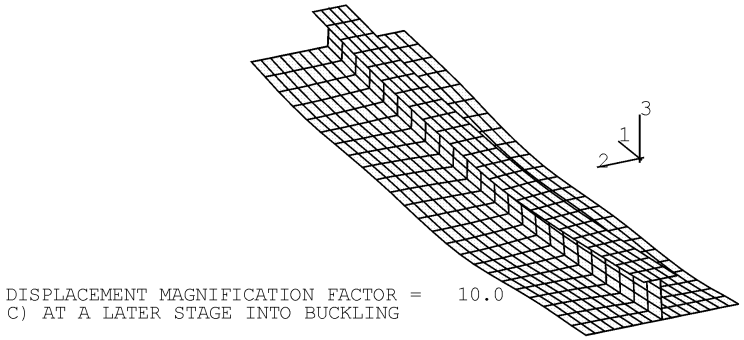

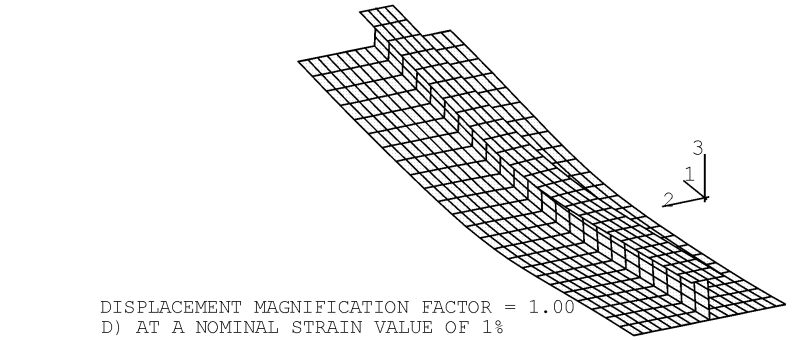

Figure 4.10 Typical deformed shape history of stiffener induced overall buckling mode

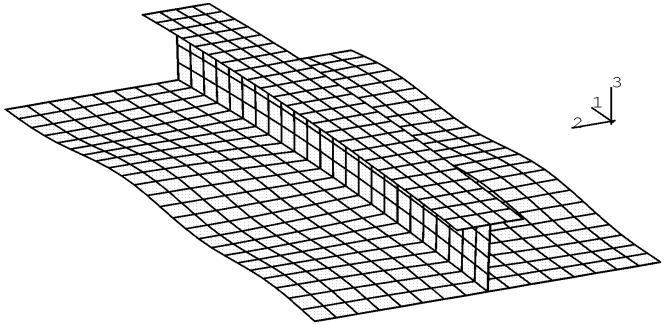

DISPLACEMENT MAGNIFICATION FACTOR = 25.0
A) AFTER APPLICATION OF 20% OF PLASTIC MOMENT

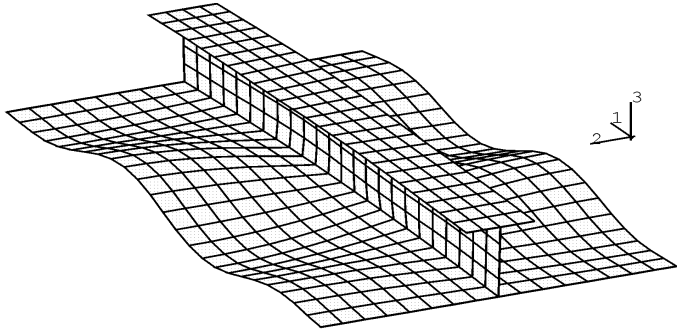

DISPLACEMENT MAGNIFICATION FACTOR = 10.0
B) AT THE INITIATION OF BUCKLING

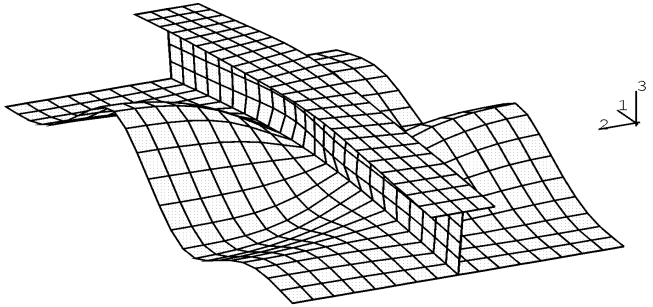

DISPLACEMENT MAGNIFICATION FACTOR = 10.0
C) AT A LATER STAGE INTO BUCKLING

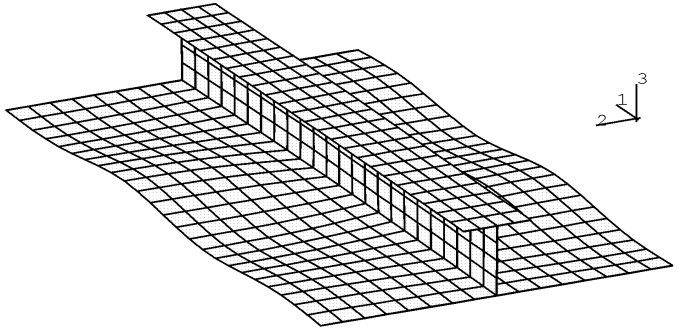

DISPLACEMENT MAGNIFICATION FACTOR = 1.00
D) AT A VALUE OF 1% NOMINAL STRAIN

Figure 4.11 Typical deformed shape history of plate buckling mode

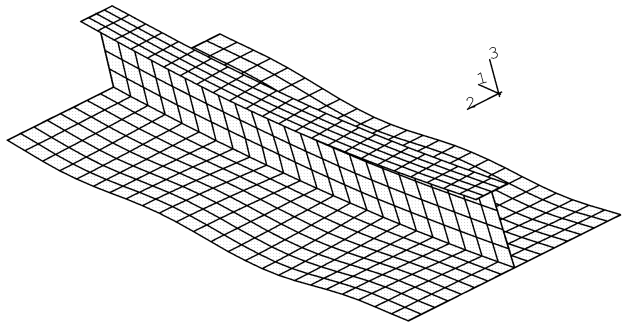

DISPLACEMENT MAGNIFICATION FACTOR = 25.0
A) AFTER APPLICATION OF 20% OF PLASTIC MOMENT

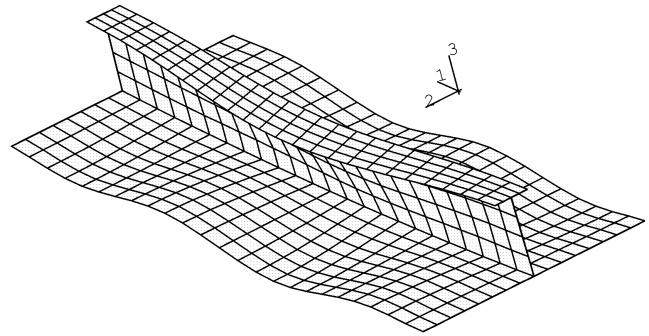

DISPLACEMENT MAGNIFICATION FACTOR = 10.0
B) AT THE INITIATION OF STIFFENER TRIPPING

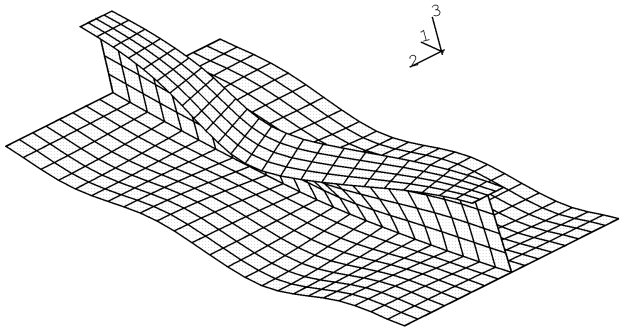

DISPLACEMENT MAGNIFICATION FACTOR = 10.0
C) AT A LATTER STAGE INTO STIFFENER TRIPPING

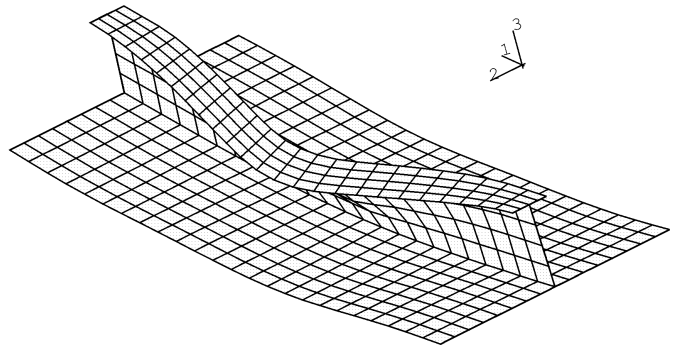

D) AT A NOMINAL STRAIN VALUE OF 1%
DISPLACEMENT MAGNIFICATION FACTOR = 1.00

Figure 4.12 Typical deformed shape history of stiffener tripping mode

CHAPTER 5

PARAMETRIC STUDY

5.1 INTRODUCTION

The parameters characterising the strength and behaviour of stiffened steel plates were established in Chapter 4 using the finite element model presented in Chapter 3. The main objective of this chapter is to carry out a detailed parametric study of the main input parameters established in Chapter 4 to find the conditions that lead to stiffener tripping. The study focuses on the behaviour in the inelastic range of material response. Since a full factorial parametric study of the nine parameters identified in Chapter 4 would result in 3^9 (19683) runs when only three values are used for each of the β parameters, it is necessary to restrict the scope to the geometric parameters β_1 through β_5. The magnitude and the distribution of the initial imperfections (β_6 and β_7) and residual stresses (β_8) in the stiffener and in the plate are maintained at the most probable values as determined from the work of previous researchers (Faulkner, 1975; Carlsen and Czujko, 1978; Smith *et al*., 1991). Only two magnitudes of β_9 (ratio of the applied moment to plastic moment capacity) are investigated, namely, 0.0 and 0.2 (20% of the plastic bending moment capacity of the stiffened plate panel). The bending moment is applied so as to increase the compressive stresses in the stiffener. The results of this parametric study will be used in Chapter 6 to evaluate current design guidelines.

5.2 PARAMETRIC MATRIX

A review of the literature was conducted to determine reasonable ranges for the parameters β_1 through β_9. The range and increments for each of the input parameters are described in the following.

5.2.1 Plate Transverse Flexural Slenderness, b_1

Test results presented by Winter (1948) indicated that panels with plate transverse flexural slenderness, β_1, less than 1.28 could reach their full yield capacity before buckling. This observation was also confirmed by Faulkner (1975), Carlson (1980) and Grondin *et al.* (1999). A lower bound value of $\beta_1 = 0.7$ was therefore arbitrarily chosen for the parametric study to ensure that the plate yielding occurs before buckling. Since a review of the literature has indicated that most of the research to date has focused on the elastic behaviour of stiffened plates, the parametric study focuses mainly on the inelastic range. The upper bound value of β_1 is taken as 2.7, which corresponds to the limit of elastic buckling of the plate proposed by Soares and Gordo (1997). An intermediate value of $\beta_1 = 2.0$ was selected for the major portion of the parametric study presented in the following. Other values of β_1 as needed were investigated to refine the boundary between various buckling modes.

5.2.2 Stiffener Web Slenderness, b_2

The upper limit of stiffener web slenderness, β_2, is set to 1.5. This corresponds to the local buckling limitation for class 3 sections (CAN/CSA-S16.1, 1994) for steel yield strength of 420 MPa. Since the shape of the stiffener considered in this study is a tee, the minimum value of β_2 investigated is based on the lowest value available for a standard rolled section. An examination of the slenderness of standard rolled sections indicates that the minimum value, assuming a material yield strength of 420 MPa, is approximately 0.6. An intermediate value of 1.05 was selected to complete the test matrix.

5.2.3 Stiffeners Flange Slenderness, b_3

An examination of the slenderness of standard rolled sections (CAN/CSA-S16.1, 1994) indicates that the maximum value of β_3 is approximately 1.125 for material yield strength of 420 MPa. At this yield strength, the minimum value of β_3 is approximately 0.50. This value is reduced further to one third of the maximum value, i.e. 0.375. An intermediate value of 0.75 was selected to complete the test matrix.

5.2.4 Ratio of Stiffener Torsional Slenderness to Plate Transverse Flexural Slenderness, b_4

Since a range of values has already been established for the plate transverse flexural slenderness, β_1, the range for the parameter β_4 can be established once the range of the torsional slenderness is selected. A conservative assumption for the lower bound can be obtained by assuming that the stiffener is acting alone. According to the work of Rondal and Maquoi (1979), the minimum slenderness ratio required for the stiffener to yield before buckling is 0.6. This results in a minimum β_4 value of 0.7. This value is further lowered to 0.5 in order to ensure yielding of the stiffener before tripping. The upper bound is selected such that the slenderness of the stiffened plate, governing the overall buckling capacity, should be less than 1.414 for a yield strength of 420 MPa. The value of 1.414 is based on Bleich's (1951) derivation for overall buckling of stiffened steel plates and accounts for residual stress effects. This limit has been used widely to account for other strength reduction factors as well (Hu, 1993). Similar upper bounds were found for extreme combinations of other geometric input parameters, i.e. $\beta_1 = 2.70$, $\beta_2 = 1.50$, $\beta_3 = 0.375$ and $\beta_5 = 0.30$. The maximum value of β_4, using the extreme combinations, was found to be 2.0. An increment of 0.5 was selected for β_4 for the analysis. (Note: These slenderness values are obtained for an assumed yield strength of 420 MPa). Other values of β_4, such as 0.75 and 1.25, were also investigated for the combined compression and bending case to refine the definition of a boundary between various buckling modes.

5.2.5 Stiffener to Plate Area Ratio, b_5

The upper bound for the stiffener to plate area ratio was selected as 0.3. A stiffener to plate area ratio less than 0.3 was found to trigger stiffener tripping instead of overall buckling if the stiffener flange was initially placed under flexural compression (Grondin *et al.* 1999). A lower bound value of 0.075 was selected for this work to study the effect of stiffener to plate area ratio on stiffener tripping. An intermediate value of 0.15 was selected to complete the parametric matrix.

5.2.6 Initial Plate Imperfections, b_6

An 'average' magnitude of plate imperfection proposed by Smith *et al.* (1991), defined in Table 2.1, was used in all models in the parametric study. This magnitude corresponds to a value of β_6 equal to $0.1\beta_1^2$. Four half-sine waves along the length and two quarter-sine waves across the width of the plate were used to represent the distribution of imperfections in the plate. This is consistent with the plate imperfection pattern proposed by Grondin *et al.* (1999).

5.2.7 Initial Stiffener Imperfections, b_7

An 'average' magnitude of stiffener imperfection (Table 2.2) was defined by Smith *et al.* (1991). This magnitude (β_7 = 0.0015) and the shape of the initial imperfection in the stiffener defined in Section 4.2.2.7 were kept constant for all models in this study.

5.2.8 Residual Stresses, b_8

A residual stress pattern as shown in Figure 4.4 with a maximum magnitude classified as "severe" according to Smith *et al.* (1991) was used for the following parametric study. This "severe" magnitude corresponds to β_8 = 0.3 (Table 2.1).

5.2.9 Applied to Plastic Moment Ratio, b_9

Two values of β_9 were used, namely, a magnitude of 0.0, representing uniaxial compression, and a magnitude of 0.2, representing the combined uniaxial compression and bending case. A value of 0.2 corresponds to a bending moment equal to 20 percent of the plastic moment capacity of the stiffened panel cross-section, applied to create compression at the extreme fibre of the stiffener flange. Grondin *et al.* (1998) have shown that small values of β_9 did not trigger tripping failure.

5.2.10 Other Parameters

The flange to web area ratio, A_f/A_w, reflects the distribution of material in the stiffener. The minimum area ratio for a standard rolled tee section was selected for the

study since this would result in the maximum area in the web for a given stiffener web slenderness ratio, thus reducing the stiffener tripping capacity.

The complete input parametric matrix, excluding a select number of cases used to refine boundaries between buckling modes, can be summarised as follows:

b_1	b_2	b_3	b_4	b_5	b_6	b_7	b_8	b_9
$\begin{bmatrix}0.70\\1.28\\2.00\\2.70\end{bmatrix}$	$-\begin{bmatrix}1.50\\1.05\\0.60\end{bmatrix}$	$-\begin{bmatrix}1.125\\0.750\\0.375\end{bmatrix}$	$-\begin{bmatrix}0.50\\1.00\\1.50\\2.00\end{bmatrix}$	$-\begin{bmatrix}0.300\\0.150\\0.075\end{bmatrix}$	$-(average)$	$-(average)$	$-(severe)$	$-\begin{bmatrix}0.0\\0.2\end{bmatrix}$

A full factorial design for the above parameters would require 864 analysis runs. To reduce this number to a more manageable size, a representative subset of the full-factorial matrix was used. A review of the literature indicated that β_4 is the main parameter controlling the stiffener tripping failure mode (Grondin *et al.*, 1999; Paik *et al.*, 1998; Rogers and Dwight, 1976). In addition, it has already been established that a variation in the plate transverse flexural slenderness, β_1, will result in a change of failure mode from plate buckling to overall buckling (Grondin *et al.*, 1999). The parameters β_1 and β_4 were, therefore, selected as the *primary parameters* and the other geometric parameters were varied in turn to study their effect. The finite element analysis was carried out with respect to the primary variables β_1 and β_4, and a secondary parameter, which was varied for a particular series of runs.

Tables 5.1 through 5.10 define the geometric non-dimensional parameters, i.e. β_1 through β_5, used to describe the models in the parametric study. The tables also list the strength ratio, P_c / P_y, as an output parameter. The failure mode, determined from the deformed shape and the load-deformation plots for each analysis run, are also reported in these tables. Any other variable used is defined when first introduced.

The main objective of the following investigation is to determine the effect of various geometric parameters on the behaviour and strength of stiffened steel plates. Two broad categories of graphs are, therefore, produced: one to illustrate the effect of the

parameter investigated on behaviour and another to illustrate the effect of the parameter on the plate strength.

5.3 STIFFENED STEEL PLATES UNDER UNIAXIAL COMPRESSION

Three magnitudes of β_5, namely, 0.30, 0.15 and 0.075, were analysed for all the combinations of β_1 and β_4 presented in the parametric matrix for the least stable geometric configuration of stiffener cross-section, i.e. β_2 = 1.50. The stiffener flange slenderness ratio, β_3, was kept at 0.375 to prevent local buckling in the stiffener flange.

The results and corresponding failure modes for the uniaxial compression cases are reported in Tables 5.1 through 5.3. The failure modes observed were either plate buckling or plate induced overall buckling, with few exceptions in which dual failure modes were detected. These dual failure modes are characterised by plate induced overall buckling mode following plate buckling and resulting in a sharp decrease in the load carrying capacity as illustrated in Figure 5.15. The axial deformation at onset of the dual failure mode, designated as U_{dm} and non-dimensionalised with respect to the axial deformation at the peak load, U_c, is also reported in Tables 5.1 through 5.3.

5.3.1 Effect of Plate Transverse Flexural Slenderness, b_1

In this section the effect of plate transverse flexural slenderness, β_1, for four magnitudes of β_1 (0.70, 1.28, 2.00 and 2.70) combined with four different magnitudes of β_4 and three magnitudes of β_5 are investigated. To determine the effect of β_1 on the load-deformation behaviour, the non-dimensional load-deformation plots, for extreme values of β_4 (0.5 and 2.0), are plotted for all the values of β_1 and β_5 in Figures 5.1 through 5.3. These plots are separated on the basis of stiffener to plate area ratio, β_5.

For torsionally stiff plates (small β_4) the pre-buckling response is identical for all values of β_1 at any given value of β_5. However, as β_1 increases, the ultimate strength decreases and the failure mode changes from plate induced overall buckling to plate buckling. The post-buckling response becomes increasingly unstable as β_1 increases.

For torsionally flexible plates (large β_4) these plots show almost the same pre-buckling response for stocky plates (β_1 = 0.7 and 1.28) and all values of β_5 and a stable post-buckling response typical of plate induced overall buckling mode. In contrast, the pre-buckling response of relatively slender plates (β_1 = 2.0 and 2.7) shows a greater flexibility for larger values of β_1. The load carrying capacity reduces as β_1 increases, but the post-buckling response remains relatively stable. The different pre-buckling response is due to the sensitivity of plate buckling failure mode to the magnitude of initial imperfections in the plate (Smith *et al.*, 1991). The initial plate imperfections are a function of β_1, thus affecting the pre-buckling response for plates with large β_1 values.

Some models show an abrupt drop in load carrying capacity in the post-buckling range (see for example β_1= 1.28, β_4 = 2.0 in Figure 5.2). This type of load-deformation behaviour is not typical of any of the failure modes identified in Figure 4.2. This load-deformation behaviour is attributed to a dual failure mode discussed later in this chapter.

A summary of the effect of β_1 in terms of the peak strength P_c / P_y is presented in Figure 5.4. The figure shows a decrease in strength with an increase in the value of β_1. The strength is affected only by β_1 when the failure mode is either overall buckling or plate buckling. For example, for β_1 = 0.7, stiffened plates with extreme values of β_4, i.e. 0.5 and 2.0, have the same peak strength ratio because they are exhibiting the typical overall buckling behaviour (Figure 5.1). This behaviour was also observed by previous researchers (Faulkner, 1975; Carlsen, 1980; Smith *et al.*, 1991; Grondin *et al.*, 1999). The peak capacity of stiffened plates failing by failure modes other than plate buckling or overall buckling seems to be affected by other parameters as well. For example, for β_1 = 2.70, stiffened plates with different values of β_4 (0.5 and 2.0) have different peak strength ratios (see Figure 5.4). For a plate with β_1 = 2.70 and β_4 = 2.0 the stiffened panel is exhibiting different load-deformation behaviour than the typical overall buckling or plate buckling failure mode (Figure 5.1). This failure mode is discussed in a later section.

5.3.2 Effect of Ratio of Stiffener Torsional Slenderness to Plate Transverse Flexural Slenderness, β_4

To determine the effect of β_4 on the load-deformation behaviour of stiffened steel plates, the non-dimensional load-deformation plots, for extreme values of β_1 (0.7 and 2.7), are plotted for all the values of β_4 in Figure 5.5 through Figure 5.7. These plots are separated on the basis of stiffener to plate area ratio, β_5.

The plots show a clear separation of the response with respect to β_1. Models with stocky plates (small β_1) have a nearly constant strength ratio and a nearly constant pre-buckling response regardless of the value of β_4. These models also exhibit a stable post-buckling response except for very small values of β_1 where the so-called dual failure mode is observed for torsionally flexible models (large β_4).

Models with slender plates (large β_1) show a marked decrease in strength that becomes more evident as β_4 increases. The pre-buckling response also changes somewhat, but the post-buckling response becomes increasingly unstable as β_1 increases.

A summary of the effect of β_4 on the peak strength (P_c / P_y) is presented in Figure 5.8. The strength ratio (P_c/P_y) remains constant for stocky plates (β_1 = 0.7), whereas for relatively slender plates (β_1 = 2.7) there is a drop in peak strength with an increase in β_4 value (Figure 5.8). The value of β_4 was varied by changing the length of the stiffened plate panel, resulting in a change of plate aspect ratio. Figure 5.8, therefore, shows that the strength of a stiffened plate failing by plate buckling changes with a change in plate aspect ratio. This observation seems to be in contradiction with the observations made by earlier researchers (Carlsen, 1980, Grondin *et al*., 1999), i.e. plate buckling strength remains unaffected by the change in plate aspect ratio. The results can be reconciled if one considers only the plate buckling failure mode, as determined from the behaviour plots (Figure 5.5 through Figure 5.7). The change in plate buckling strength with a change in plate aspect ratio can be attributed to dual failure mode. The stiffened

plates showing a decrease in strength with an increase in plate aspect ratios are exhibiting the dual failure mode.

5.3.3 Effect of Stiffener to Plate Area Ratio, b_5

Three values of β_5 were investigated, namely, 0.30, 0.15, and 0.075. Non-dimensional load-deformation plots for values of β_1 of 0.7 and 2.7 are presented in Figures 5.9 to 5.11 for all the values of β_5. Figures 5.9 to 5.11 are applicable to values of β_4 from 0.50 to 2.00, respectively. Similar to the response of the model to β_4, the response here is once more strongly dependent on β_1. Stocky plates (β_1 of 0.7) exhibit identical response in the pre-buckling range, nearly identical strength ratios and a similar stable post-buckling response. Only the models with (β_5, β_4) combination of (0.075, 1.50), (0.075, 2.00) and (0.15, 2.00) show a distinct discrepancy from the other plates with β_1 of 0.7. These plates were found to fail by overall buckling subsequent to plate buckling (dual failure mode). All other models showed either only plate buckling failure or plate induced overall buckling with a peak load within 5% of the yield load.

For stiffened steel plates with a large value of β_1 (2.7) the strength is markedly reduced and dependent on β_5. The pre- and post-buckling ranges are also dependent on β_5, becoming increasingly unstable as β_5 decreases. All the plots that show a stable post-buckling range are typical of plate buckling, whereas the plots showing a sharp drop of capacity in the post-peak range are representative of plate buckling followed by overall buckling (i.e. dual failure mode). The peak load for the models with $\beta_1 = 2.7$ ranged from a high of 54% of the yield load and a low of 12% of the yield load.

A summary of the effect of β_5 in terms of peak strength (P_c / P_y) is presented in Figure 5.13. It is apparent from the figure that the effect of β_5 is insignificant for stocky plates ($\beta_1 = 0.7$), whereas for slender plates ($\beta_1 = 2.7$) the peak strength decreases with a decrease in β_5 value. This observation is not in agreement with observations made by earlier researchers (Carlsen, 1980, Grondin *et al.*, 1999) who concluded that the plate buckling strength remains unaffected by the variation of stiffener to plate area ratio. The discrepancy between these findings and the findings of the other researchers is once again

attributed to the dual failure mode, which was not observed in the work of the other researchers, but was observed in the work presented here.

5.3.4 Failure Modes under Uniaxial Compression

With few exceptions, two failure modes were observed for all models subjected to uniaxial compression, namely, plate induced overall buckling and plate buckling. A boundary between plate induced overall buckling and plate buckling was found by plotting all the analysis points in a β_1 versus β_4 plot (Figure 5.14-a) for a β_5 value of 0.3. The plot shows that the failure mode is strongly dependent on β_1 and less so on β_4, although an increase in β_4 slightly shifts the mode from plate buckling to overall buckling. This behaviour can be explained if one considers the shift of the centroid of the cross-section resulting from a reduction of the effective width of the plate. This shift in centroid towards the stiffener results in an eccentricity causing the stiffened panel to bend under the action of the eccentric load with the plate side under flexural compression (plate induced overall buckling). The effect of this eccentricity is more severe for a longer panel (β_4= 2.0), causing a larger P-δ moment, than for a shorter panel (β_4= 0.5).

Figures 5.14 a, b, c show that the failure mode shifts from plate buckling to dual failure mode with a decrease in stiffener to plate area ratio. The shift in failure mode from plate buckling to dual failure mode is discussed in the following section.

5.3.5 Dual Failure Mode

The term "dual failure mode" is used in this work to define a mode in which failure is initiated with a plate buckling mode that switches to a plate induced overall buckling mode taking over the plate buckling mode in the post-buckling range. Both the plate induced overall buckling and plate buckling failure modes are considered to be stable failure modes (Murray, 1973; Carlsen, 1980; Smith et al., 1991, Grondin et al., 1999). The dual failure mode is a combination of plate buckling and plate induced overall buckling (Figure 5.15) and shows an abrupt loss in load carrying capacity.

When a plate buckles, the stresses across the plate width are not uniform. In simplified idealisations this effect is accounted for by using the effective width concept (Galambos, 1998). Plate buckling causes a reduction in the effective plate width, which in turn causes a shift of the cross-section centroid towards the flange of the stiffener. This results in an effective axial load eccentricity and produces a couple that places the plate under increasing compressive stresses thus aiding the stiffened plate to undergo deformation in the manner of plate induced overall buckling mode.

The axial shortening at which the mode of failure changes from plate buckling to a dual failure mode is denoted U_{dm} (Figure 5.15) and is non-dimensionalised with respect to the deformation at the peak load, U_c, and reported in the results reported in Tables 5.1 to 5.3. The most critical condition for dual failure mode is the one where overall buckling overtakes plate buckling at, or immediately after, attaining the peak load, i.e. $U_{dm}/U_c = 1.0$ (Figure 5.17).

A typical load versus deformation response (Figure 5.15) for dual failure mode can be divided into four segments: an initial pre-buckling segment (OA), a first stable post-buckling segment (AB), an unstable post-buckling segment (BC) and a stable second post-buckling segment (CD). Letters A, B, C and D in Figure 5.15 denote the end points of these segments. The unstable post-buckling segment corresponds to onset of plate induced overall buckling, which followed plate buckling. The peak load corresponds to the plate buckling load. Note also that the dual failure mode is also characterised by a stable post-buckling phase at a load level significantly lower than the plate post-buckling stage.

Figure 5.16 shows longitudinal normal stress contour plots in a stiffened plate at various stages of loading. Figure 5.16(a) shows the stress contour plot on the deformed shape at the peak load (point A in Figure 5.15), corresponding to onset of plate buckling. At this point the compressive stresses in the stiffener are small. As deformations increase in the post-buckling range, the stresses in the stiffener have reversed as depicted in Figure 5.16 (b). This stage is designated as point B in Figure 5.15, corresponding to onset of plate induced overall buckling. Figure 5.16 (c) shows the formation of a plastic hinge at mid length and corresponds to point C in Figure 5.15. The stable range following the

second buckling is characterised by the rotation of the plastic hinge. The stress contour plot and deformed shape of the plate at point D in Figure 5.15 is depicted in Figure 5.16 (d).

Higher plate slenderness results in a larger reduction of the effective width of the buckled plate. Figures 5.14 (a), (b) and (c) clearly show that the dual failure mode is associated with higher values of β_1. Figures 5.14 (a), (b) and (c) indicate also a possible dependence on β_4. This could result from the fact that β_4 is increased by increasing the length of the stiffened plate panel, thus making the panel more susceptible to overall buckling (which is triggered by plate buckling and the eccentricity of the load created by this eccentricity). A reduction in β_5 usually results in a greater dominance of the plate behaviour and a larger shift of the cross section centroid when plate buckling takes place.

In order to investigate whether a dual failure mode could be triggered as a result of an unloading cycle, a few analyses were performed where the stiffened plate was unloaded after the peak load was reached and the plate was reloaded well into the post-buckling range. Figure 5.17 shows numerical simulations of this scenario. The load versus deformation response of monotonic case and cyclic loading case are almost identical. An unloading cycle does not seem to trigger the dual failure mode.

5.4 STIFFENED STEEL PLATES UNDER COMBINED COMPRESSION AND BENDING, b_9=0.2

For all the cases investigated under uniaxial compression, stiffener tripping was not observed as a failure mode, even under the most unstable stiffener configurations. In an attempt to trigger stiffener tripping, combined bending and compression is, therefore, investigated. A bending moment equal to 20% of the plastic bending moment capacity of the stiffened plate (β_9=0.2) was applied to place the stiffener flange under flexural compression. This was followed by the gradual application of axial compression up to a nominal axial strain of 0.01. The results for the combined bending and compression cases are tabulated in Tables 5.4 through 5.10 with respect to the set of non-dimensional geometric parameter values.

5.4.1 Effect of Stiffener Flange Slenderness, b_3

The effect of stiffener flange slenderness, β_3, on the stiffener tripping failure mode was is compared for two different ranges of plate capacity, namely, plates with a peak capacity of about 80% of the yield strength, and plates with a capacity of only about 30% of the yield capacity. Higher plate capacities were obtained with low values of β_1 and β_4 (0.70 and 0.50, respectively). At 80% of yield, part of the cross-section had yielded before the peak capacity was reached. Figure 5.18 shows that the peak capacity is not affected by the value of β_3. For high stiffener flange slenderness (β_3 = 1.125) the post-buckling behaviour is not stable, showing a sudden drop in post-buckling capacity of close to 40%. As the stiffener flange slenderness decreases, the post-buckling behaviour becomes stable as illustrated by the response for β_3 = 0.375 in Figure 5.18. The effect of stiffener flange slenderness on the post-buckling behaviour of stiffened plates in which tripping initiates in elastic range is insignificant, as illustrated in Figure 5.19.

The effect of stiffener flange slenderness, β_3, on the plate buckling failure mode is also compared for two different ranges of plate capacity, namely, plates with a peak capacity of about 70% of the yield strength, and plates with a capacity of about 60% of the yield capacity. The results are presented in Figures 5.20 and 5.21. Again, higher plate capacities were obtained with low values of β_1 and β_4. Figure 5.20 shows an identical load versus deformation behaviour for the full range of β_3 investigated. Figure 5.21, which shows the models with a slightly lower capacity than those in Figure 5.20, shows little effect of β_3 on the stiffened plate behaviour both in the pre- and post-buckling ranges.

A summary of the effect of β_3 in terms of the peak to yield strength ratio, P_c/P_y, is presented in Figure 5.22. The figure confirms what has been observed in the previous figures, namely, that the peak capacity and post-buckling strength of stiffened steel plates is not affected by the stiffener flange slenderness, β_3.

5.4.2 Effect of Stiffener Web Slenderness, b_2

The effect of β_2 on the behaviour of stiffened steel plates under combined compression and bending is compared in two ranges of plate capacity, namely, plates with a peak capacity of about 80% of the yield strength, and plates with a capacity of only about 30% of the yield capacity. At a capacity of 80% of yield, part of the cross-section had yielded before the peak capacity was reached. Figure 5.23 shows the load-deformation response of stiffened plates for values of β_2 varying from 0.6 to 1.5. Although the pre-buckling range and the peak load are not significantly affected by a change in β_2, the post-buckling behaviour is affected by the change in β_2. The stiffened plates with lower values of β_2 show a more stable post-buckling behaviour, even though stiffener tripping is the mode of failure for all three cases shown in Figure 5.23. A similar pattern is observed for stiffened plates in which tripping initiate in the elastic range ($P_c / P_y = 0.3$) (Figure 5.24).

The effect of stiffener web slenderness, β_2, on the plate buckling failure mode was also investigated for two different levels of plate capacity, namely, plates with a peak capacity of about 70% of the yield strength, and plates with a peak capacity of about 60% of the yield capacity. The results are presented in Figures 5.25 and 5.26. It is observed once again that higher plate capacities are obtained for low values of β_1 and β_4. Figure 5.25 shows an identical load versus deformation behaviour for the full range of β_2 investigated. Figure 5.26, which shows the models with a slightly lower capacity than those in Figure 5.25, shows little effect of β_2 on stiffened plate behaviour.

A summary of the effect of β_2 in terms of the peak strength ratio, P_c/P_y, is presented in Figure 5.27. The figure shows readily that the capacity of stiffened steel plates is not affected by the stiffener web slenderness, β_2.

5.4.3 Effect of Stiffener to Plate Area Ratio, b_5

The effect of β_5 on the behaviour of stiffened steel plates under combined compression and bending is compared in two ranges of plate capacity, namely, plates with a peak capacity of about 80% of the yield strength, and plates with a capacity of

only about 30% of the yield capacity. Figure 5.28 shows the load-deformation response of stiffened plates failing by inelastic stiffener tripping for values of β_5 varying from 0.30 to 0.15. The pre-buckling range, the peak load as well as the post-buckling behaviour are not affected significantly by a change in β_5 for inelastic stiffener tripping failure mode. Figure 5.29 shows the load-deformation response of stiffened plates failing by elastic stiffener tripping for values of β_5 varying from 0.30 to 0.075. The peak load and the post-buckling response are affected by a change in β_5 for elastic stiffener tripping failure. A reduction in capacity of approximately 56 percent is observed as the value of β_5 decreased from 0.3 to 0.075.

The effect of stiffener to plate area ratio, β_5, on the plate buckling failure mode was also investigated for two different ranges of plate capacity, namely, plates with β_1 and β_4 of 2.0 and 0.5, respectively, resulting is a peak strength variation from 0.60 to 0.68 of the yield strength, and plates with β_1 and β_4 of 2.7 and 1.0, respectively, resulting is a peak strength variation from 0.34 to 0.57. The results are presented in Figures 5.30 and 5.31. Higher plate capacities were obtained for low values of β_1 and β_4. Figure 5.30 shows similar load versus deformation behaviour for the full range of β_5 investigated, but with a tendency for the peak load to decrease with a decreases value of β_5. Figure 5.31, shows that both the peak load as well as post-buckling capacity of plates have decreased very significantly with the decrease in stiffener to plate area ratio. The decrease in peak load as well as post-buckling response can be attributed to dual failure mode (section 5.3.5). The plate with the largest capacity (β_5 = 0.30) failed by plate buckling, whereas the two other plates (β_5 = 0.15, 0.075) failed in a dual buckling mode, with the lowest capacity plate (β_5 = 0.075) showing the overall buckling at an earlier stage than the plate of intermediate capacity (β_5 = 0.15).

A summary of the effect of β_5 in terms of the peak strength ratio, P_c/P_y, is presented in Figure 5.32. The figure shows that the capacity of stiffened steel plates is not affected by the stiffener to plate area ratio, β_5, for stocky plate with stiff stiffeners. A decrease in strength with a decrease in β_5 is observed for slender plates stiffened with

flexible stiffeners. It can be deduced that slender plates stiffened with flexible stiffeners are susceptible to the value of β_5.

5.4.4 Effect of Plate Transverse Flexural Slenderness, b_1

The effect of β_1 on the stiffener tripping failure mode was investigated for two different ranges of plate capacity, namely, inelastic and elastic range. Higher plate capacities were obtained for low values of β_1 and β_4. In the inelastic range, part of the cross-section had yielded before the peak capacity (approximately 80 percent of the yield capacity) was reached. The data plotted in Figure 5.33 are summarised in Table 5.7. The figure shows that for a moderate value of β_1 (1.46), the post-buckling behaviour is relatively less stable than for a low value of β_1 (0.7). As β_1 decreases, the post-buckling behaviour becomes stable as illustrated by the upper curve in Figure 5.33. Figure 5.34 indicates a similar effect, i.e. drop in post-buckling strength with an increase β_1, for plates failing by elastic stiffener tripping. As opposed to the plates that failed by inelastic stiffener tripping, the plates presented in Figure 5.34 indicate a significant decrease in peak load with an increase in β_1. The data presented in Figure 5.34 are also summarised in Table 5.7.

The effect of β_1 on the plate buckling failure mode was investigated for two different magnitudes of β_4 values, namely, for β_4 = 0.5 and 1.0. The results are presented in Figures 5.35 and 5.36, respectively. Higher plate capacities were obtained for low values of β_1. A drop in both the peak load and post-buckling response is observed for an increase in β_1. A comparison of Figure 5.35 with Figure 5.36 shows that the effect of β_4 is minimal on the plate buckling failure mode.

A summary of the effect of β_1 in terms of the peak strength ratio, P_c/P_y, is presented in Figure 5.37. The figure shows clearly that the plate buckling capacity and stiffener tripping capacity of stiffened steel plates are affected by β_1. The peak strength ratio decreases with an increase in β_1. The line that marks the boundary between stiffener tripping and plate buckling is not a vertical line, which indicates that the failure mode is not governed strictly by the plate slenderness parameter β_1.

5.4.5 Effect of Ratio of Stiffener Torsional Slenderness to Plate Transverse Flexural Slenderness, β_4

The effect of β_4 on stiffener tripping was also investigated for the inelastic and elastic ranges of material response. Higher plate capacities were once again obtained using low values of β_1 and β_4. In the inelastic range, part of the cross-section had yielded before the peak capacity was reached. Figure 5.38 shows that as β_4 increases stiffened plates become less stable in the post-buckling range (a drop of capacity of close to 55 percent is observed over a nominal strain of 0.01 for a stiffened plate with $\beta_4 = 1.50$). A drop in post-buckling capacity was also observed to take place with an increase in β_4 for plates failing by elastic stiffener tripping failure mode (Figure 5.39). A significant loss of peak capacity was also observed in the elastic range.

The effect of β_4 on the plate buckling failure mode was investigated for two different magnitudes of β_1 values, namely, for plates with β_1 of 2.0 and 2.25. The results are presented in Figures 5.40 and 5.41. Both figures indicate that the peak load is not significantly affected by a change in β_4 values. The post-buckling capacity, however, decreases with an increase in β_4 value.

A summary of the effect of β_4 in terms of the peak strength ratio, P_c/P_y, is presented in Figure 5.42. The figure shows that β_4 is only affecting the capacity of stiffened steel plates failing by stiffener tripping failure mode. The peak strength ratio decreased with an increase in β_4. No effect is found on the peak strength ratio for plates failing by plate buckling failure mode.

5.4.6 Failure Modes under Combined Compression and Bending

As was observed in the case of stiffened plates under uniaxial compression, the effect of β_1 and β_4 is once again significant. The effect of these two parameters on the failure mode is illustrated in Figure 5.43. The figure is plotted for all the values of β_2, β_3 and β_5 included in the parametric study. The figure shows that the failure mode is not affected with the change in β_2, β_3 and β_5 values. Consequently, each points represent more than one specimen. Mainly two different failure modes were observed for all

models subjected to combined compression and bending, namely, plate buckling and stiffener tripping. Only two cases showed a dual failure mode, namely, the cases with β_5 of 0.150 and 0.075 as identified in Figure 5.43. Stiffener tripping is observed for most of the combinations of β_1 and β_4 for all the values of β_2, β_3 and β_5, investigated in this study. Plate buckling was limited to high values of β_1 and low values of β_4, namely in the range of $0.5 \leq \beta_4 \leq 1$, and for $\beta_1 \geq 2.0$.

A boundary between stiffener tripping and plate buckling was found by refining the grid between already available bounds. The refinement around the apparent boundary seen in Figure 5.43 was performed for a β_5 value of 0.3. The results of this refinement are illustrated in Figure 5.44. An approximate description of this boundary can be described as:

Stiffener tripping if $(\beta_1 - 2.75)^2 + \beta_4^2 > 1.25^2$

Plate buckling if $(\beta_1 - 2.75)^2 + \beta_4^2 < 1.25^2$

5.4.7 Effect of Applied to Plastic Moment Ratio, b_9

Two magnitudes of β_9 were investigated, namely, 0.0 and 0.2. Since only one value of β_2 (1.5) was investigated for the uniaxial compression cases, the comparison is therefore restricted to plates with a β_2 factor of 1.5, the least stable web geometry included in this study, and to a stiffener to plate area ratio, β_5, of 0.3. Since the applied to plastic moment ratio was not varied over the full range of –1.0 to +1.0, the conclusions cannot be generalised over the full range of applied moments.

A summary of peak strength ratio (P_c/P_y) is presented in Figure 5.45. The strength of stiffened steel plates exhibiting a plate buckling failure mode is not affected by β_9. In fact, the peak strength capacity has increased for panels with $\beta_1 = 2.7$. This increase in strength for combined compression and bending as compared to uniaxial compression only case can be explained by the loss in effective plate width with the increase in plate slenderness. For a plate under uniaxial compression a loss in effective plate width will result in a shift of the cross section centroid and an effective eccentricity that places the flange of the stiffener under tension. By contrast, the initial applied bending that places

the stiffener under compression is partially offset by the secondary moment that result from the effective eccentricity of the applied axial load when the centroid of the cross-section shifts.

The above argument suggests that for a given combination of applied axial load and bending moment, there exists a unique stiffened plate configuration that could give an optimum section (giving maximum strength) with the least amount of material.

The introduction of bending moment has also resulted in the shift of failure modes from plate induced overall buckling, and in some cases from plate buckling, to stiffener tripping. For specimens failing by stiffener tripping, there is a decrease in capacity with an increase in β_1 and β_4 values. This observation is consistent with the work of Grondin *et al*. (1999).

5.5 SUMMARY AND CONCLUSIONS

Under uniaxial compression and "average" initial imperfections combined with "severe" magnitude of residual stresses, three types of failure modes were observed, namely plate induced overall buckling, plate buckling, and a dual failure mode. The dual failure mode is characterised by plate induced overall buckling taking over the plate buckling failure mode in the post-buckling range. The influence of the ratio of stiffener torsional slenderness to plate transverse flexural slenderness (β_4) and stiffener to plate area ratio (β_5) on the peak strength ratio (P_c/P_y) was found to be negligible for stiffened plate failing by either plate buckling or plate induced overall buckling. The dual failure mode, characterised by plate induced overall buckling mode taking over the plate-buckling mode, was observed for some of the cases investigated. This type of failure mode results in a loss in peak strength as well as an abrupt drop in the post-buckling response of the stiffened steel plates. The dual failure mode was affected primarily by the stiffener to plate area ratio (β_5) and by the plate slenderness ratio (β_1).

The failure mode shifted from plate induced overall buckling, and in some cases from plate buckling, to stiffener tripping with the application of a bending moment to place the stiffener flange initially under flexural compression.

For a range of stiffener flange slenderness (β_3) precluding flange local buckling, the value of β_3 had no influence on either the strength nor the behaviour of stiffened plates. The stiffener web slenderness (β_2) only affected the post-buckling response of stiffened plates failing by stiffener tripping failure mode.

The stiffener to plate area ratio (β_5) neither affected the strength nor the behaviour of the stocky plates stiffened with stocky stiffeners for both the stiffener tripping and plate buckling failure modes. A decrease in both the peak strength and post-buckling response for stiffener tripping and plate buckling failure modes was observed with the decrease in stiffener to plate area ratio.

The plate transverse flexural slenderness (β_1) affected both the behaviour and strength of both the plate buckling and stiffener tripping failure modes. A decrease in peak strength as well as post-buckling response was observed with an increase in plate transverse flexural slenderness.

The ratio of stiffener torsional slenderness to plate transverse flexural slenderness (β_4) only affected the peak strength and behaviour of stiffened plates failing by stiffener tripping. A decrease in strength as well as post-buckling response was observed with an increase in β_4.

The observed failure modes, for combined compression and bending case, were found to be affected by β_1 and β_4 only. It was also found that for only a certain range of β_1 and β_4 the boundary between stiffener tripping and plate buckling is affected. For the rest of the range the boundary between stiffener tripping and plate buckling is only dictated by β_4.

The main effect of the application of a bending moment on an axially loaded stiffened plate was to trigger stiffener tripping. Compared to plates loaded under axial compression only, the peak strength of plates subjected to combined bending and compression was decreased when the failure mode under combined bending and axial load was stiffener tripping. By contrast, the strength of the stiffened steel plates failing by plate buckling increased with the application of a bending moment.

Table 5.1 Effect of β_1 and β_4 for uniaxial compression

b_1	b_4	U_{dm} / U_c	P_c / P_y	**Failure mode**
0.25	**0.50**	—	1.025	Plate induced overall buckling
0.40	**0.50**	—	1.018	Plate induced overall buckling
0.55	**0.50**	—	1.013	Plate buckling
0.70	**0.50**	—	1.003	Plate buckling
1.28	**0.50**	—	0.833	Plate buckling
2.00	**0.50**	—	0.632	Plate buckling
2.70	**0.50**	—	0.541	Plate buckling
0.55	**1.00**	—	1.008	Plate induced overall buckling
0.70	**1.00**	—	1.002	Plate buckling
1.28	**1.00**	—	0.875	Plate buckling
2.00	**1.00**	—	0.656	Plate buckling
2.70	**1.00**	—	0.527	Plate buckling
0.70	**1.50**	—	0.993	Plate induced overall buckling
0.85	**1.50**	—	0.981	Plate buckling
1.00	**1.50**	—	0.964	Plate buckling
1.14	**1.50**	—	0.945	Plate buckling
1.28	**1.50**	—	0.923	Plate buckling
1.30	**1.50**	—	0.916	Plate buckling
1.39	**1.50**	—	0.892	Plate buckling
1.50	**1.50**	—	0.850	Plate buckling
2.00	**1.50**	—	0.647	Plate buckling
2.70	**1.50**	1.294	0.440	Dual failure mode
0.70	**2.00**	—	0.975	Plate induced overall buckling
0.85	**2.00**	—	0.953	Plate induced overall buckling
1.00	**2.00**	—	0.926	Plate buckling
1.15	**2.00**	—	0.892	Plate buckling
1.28	**2.00**	—	0.856	Plate buckling
2.00	**2.00**	1.83	0.600	Dual failure mode
2.70	**2.00**	2.07	0.314	Dual failure mode

at $\beta_2 = 1.50$; $\beta_3 = 0.375$; $\beta_5 = 0.30$; $\beta_9 = 0.0$

Table 5.2 Effect of β_1 and β_4 for uniaxial compression

b_1	b_4	U_{dm} / U_c	P_c / P_y	**Failure mode**
0.70	**0.50**	—	1.002	Plate induced overall buckling
1.28	**0.50**	—	0.835	Plate buckling
2.00	**0.50**	—	0.590	Plate buckling
2.70	**0.50**	—	0.493	Plate buckling
0.70	**1.00**	—	0.996	Plate induced overall buckling
1.28	**1.00**	—	0.829	Plate buckling
2.00	**1.00**	1.89	0.598	Dual failure mode
2.70	**1.00**	1.04	0.463	Dual failure mode
0.70	**1.50**	—	0.990	Plate induced overall buckling
1.28	**1.50**	1.83	0.843	Dual failure mode
2.00	**1.50**	1.05	0.523	Dual failure mode
2.70	**1.50**	1.00	0.311	Dual failure mode
0.70	**2.00**	2.23	0.974	Dual failure mode
1.28	**2.00**	1.10	0.779	Dual failure mode
2.00	**2.00**	1.00	0.399	Dual failure mode
2.70	**2.00**	1.00	0.211	Dual failure mode

at $\beta_2 = 1.50$; $\beta_3 = 0.375$; $\beta_5 = 0.15$; $\beta_9 = 0.0$

Table 5.3 Effect of β_1 and β_4 for uniaxial compression

b_1	b_4	U_{dm} / U_c	P_c / P_y	**Failure mode**
0.70	**0.50**	—	1.020	Plate Induced Overall buckling
1.28	**0.50**	—	0.854	Plate buckling
2.00	**0.50**	3.11	0.625	Dual failure mode
2.70	**0.50**	2.44	0.463	Dual failure mode
0.70	**1.00**	—	0.992	Plate Induced Overall buckling
1.28	**1.00**	1.83	0.807	Dual failure mode
2.00	**1.00**	1.00	0.520	Dual failure mode
2.70	**1.00**	1.00	0.324	Dual failure mode
0.70	**1.50**	1.83	0.980	Dual failure mode
1.28	**1.50**	1.00	0.751	Dual failure mode
2.00	**1.50**	1.00	0.332	Dual failure mode
2.70	**1.50**	1.00	0.179	Dual failure mode
0.70	**2.00**	1.23	0.956	Dual failure mode
1.28	**2.00**	1.00	0.587	Dual failure mode
2.00	**2.00**	1.00	0.219	Dual failure mode
2.70	**2.00**	1.00	0.118	Dual failure mode

at $\beta_2 = 1.50$; $\beta_3 = 0.375$; $\beta_5 = 0.075$; $\beta_9 = 0.0$

Table 5.4 Effect of β_1 and β_4 for combined compression and bending

b_1	b_4	P_c / P_v	**Failure mode**
0.70	**0.50**	0.784	Stiffener tripping
1.28	**0.50**	0.768	Stiffener tripping
2.00	**0.50**	0.681	Plate buckling
2.70	**0.50**	0.591	Plate buckling
0.70	**1.00**	0.752	Stiffener tripping
1.28	**1.00**	0.702	Stiffener tripping
2.00	**1.00**	0.655	Plate buckling
2.70	**1.00**	0.604	Plate buckling
0.70	**1.50**	0.718	Stiffener tripping
1.28	**1.50**	0.646	Stiffener tripping
2.00	**1.50**	0.497	Stiffener tripping
2.70	**1.50**	0.350	Stiffener tripping
0.70	**2.00**	0.691	Stiffener tripping
1.28	**2.00**	0.577	Stiffener tripping
2.00	**2.00**	0.372	Stiffener tripping
2.70	**2.00**	0.234	Stiffener tripping

at $\beta_2 = 1.50$; $\beta_3 = 0.375$; $\beta_5 = 0.3$; $\beta_9 = 0.2$

Table 5.5 Effect of β_1 and β_4 for combined compression and bending

b_1	b_4	P_c / P_v	**Failure mode**
0.70	**0.50**	0.783	Stiffener tripping
1.28	**0.50**	0.769	Stiffener tripping
2.00	**0.50**	0.680	Plate buckling
2.70	**0.50**	0.585	Plate buckling
0.70	**1.00**	0.756	Stiffener tripping
1.28	**1.00**	0.707	Stiffener tripping
2.00	**1.00**	0.728	Plate buckling
2.70	**1.00**	0.595	Plate buckling
0.70	**1.50**	0.723	Stiffener tripping
1.28	**1.50**	0.649	Stiffener tripping
2.00	**1.50**	0.491	Stiffener tripping
2.70	**1.50**	0.342	Stiffener tripping
0.70	**2.00**	0.691	Stiffener tripping
1.28	**2.00**	0.566	Stiffener tripping
2.00	**2.00**	0.354	Stiffener tripping
2.70	**2.00**	0.219	Stiffener tripping

at $\beta_2 = 1.50$; $\beta_3 = 0.75$; $\beta_5 = 0.3$; $\beta_9 = 0.2$

Table 5.6 Effect of β_1 and β_4 for combined compression and bending

b_1	b_4	P_c / P_v	**Failure mode**
0.70	**0.50**	0.780	Stiffener tripping
1.28	**0.50**	0.771	Stiffener tripping
2.00	**0.50**	0.682	Plate buckling
2.70	**0.50**	0.588	Plate buckling
0.70	**1.00**	0.755	Stiffener tripping
1.28	**1.00**	0.708	Stiffener tripping
2.00	**1.00**	0.728	Plate buckling
2.70	**1.00**	0.589	Plate buckling
0.70	**1.50**	0.726	Stiffener tripping
1.28	**1.50**	0.642	Stiffener tripping
2.00	**1.50**	0.478	Stiffener tripping
2.70	**1.50**	0.328	Stiffener tripping
0.70	**2.00**	0.696	Stiffener tripping
1.28	**2.00**	0.552	Stiffener tripping
2.00	**2.00**	0.337	Stiffener tripping
2.70	**2.00**	0.207	Stiffener tripping

at $\beta_2 = 1.50$; $\beta_3 = 1.125$; $\beta_5 = 0.3$; $\beta_9 = 0.2$

Table 5.7 Effect of β_1 and β_4 for combined compression and bending

b_1	b_4	P_c / P_v	**Failure mode**
0.70	**0.50**	0.796	Stiffener tripping
1.28	**0.50**	0.777	Stiffener tripping
1.46	**0.50**	0.780	Stiffener tripping
1.75	**0.50**	0.725	Plate buckling
2.00	**0.50**	0.675	Plate buckling
2.25	**0.50**	0.637	Plate buckling
2.70	**0.50**	0.576	Plate buckling
1.75	**0.75**	0.742	Plate buckling
2.00	**0.75**	0.693	Plate buckling
2.25	**0.75**	0.655	Plate buckling
0.70	**1.00**	0.761	Stiffener tripping
1.28	**1.00**	0.726	Stiffener tripping
1.75	**1.00**	0.697	Stiffener tripping
2.00	**1.00**	0.715	Plate buckling
2.25	**1.00**	0.664	Plate buckling
2.70	**1.00**	0.589	Plate buckling
1.75	**1.25**	0.617	Stiffener tripping
2.00	**1.25**	0.573	Stiffener tripping
2.25	**1.25**	0.527	Stiffener tripping
0.70	**1.50**	0.735	Stiffener tripping
1.28	**1.50**	0.653	Stiffener tripping
2.00	**1.50**	0.486	Stiffener tripping
2.70	**1.50**	0.333	Stiffener tripping
0.70	**2.00**	0.708	Stiffener tripping
1.28	**2.00**	0.564	Stiffener tripping
2.00	**2.00**	0.343	Stiffener tripping
2.70	**2.00**	0.212	Stiffener tripping

at $\beta_2 = 1.05$; $\beta_3 = 0.75$; $\beta_5 = 0.3$; $\beta_9 = 0.2$

Table 5.8 Effect of β_1 and β_4 for combined compression and bending

b_1	b_4	P_c / P_v	**Failure mode**
0.70	**0.50**	0.805	Stiffener tripping
1.28	**0.50**	0.780	Stiffener tripping
2.00	**0.50**	0.683	Plate buckling
2.70	**0.50**	0.565	Plate buckling
0.70	**1.00**	0.765	Stiffener tripping
1.28	**1.00**	0.723	Stiffener tripping
2.00	**1.00**	0.700	Plate buckling
2.70	**1.00**	0.570	Plate buckling
0.70	**1.50**	0.741	Stiffener tripping
1.28	**1.50**	0.644	Stiffener tripping
2.00	**1.50**	0.455	Stiffener tripping
2.70	**1.50**	0.308	Stiffener tripping
0.70	**2.00**	0.710	Stiffener tripping
1.28	**2.00**	0.543	Stiffener tripping
2.00	**2.00**	0.316	Stiffener tripping
2.70	**2.00**	0.192	Stiffener tripping

at $\beta_2 = 0.60$; $\beta_3 = 0.75$; $\beta_5 = 0.3$; $\beta_9 = 0.2$

Table 5.9 Effect of β_1 and β_4 for combined compression and bending

b_1	b_4	P_c / P_v	**Failure mode**
0.70	**0.50**	0.785	Stiffener tripping
1.28	**0.50**	0.725	Stiffener tripping
2.00	**0.50**	0.639	Plate buckling
2.70	**0.50**	0.510	Plate buckling
0.70	**1.00**	0.709	Stiffener tripping
1.28	**1.00**	0.651	Stiffener tripping
2.00	**1.00**	0.608	Dual failure mode
2.70	**1.00**	0.450	Dual failure mode
0.70	**1.50**	0.673	Stiffener tripping
1.28	**1.50**	0.535	Stiffener tripping
2.00	**1.50**	0.347	Stiffener tripping
2.70	**1.50**	0.232	Stiffener tripping
0.70	**2.00**	0.628	Stiffener tripping
1.28	**2.00**	0.410	Stiffener tripping
2.00	**2.00**	0.211	Stiffener tripping
2.70	**2.00**	0.126	Stiffener tripping

at $\beta_2 = 0.60$; $\beta_3 = 0.75$; $\beta_5 = 0.15$; $\beta_9 = 0.2$

Table 5.10 Effect of β_1 and β_4 for combined compression and bending

b_1	b_4	P_c / P_v	**Failure mode**
1.28	**0.50**	0.687	Stiffener tripping
2.00	**0.50**	0.645	Plate buckling
2.70	**0.50**	0.484	Plate buckling
0.70	**1.00**	0.682	Stiffener tripping
1.28	**1.00**	0.501	Stiffener tripping
2.00	**1.00**	0.557	Dual failure mode
2.70	**1.00**	0.345	Dual failure mode
0.70	**1.50**	0.567	Stiffener tripping
1.28	**1.50**	0.368	Stiffener tripping
2.00	**1.50**	0.205	Stiffener tripping
2.70	**1.50**	0.136	Stiffener tripping
0.70	**2.00**	0.491	Stiffener tripping
1.28	**2.00**	0.252	Stiffener tripping
2.00	**2.00**	0.121	Stiffener tripping
2.70	**2.00**	0.072	Stiffener tripping

at $\beta_2 = 0.60$; $\beta_3 = 0.75$; $\beta_5 = 0.075$; $\beta_9 = 0.2$

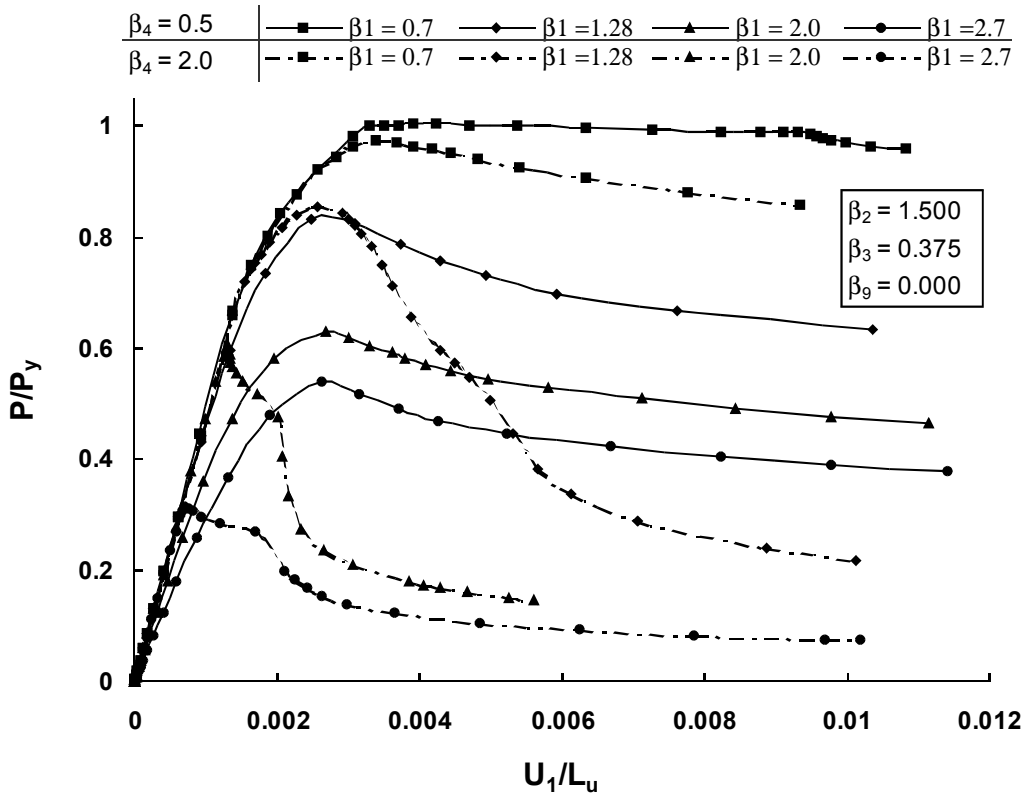

Figure 5.1 Effect of β_1 on the behaviour of stiffened plates (β_5 = 0.300)

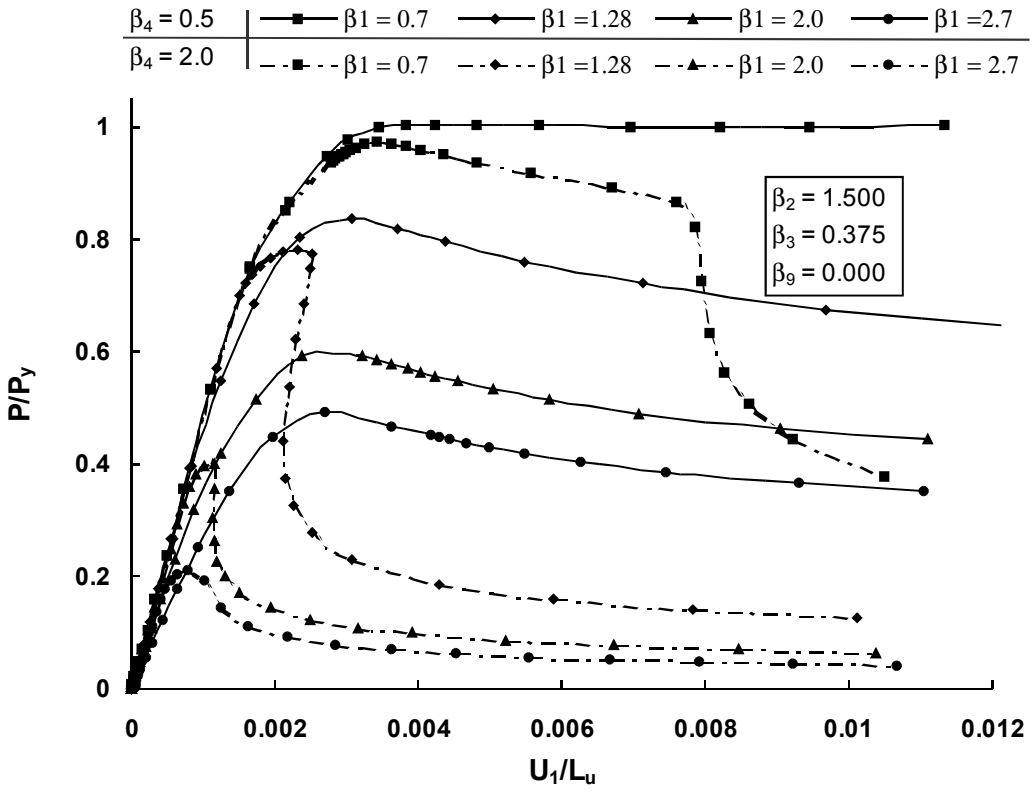

Figure 5.2 Effect of β_1 on the behaviour of stiffened plates (β_5 = 0.150)

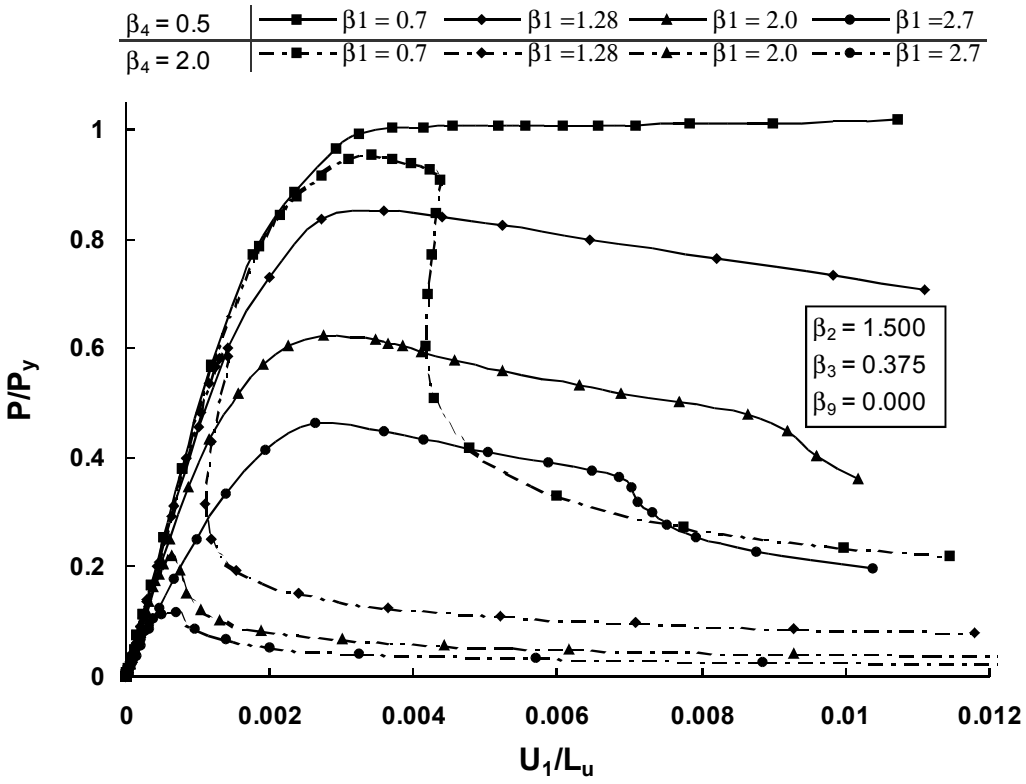

Figure 5.3 Effect of β_1 on the behaviour of stiffened plates (β_5 = 0.075)

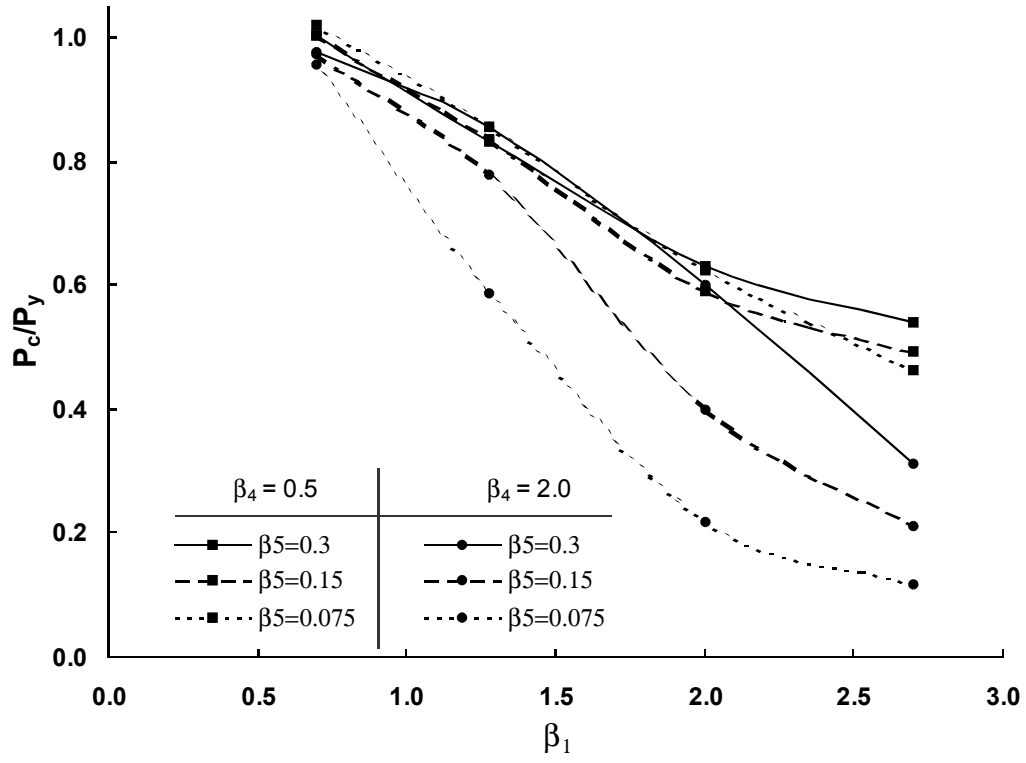

Figure 5.4 Effect of β_1 on the strength of stiffened plates

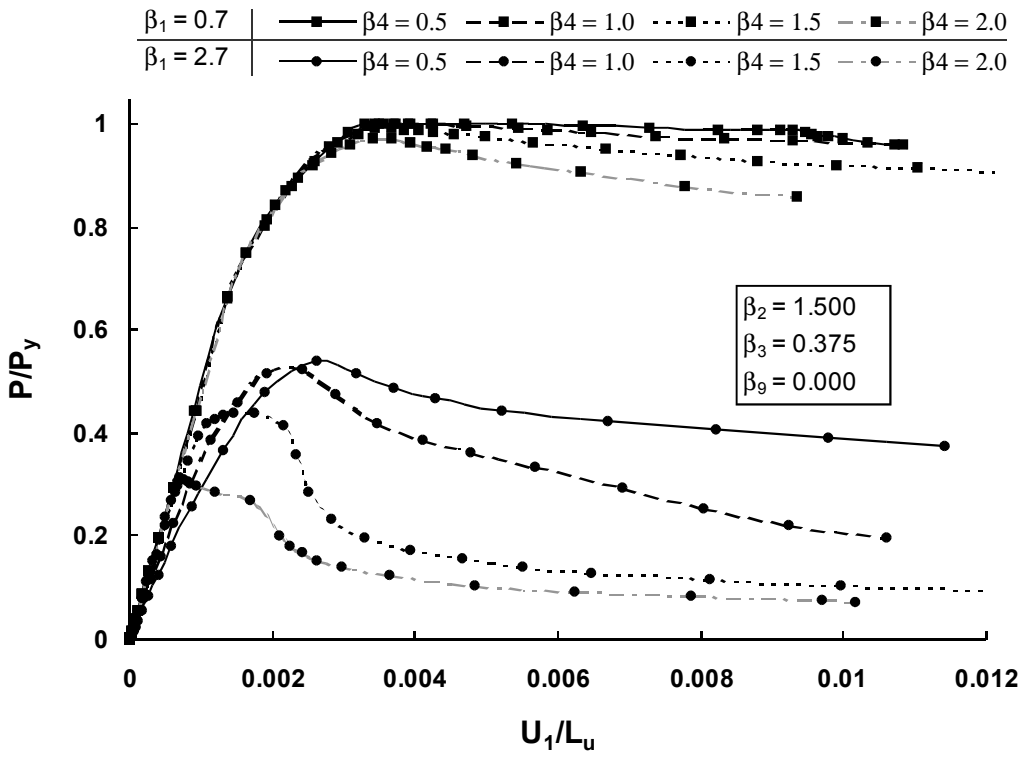

Figure 5.5 Effect of β_4 on the behaviour of stiffened plates (β_5 = 0.300)

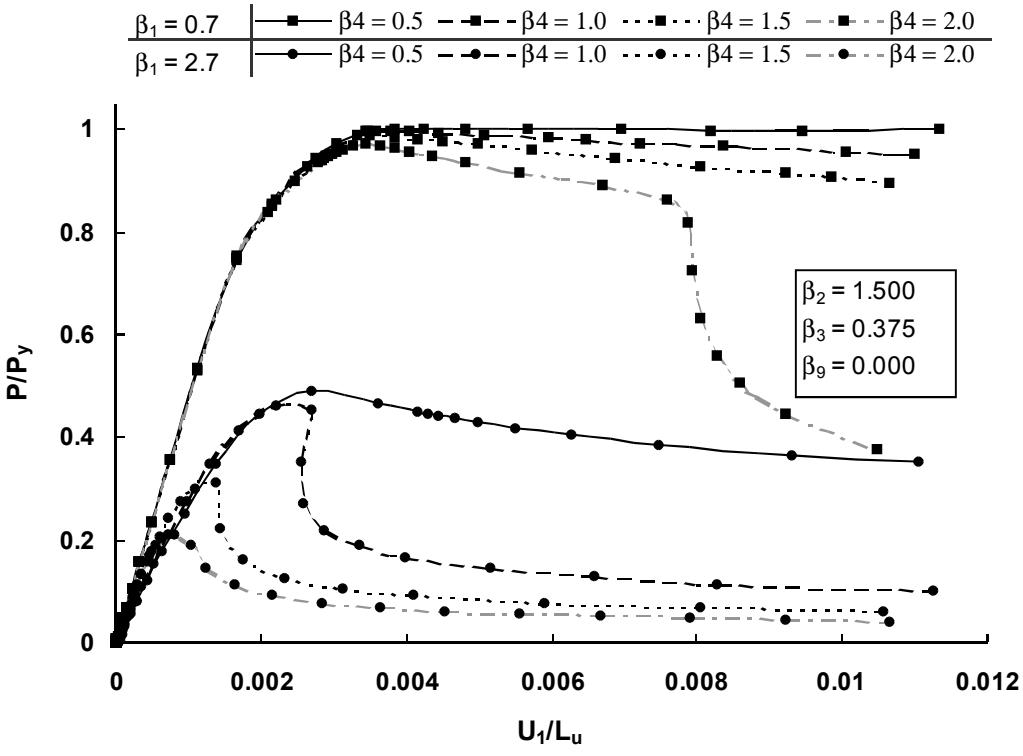

Figure 5.6 Effect of β_4 on the behaviour of stiffened plates (β_5 = 0.150)

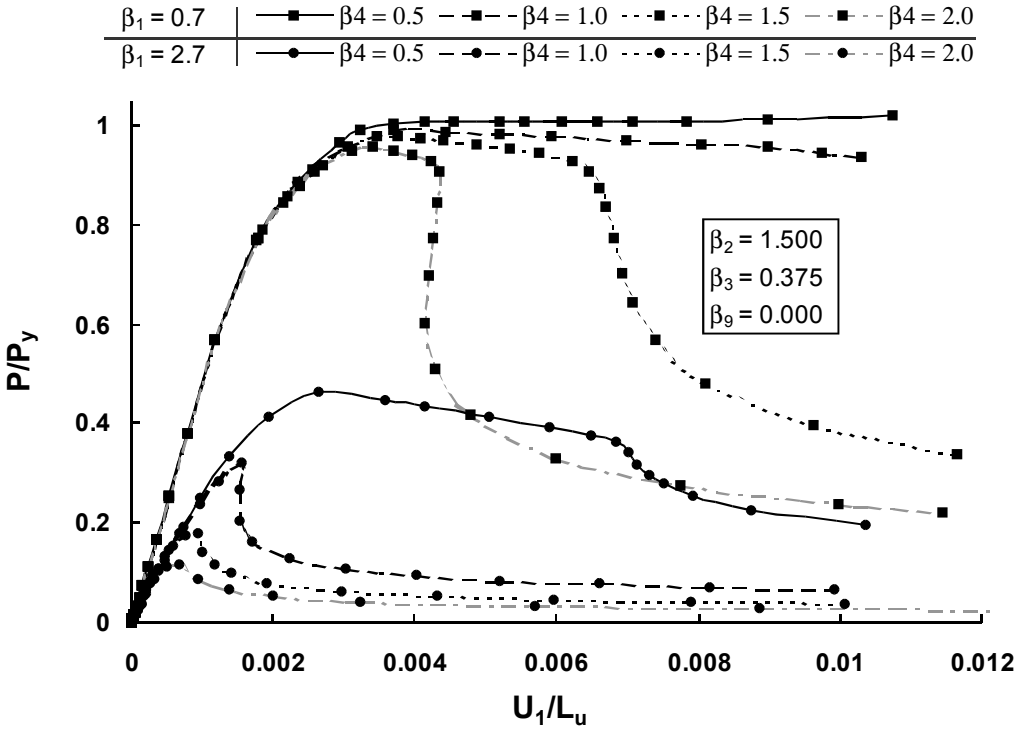

Figure 5.7 Effect of β_4 on the behaviour of stiffened plates (β_5 = 0.075)

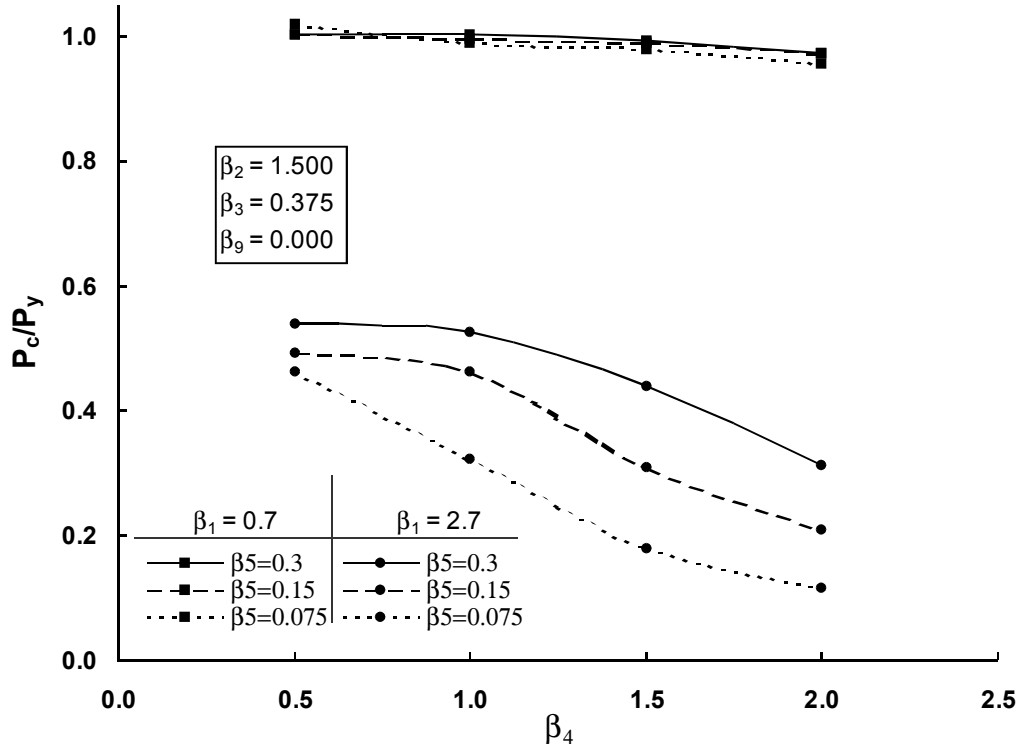

Figure 5.8 Effect of β_4 on the strength of stiffened plates

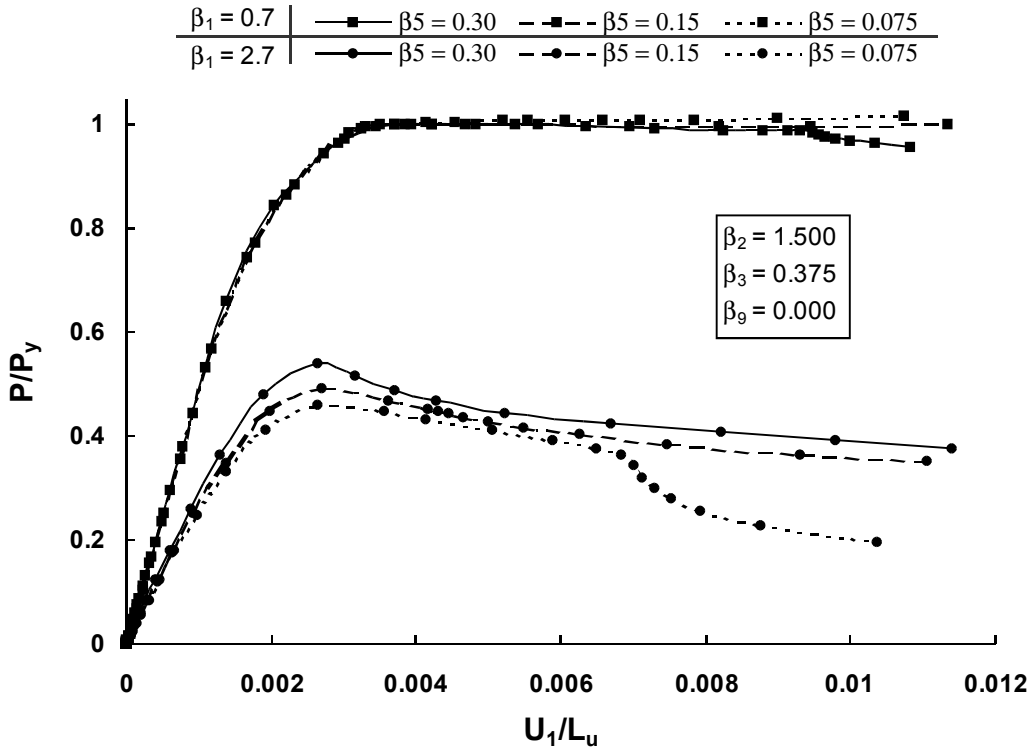

Figure 5.9 Effect of β_5 on the behaviour of stiffened plates (β_4 = 0.50)

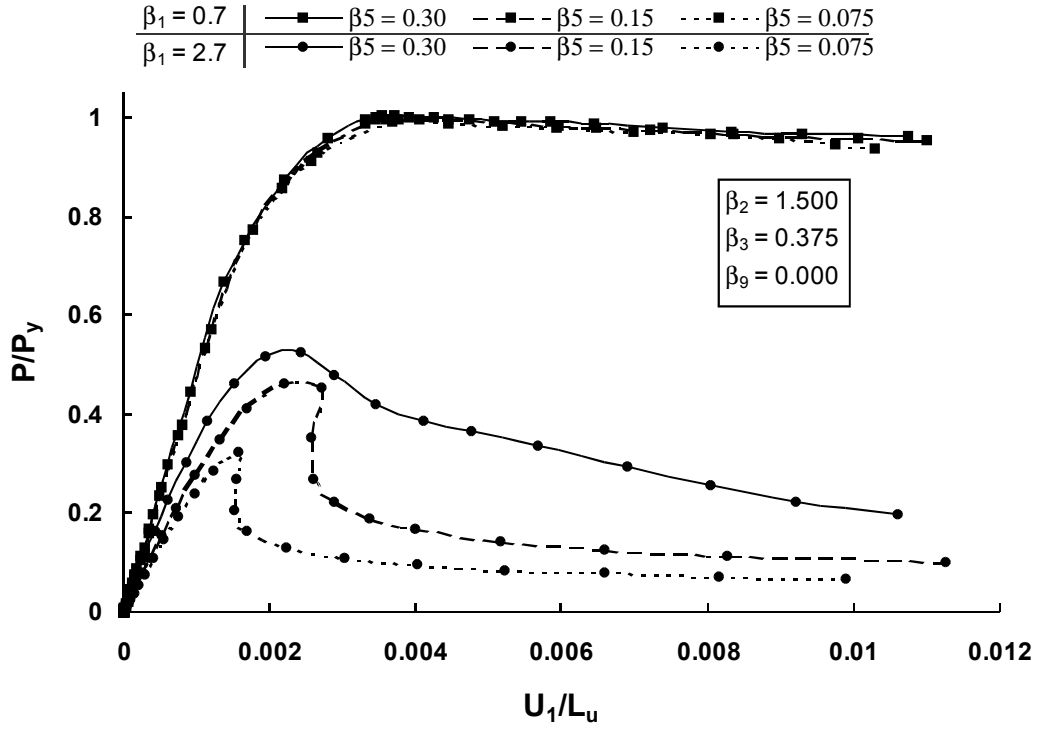

Figure 5.10 Effect of β_5 on the behaviour of stiffened plates (β_4 = 1.00)

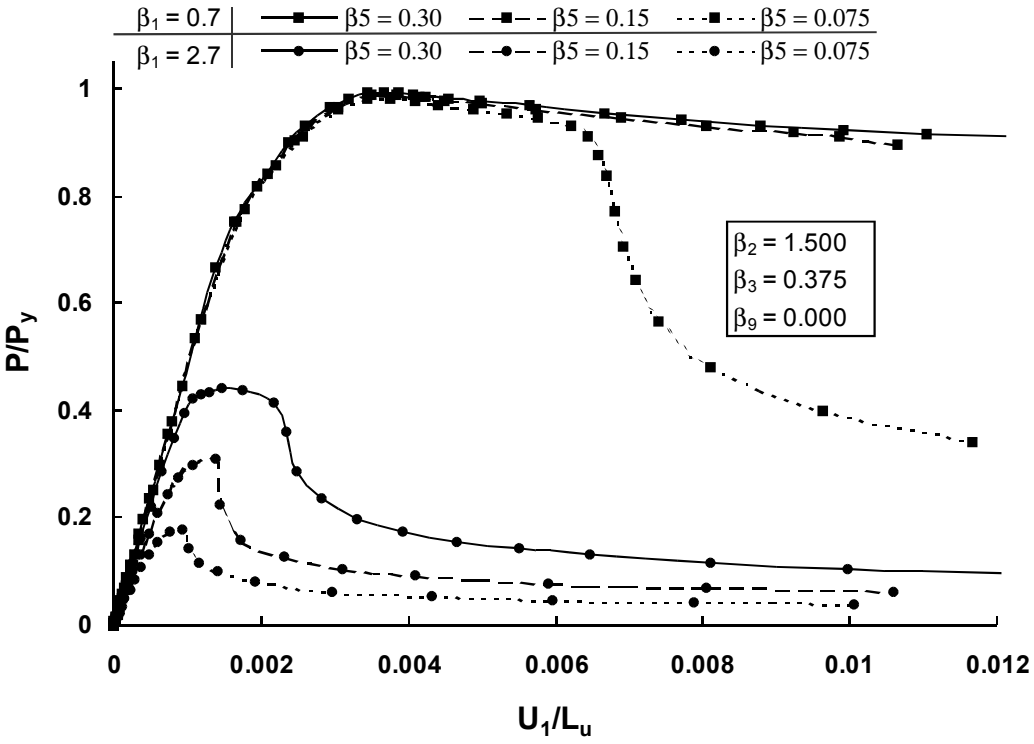

Figure 5.11 Effect of β_5 on the behaviour of stiffened plates (β_4 = 1.50)

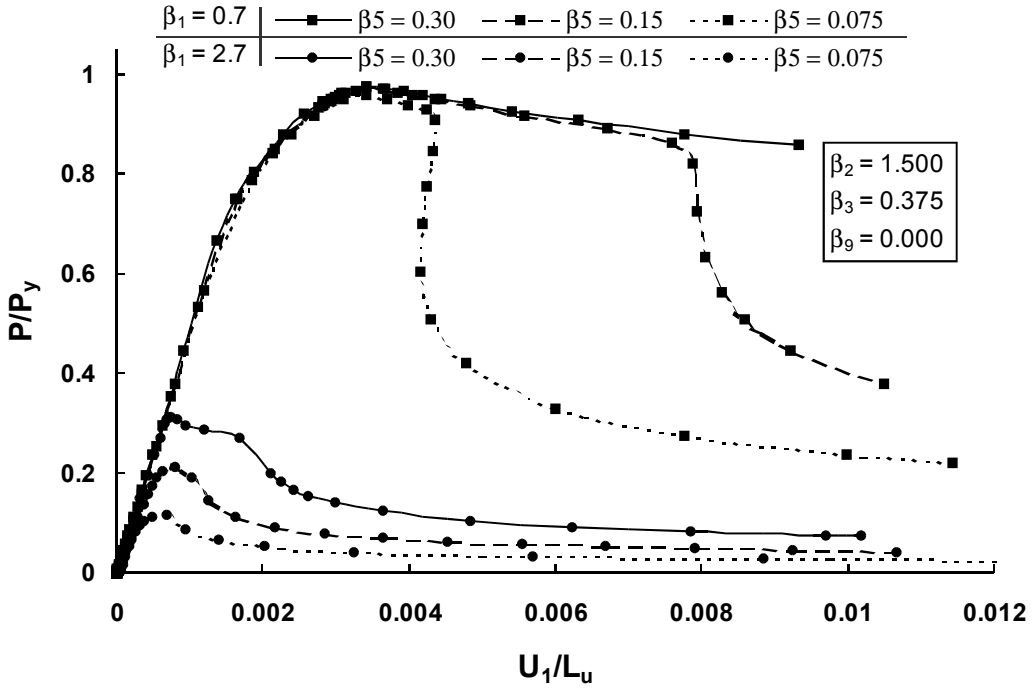

Figure 5.12 Effect of β_5 on the behaviour of stiffened plates (β_4 = 2.00)

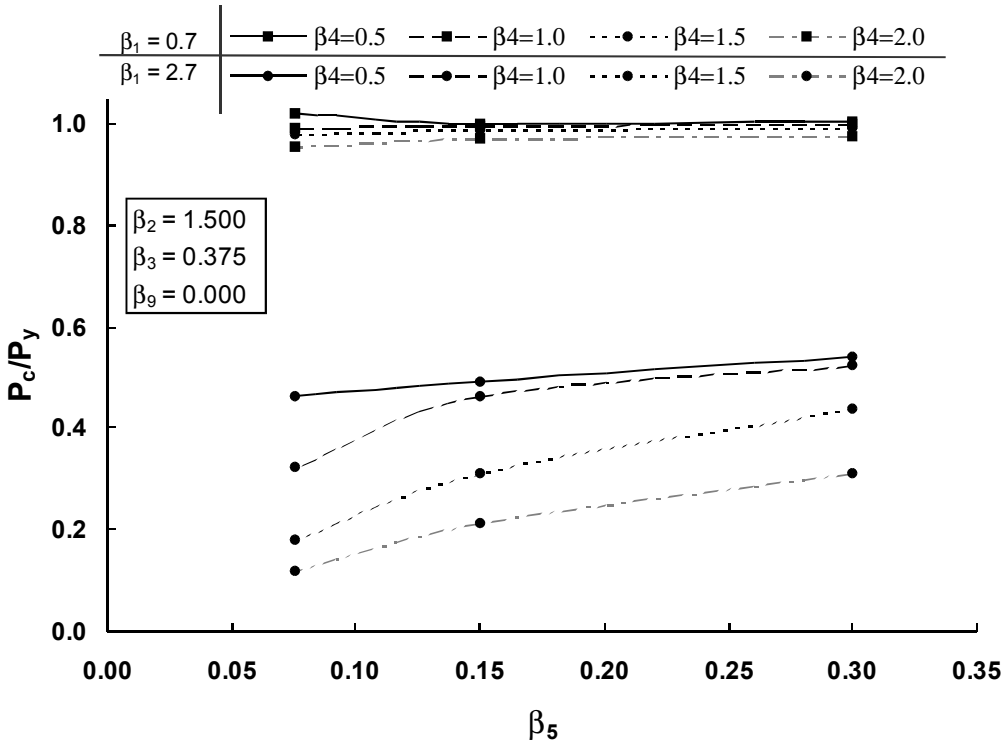

Figure 5.13 Effect of β_5 on the strength of stiffened plates

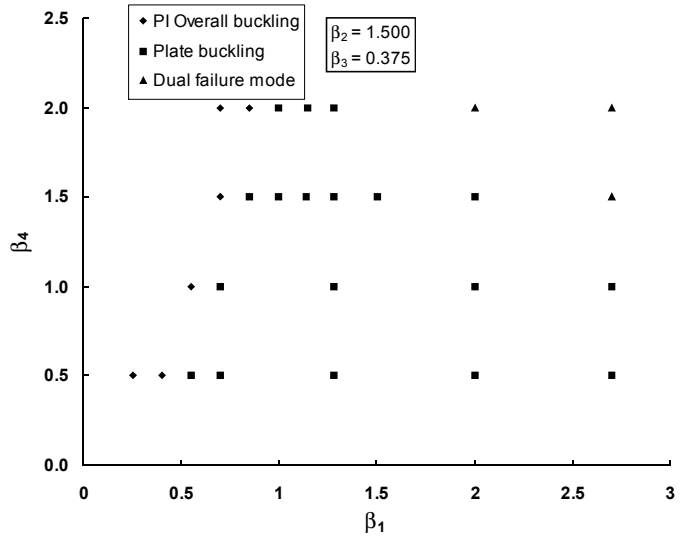

(a) $\beta_5 = 0.300$

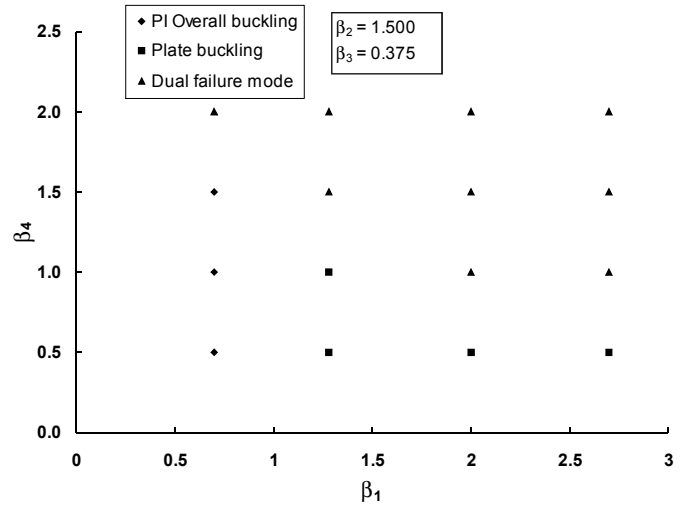

(b) $\beta_5 = 0.150$

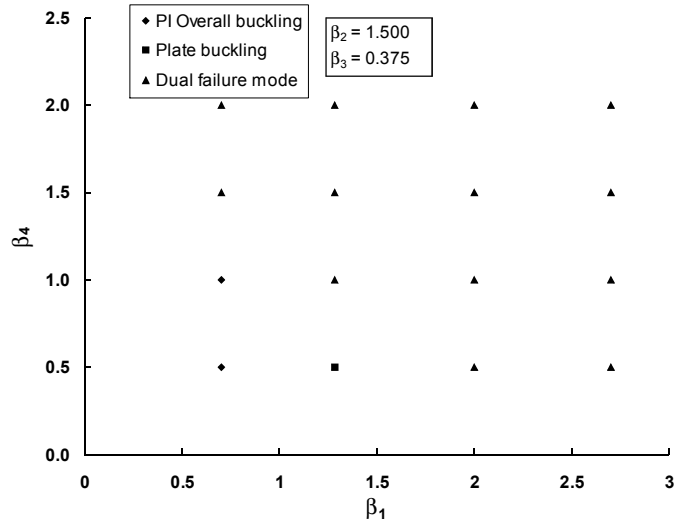

(c) $\beta_5 = 0.075$

Figure 5.14 Observed failure modes under uniaxial compression

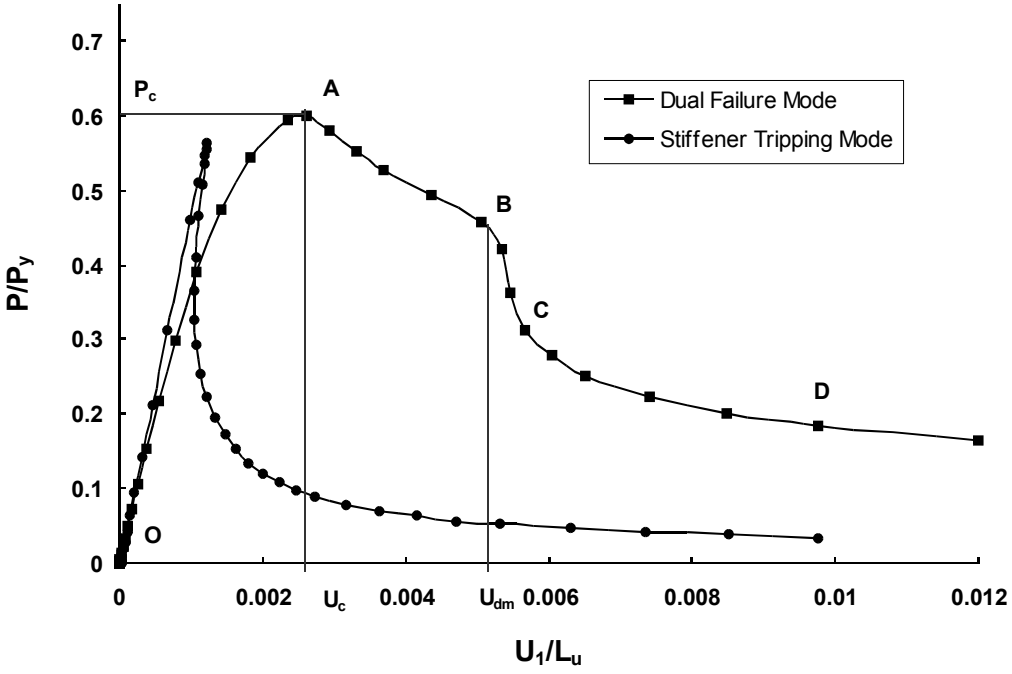

Figure 5.15 Typical load versus deformation response for dual failure and stiffener tripping modes

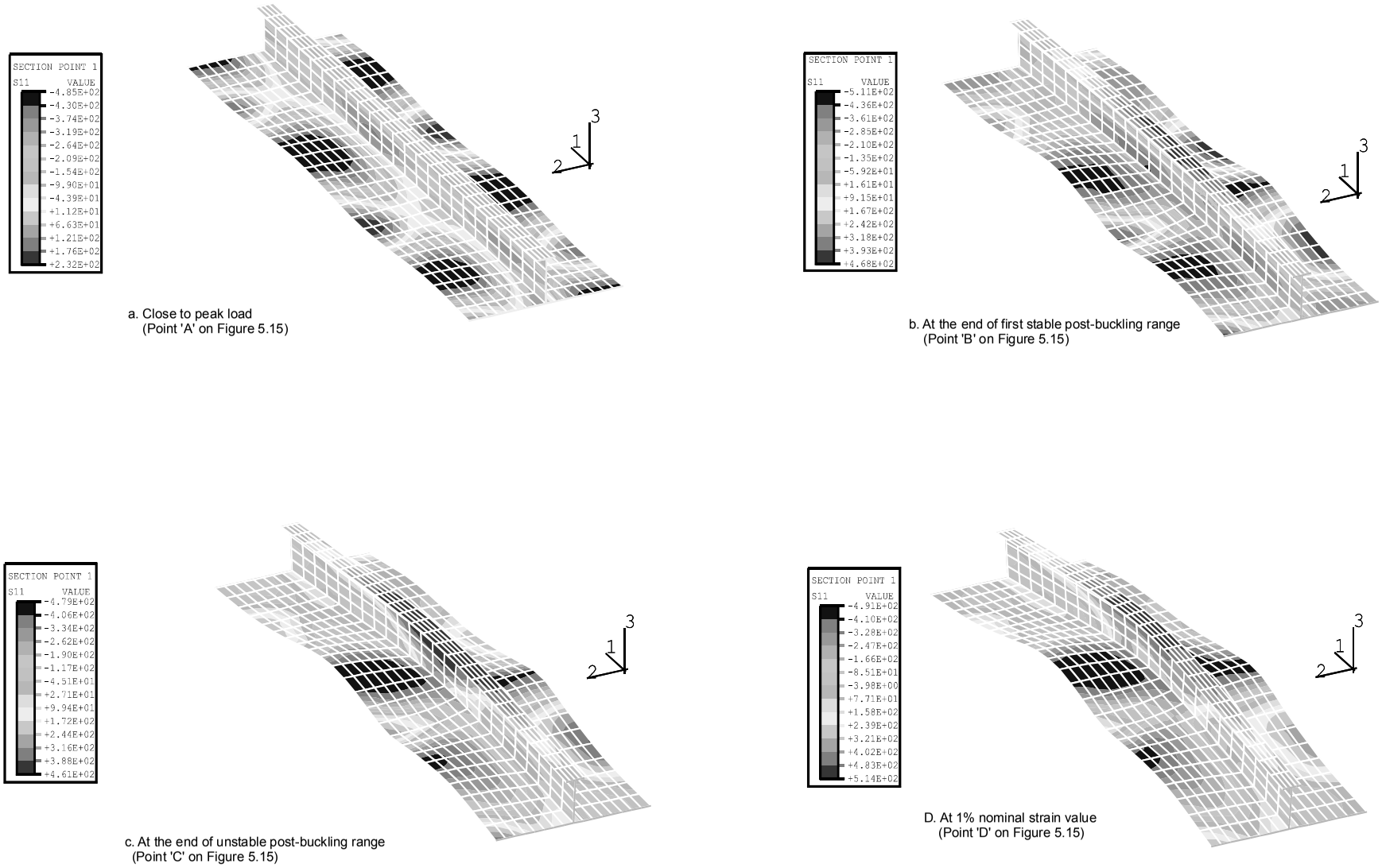

Figure 5.16 Typical stress history plot for dual failure mode

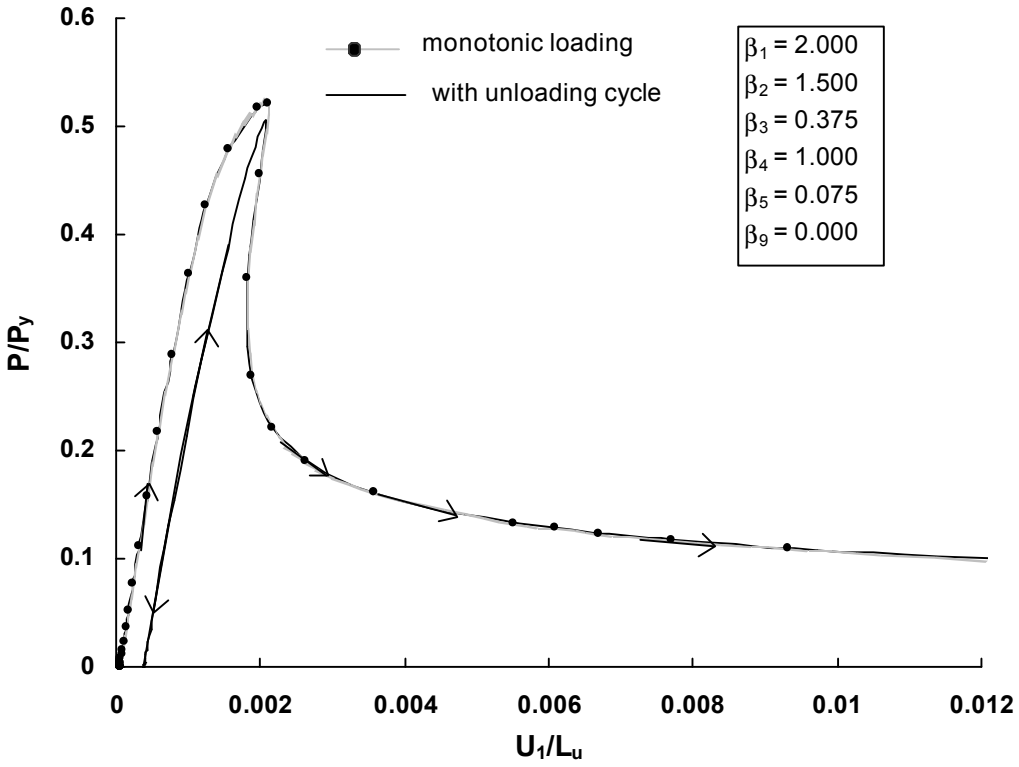

Figure 5.17 Effect of unloading cycle on stiffened plate response

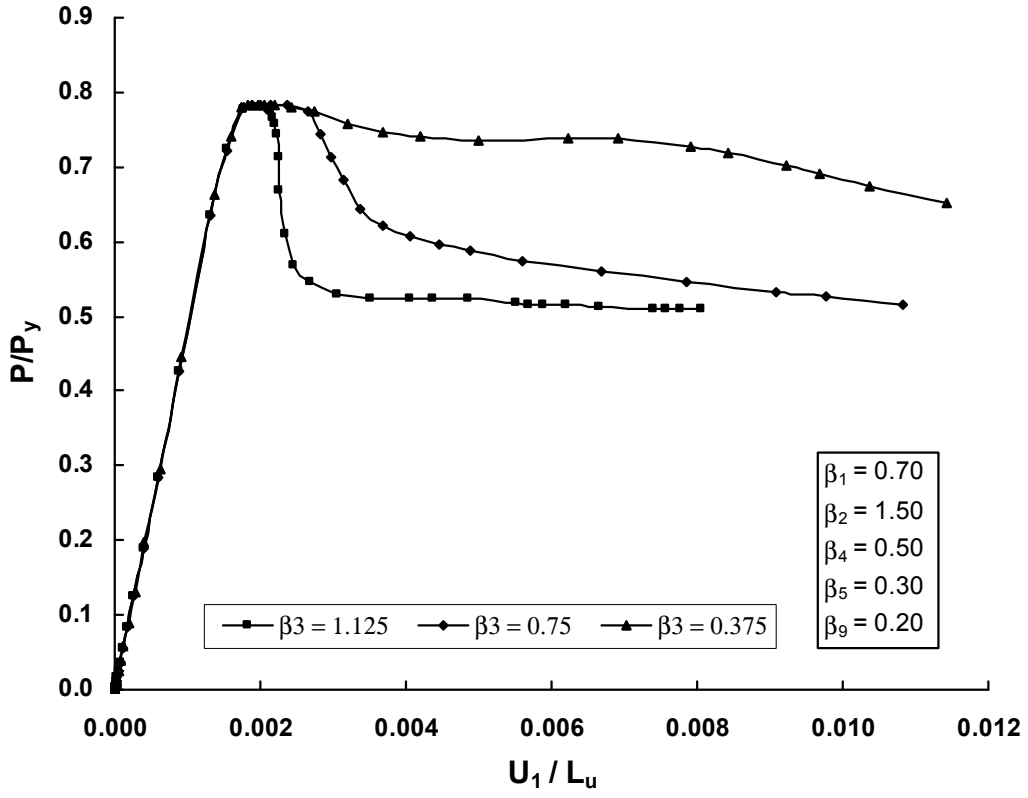

Figure 5.18 Effect of β_3 on the behaviour of plates failing by stiffener tripping at $P_c/P_Y = 0.80$

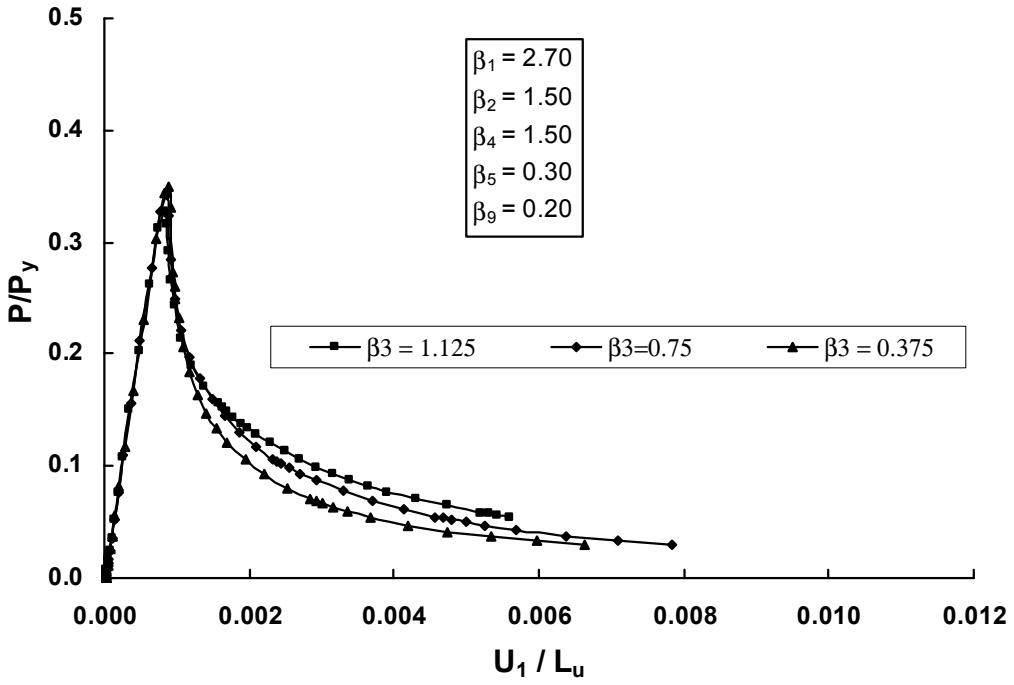

Figure 5.19 Effect of β_3 on the behaviour of plates failing by stiffener tripping at $P_c/P_Y = 0.30$

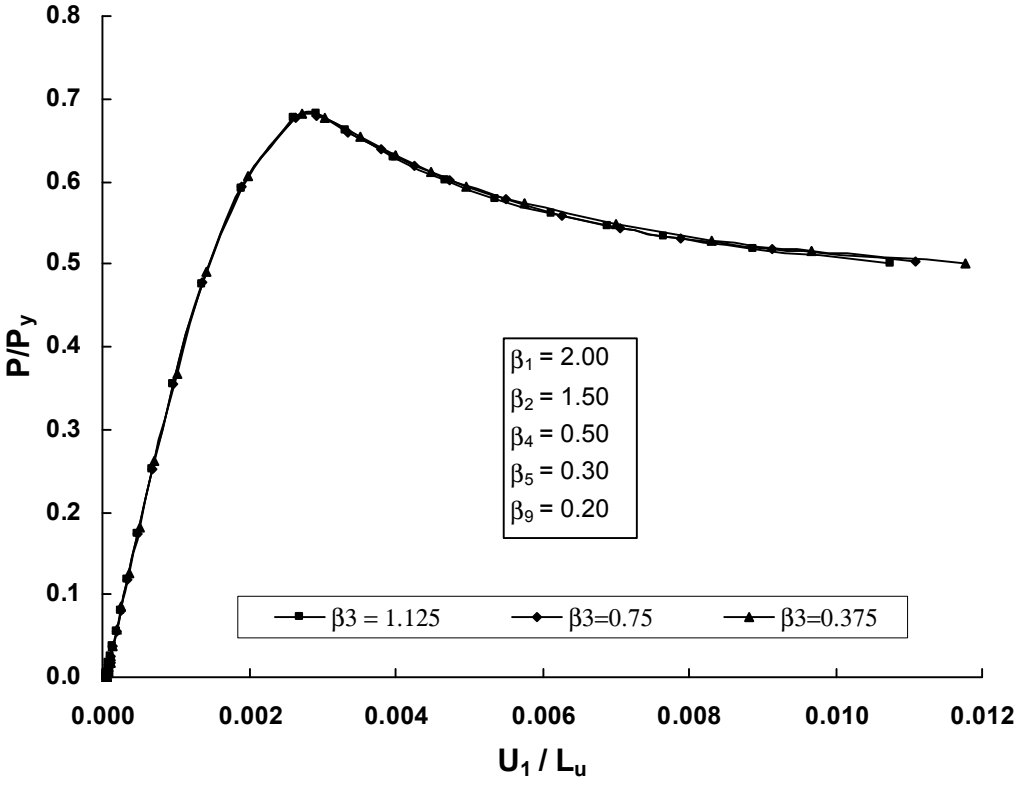

Figure 5.20 Effect of β_3 on the behaviour of plates failing by plate buckling at $P_c/P_Y = 0.70$

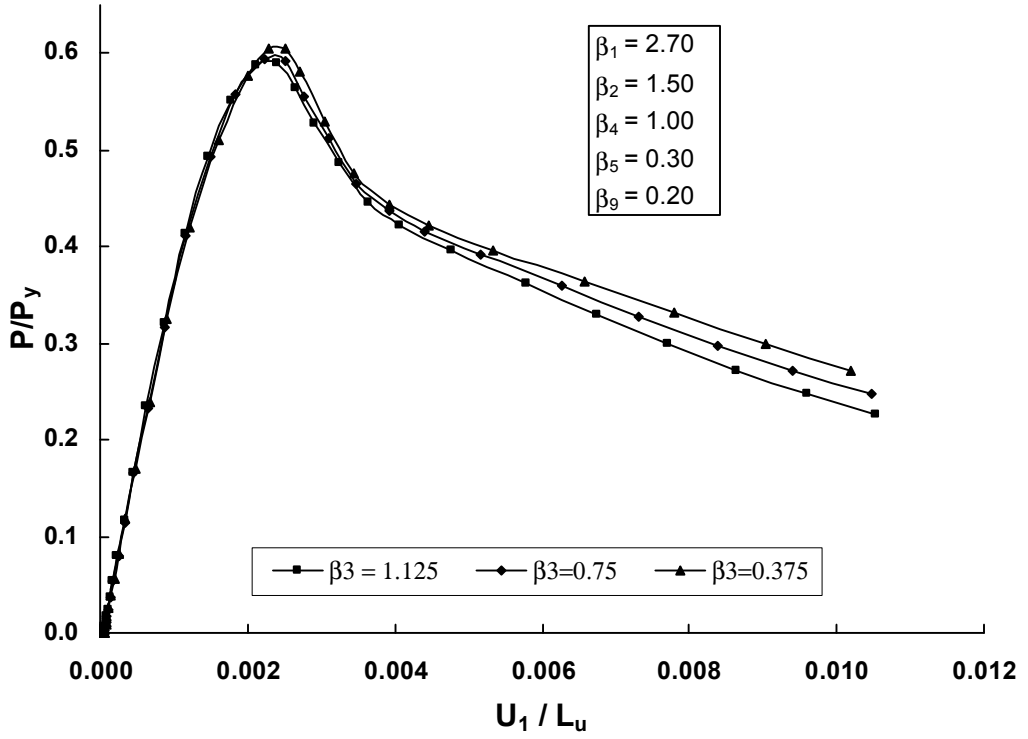

Figure 5.21 Effect of β_3 on the behaviour of plates failing by plate buckling at $P_c/P_Y = 0.60$

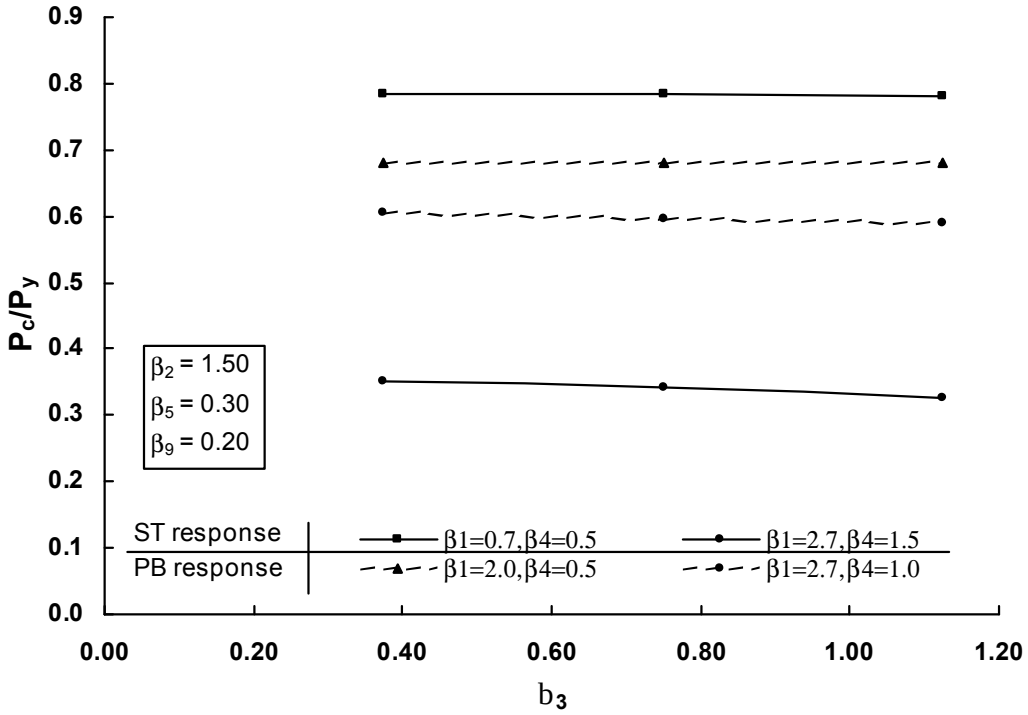

Figure 5.22 Effect of β_3 on the strength of stiffened plates

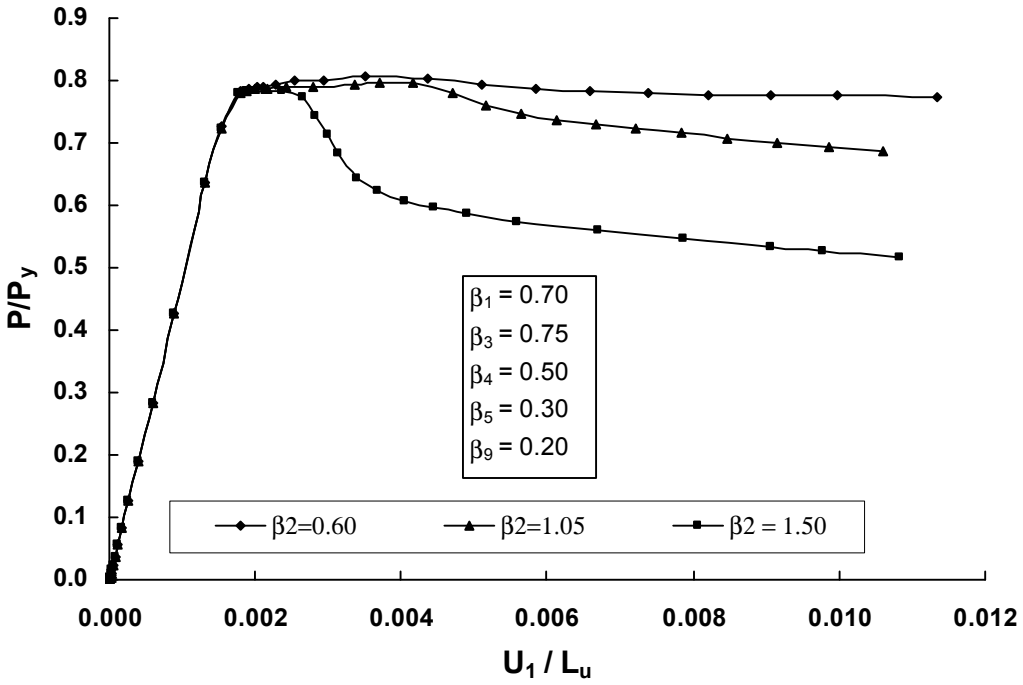

Figure 5.23 Effect of β_2 on the behaviour of plates failing by stiffener tripping at $P_c/P_Y = 0.80$

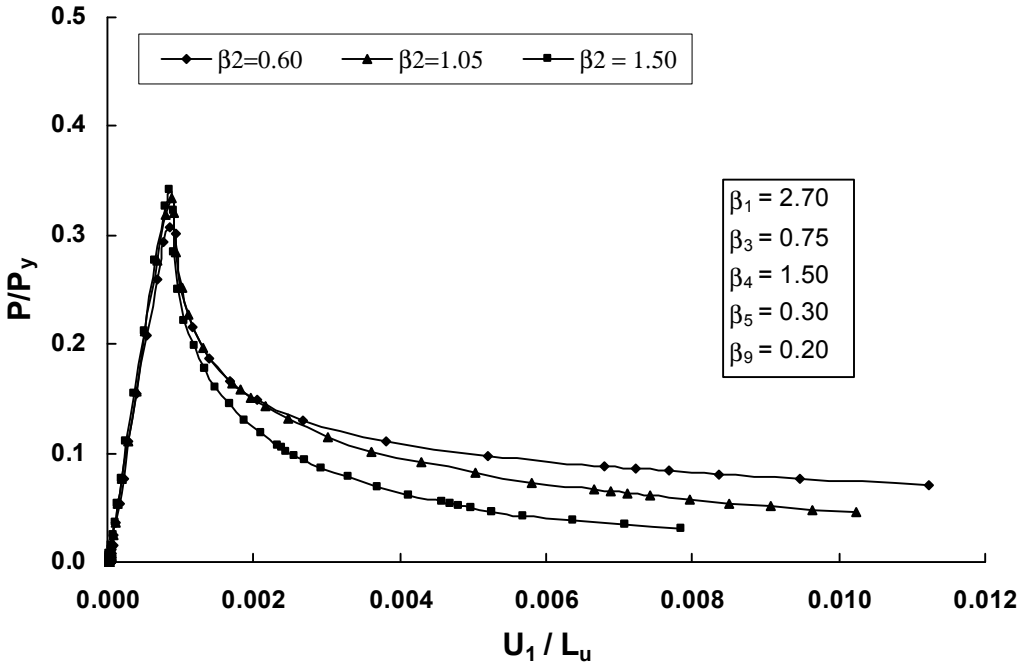

Figure 5.24 Effect of β_2 on the behaviour of plates failing by stiffener tripping at $P_c/P_Y = 0.30$

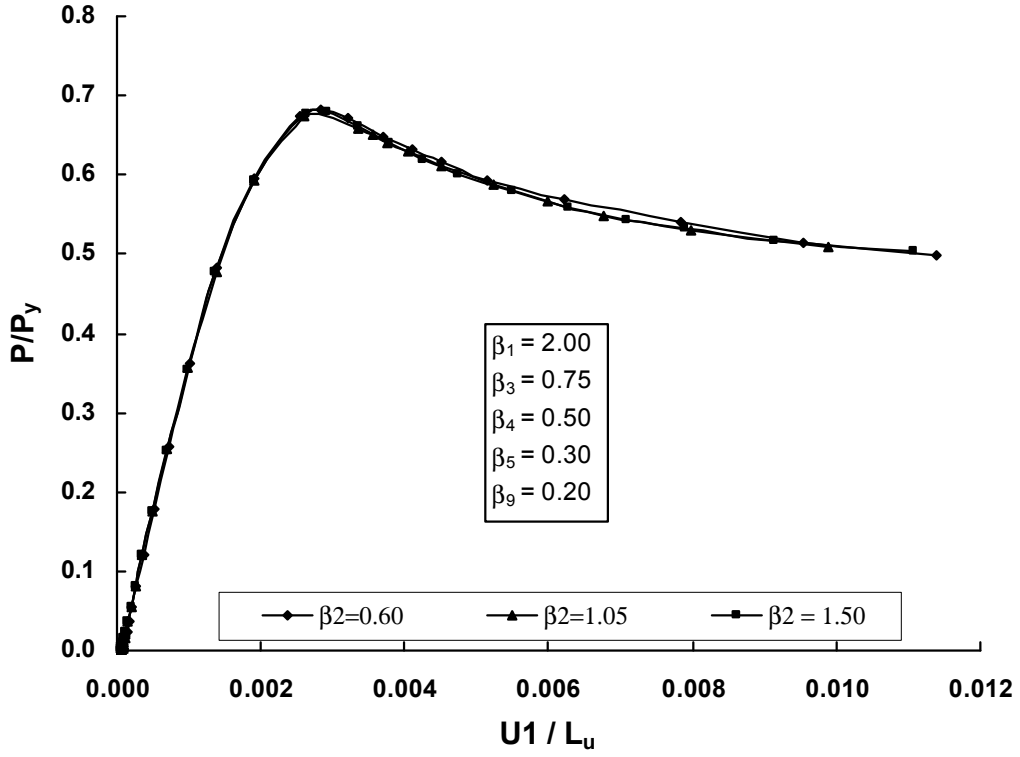

Figure 5.25 Effect of β_2 on the behaviour of plates failing by plate buckling at $P_c/P_Y = 0.70$

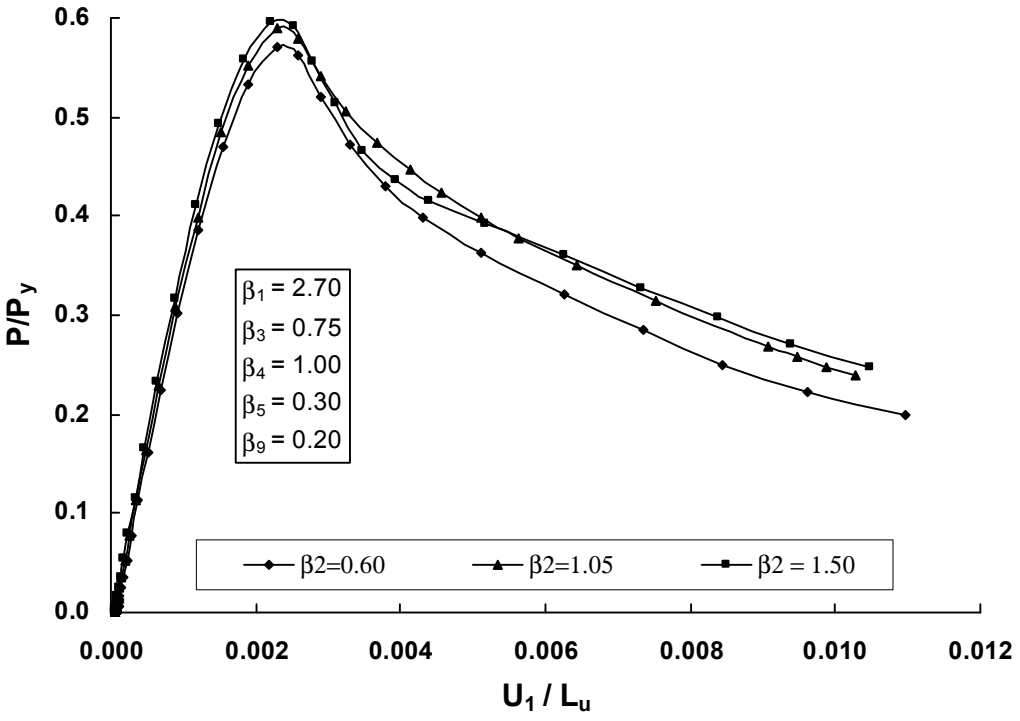

Figure 5.26 Effect of β_2 on the behaviour of plates failing by plate buckling at $P_c/P_Y = 0.60$

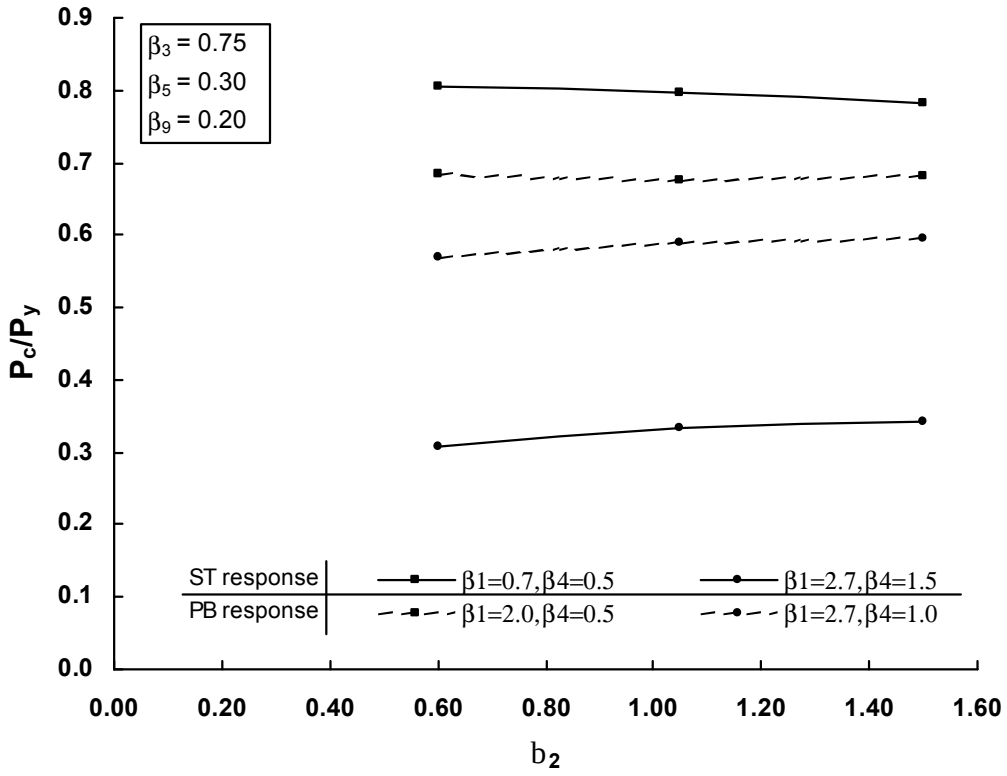

Figure 5.27 Effect of β_2 on strength of stiffened plates

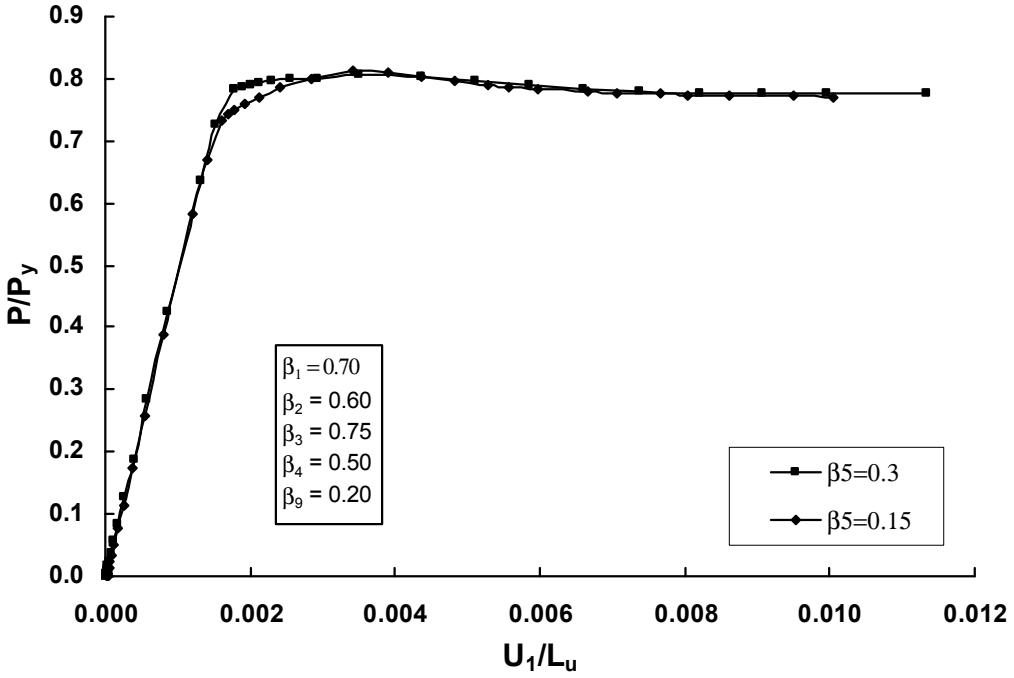

Figure 5.28 Effect of β_5 on the behaviour of plates failing by inelastic stiffener tripping

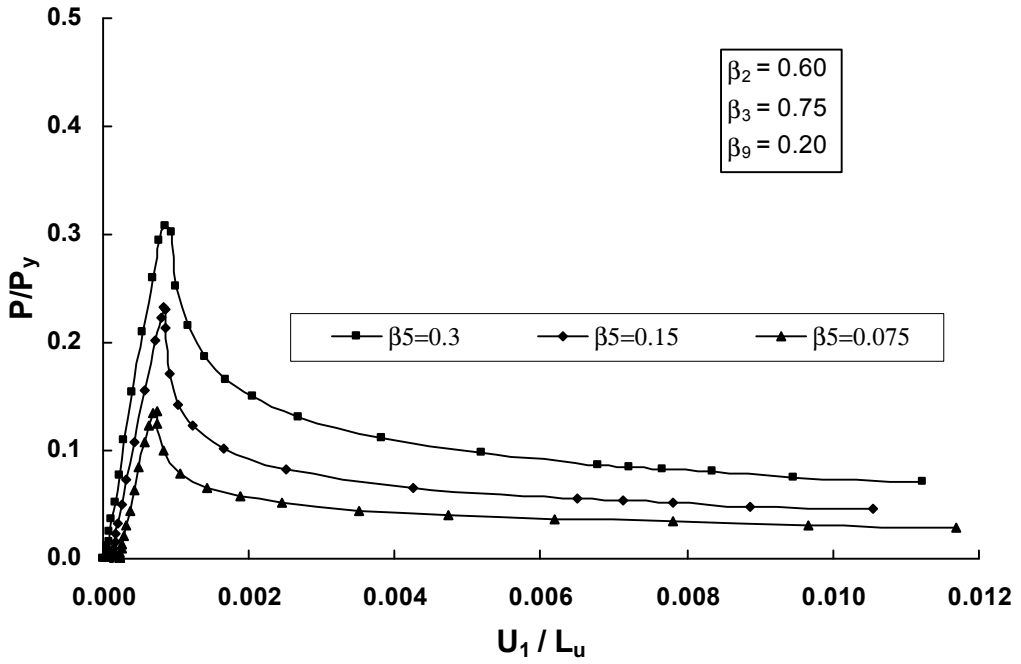

Figure 5.29 Effect of β_5 on the behaviour of plates failing by elastic stiffener tripping

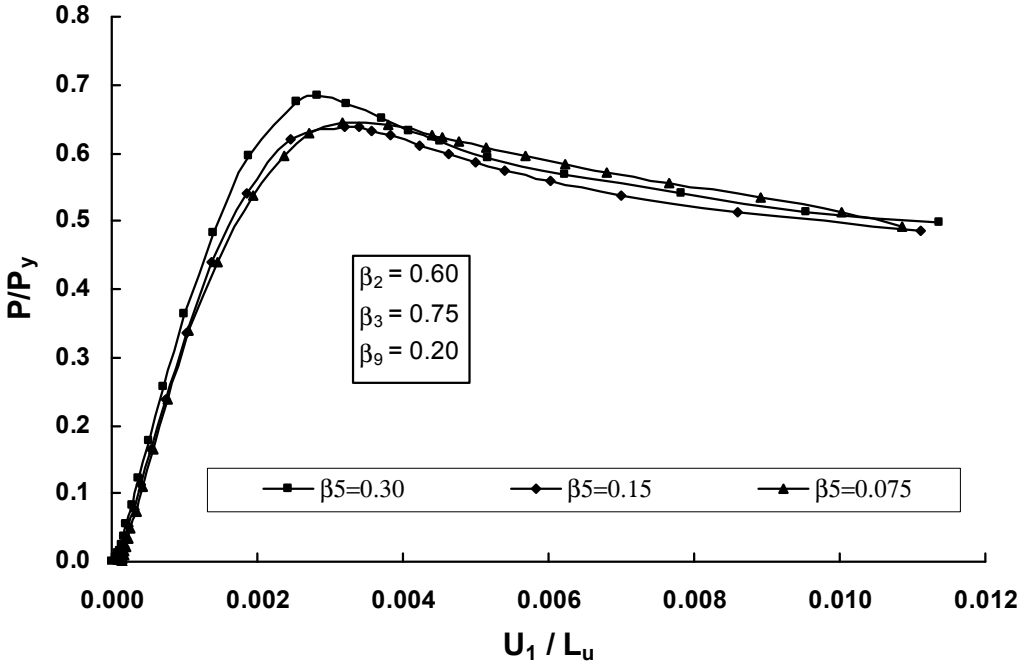

Figure 5.30 Effect of β_5 on the behaviour of plates failing by plate buckling ($\beta_1 = 2.0; \beta_4 = 0.5$)

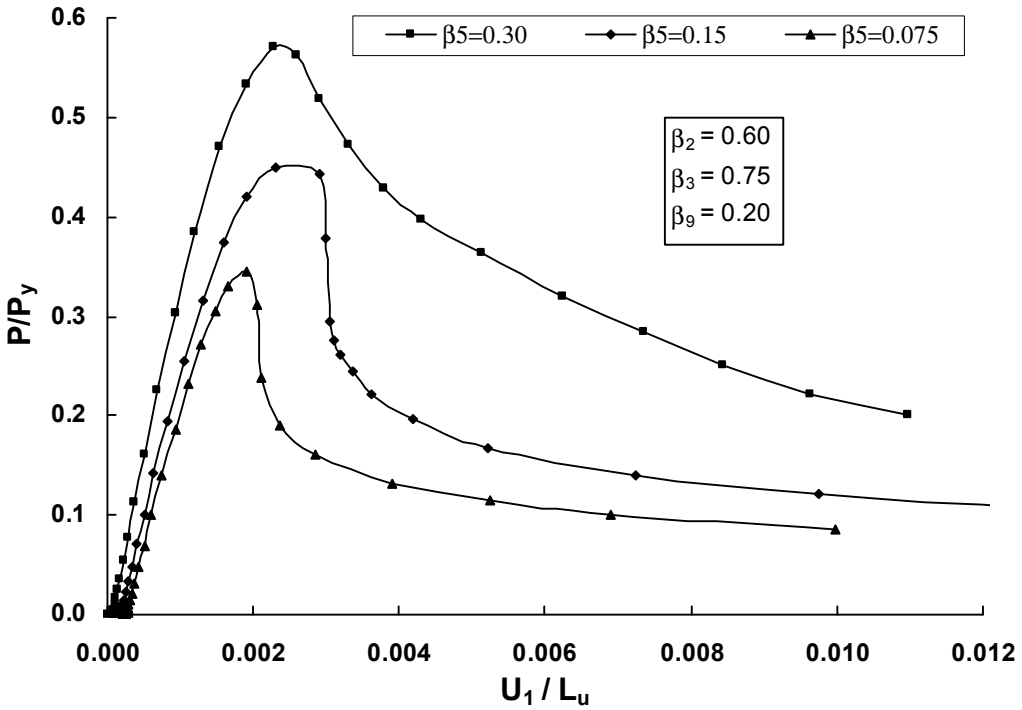

Figure 5.31 Effect of β_5 on the behaviour of plates failing by plate buckling ($\beta_1 = 2.7; \beta_4 = 1.0$)

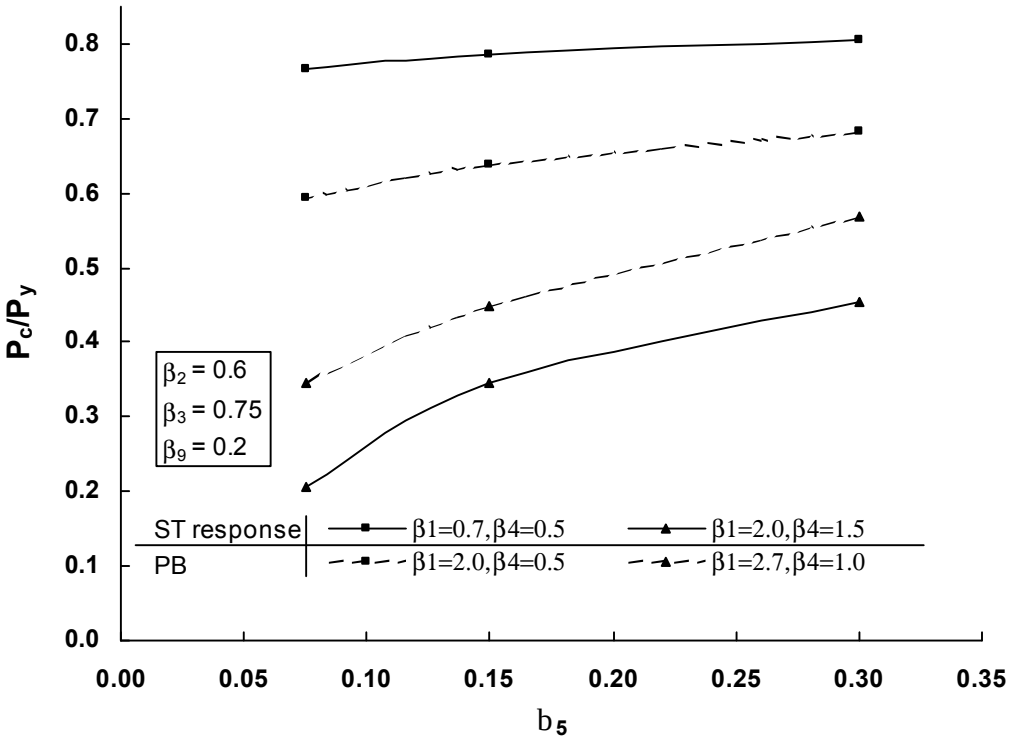

Figure 5.32 Effect of β_5 on the strength of stiffened plates

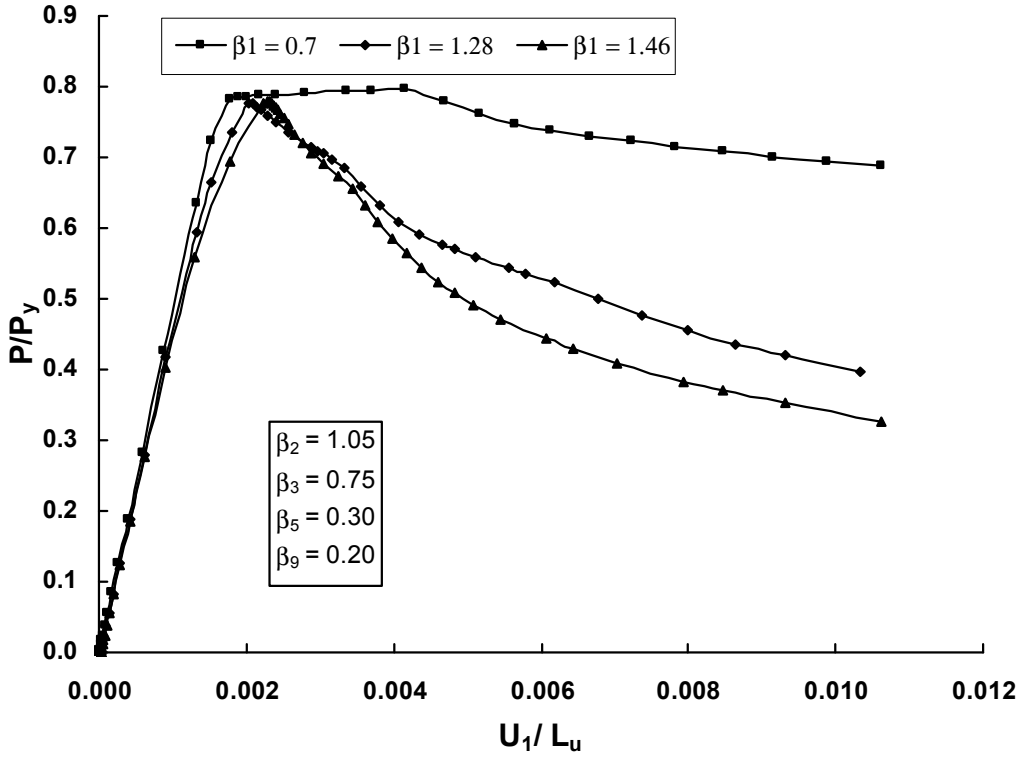

Figure 5.33 Effect of β_1 on the behaviour of plates failing by inelastic stiffener tripping

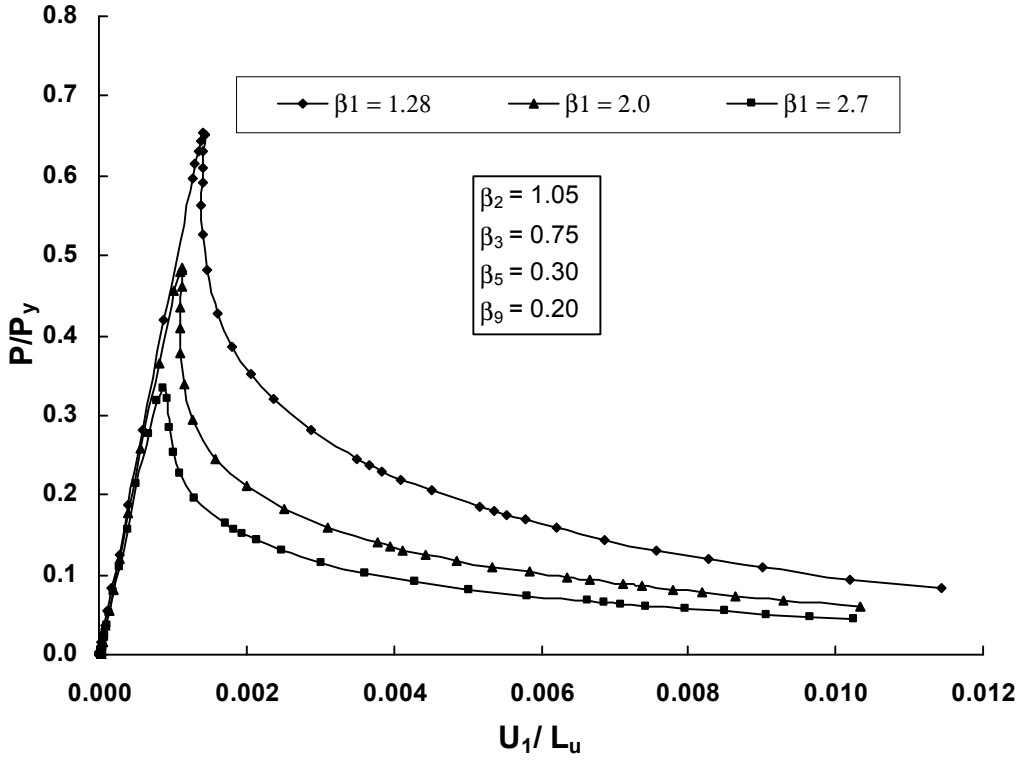

Figure 5.34 Effect of β_1 on the behaviour of plates failing by elastic stiffener tripping

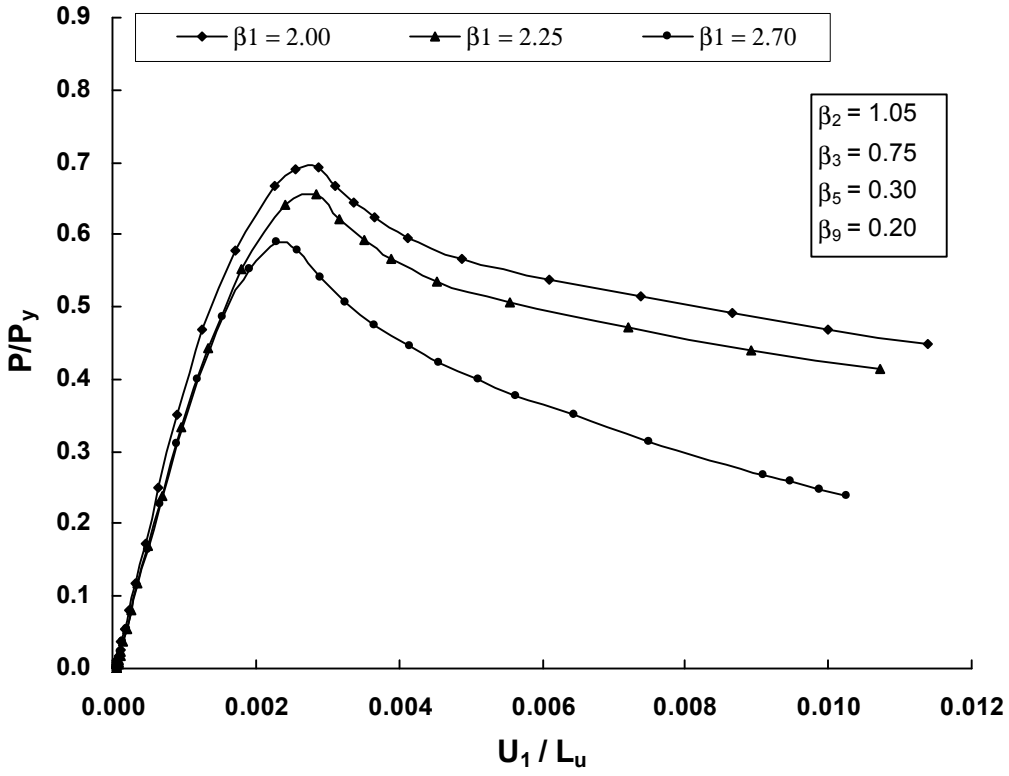

Figure 5.35 Effect of β_1 on the behaviour of plates failing by plate buckling ($\beta_4 = 0.5$)

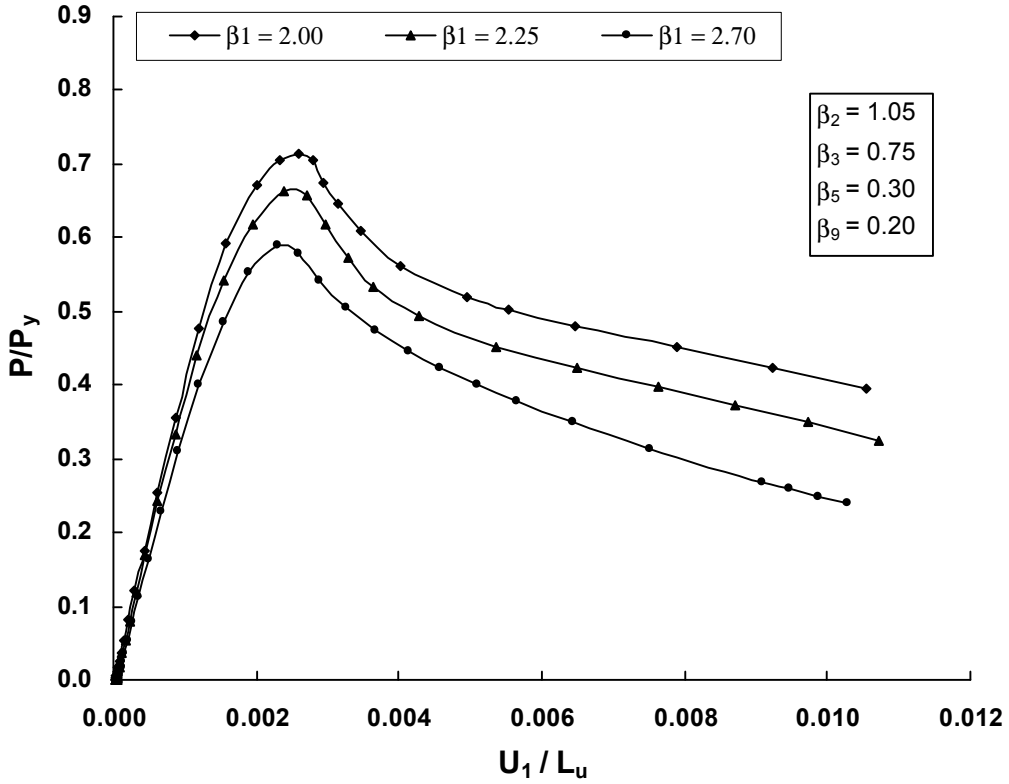

Figure 5.36 Effect of β_1 on the behaviour of plates failing by plate buckling ($\beta_4 = 1.0$)

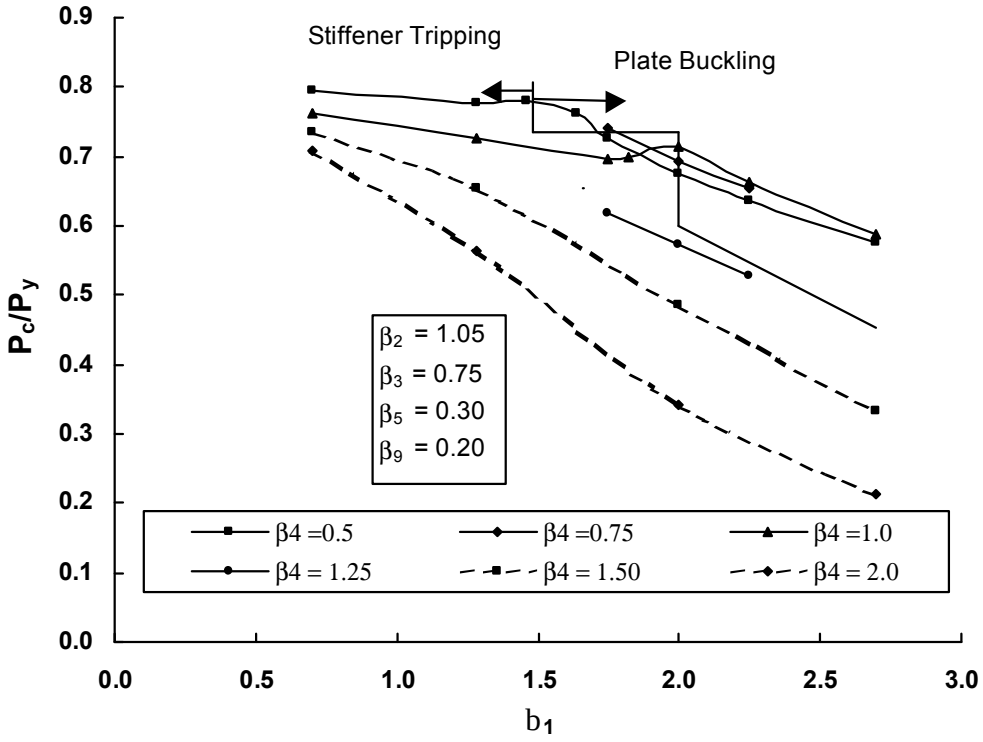

Figure 5.37 Effect of β_1 on the strength of stiffened plates

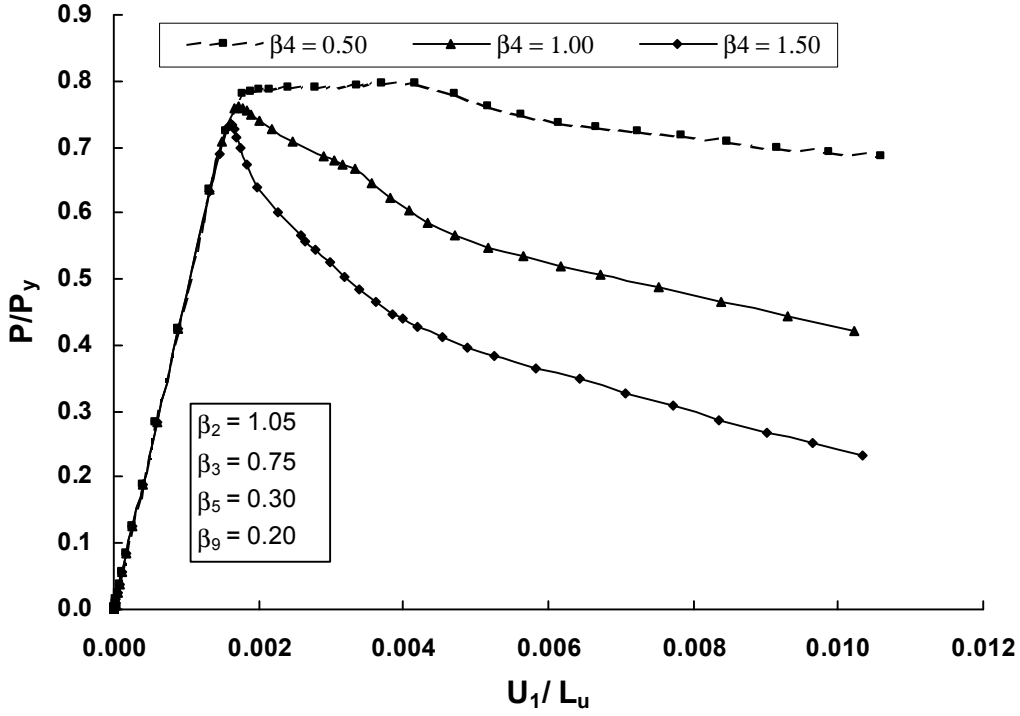

Figure 5.38 Effect of β_4 on the behaviour of plates failing by stiffener tripping ($\beta_1 = 0.70$)

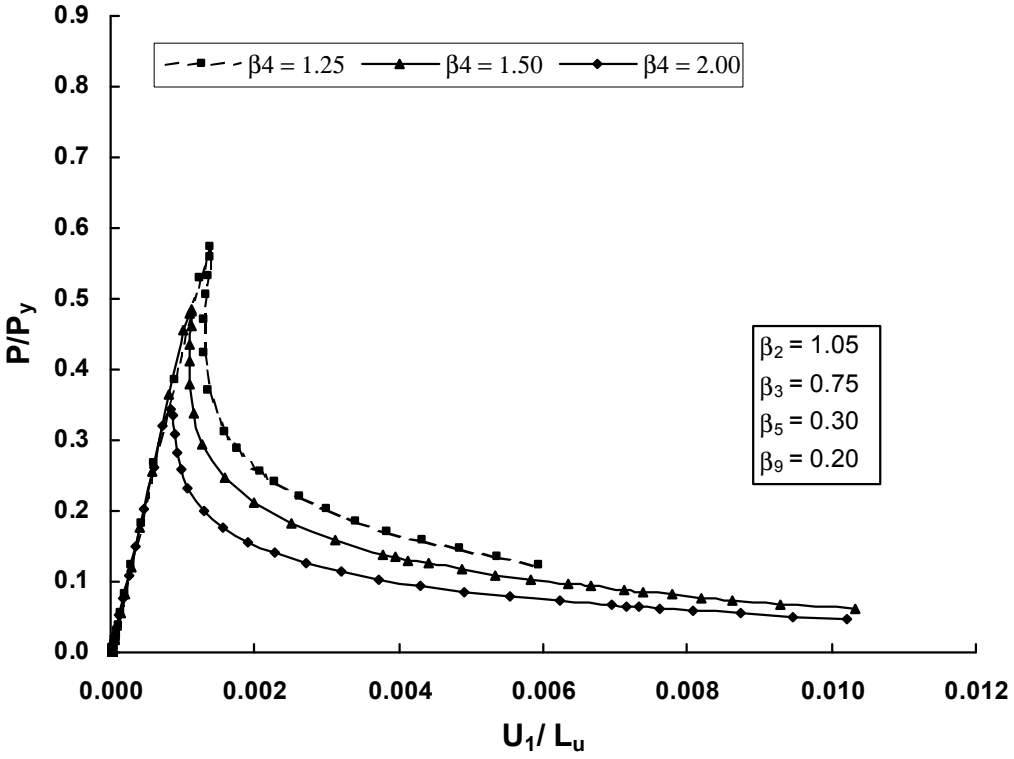

Figure 5.39 Effect of β_4 on the behaviour of plates failing by stiffener tripping ($\beta_1 = 2.0$)

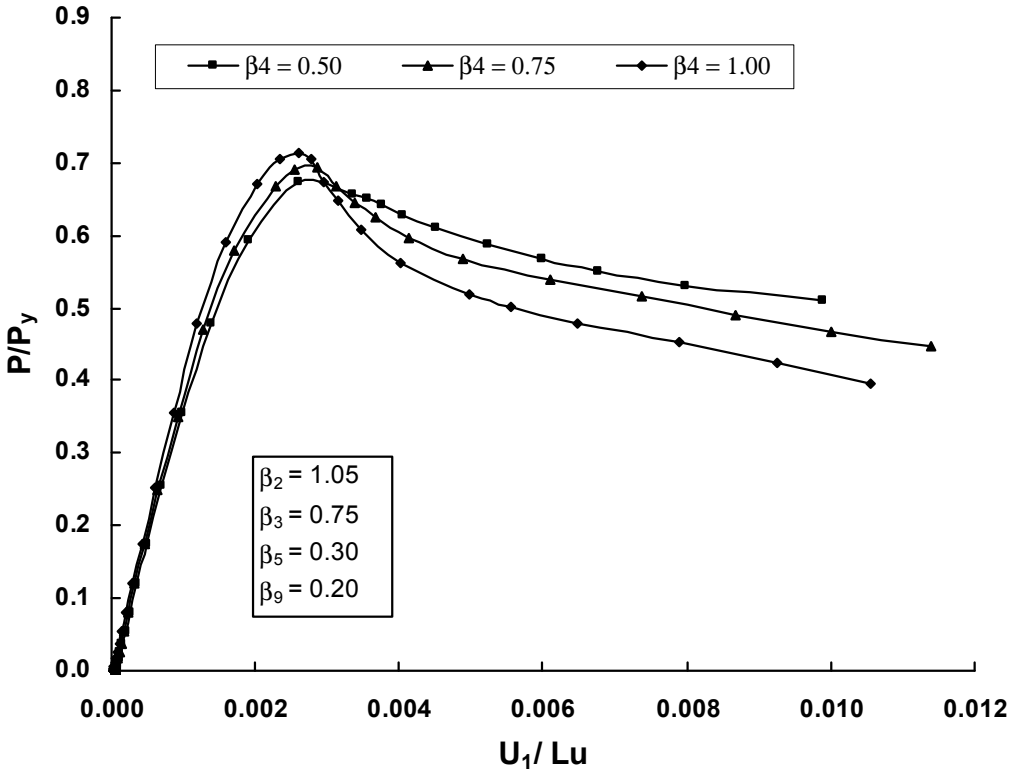

Figure 5.40 Effect of β_4 on the behaviour of plates failing by plate buckling ($\beta_1 = 2.0$)

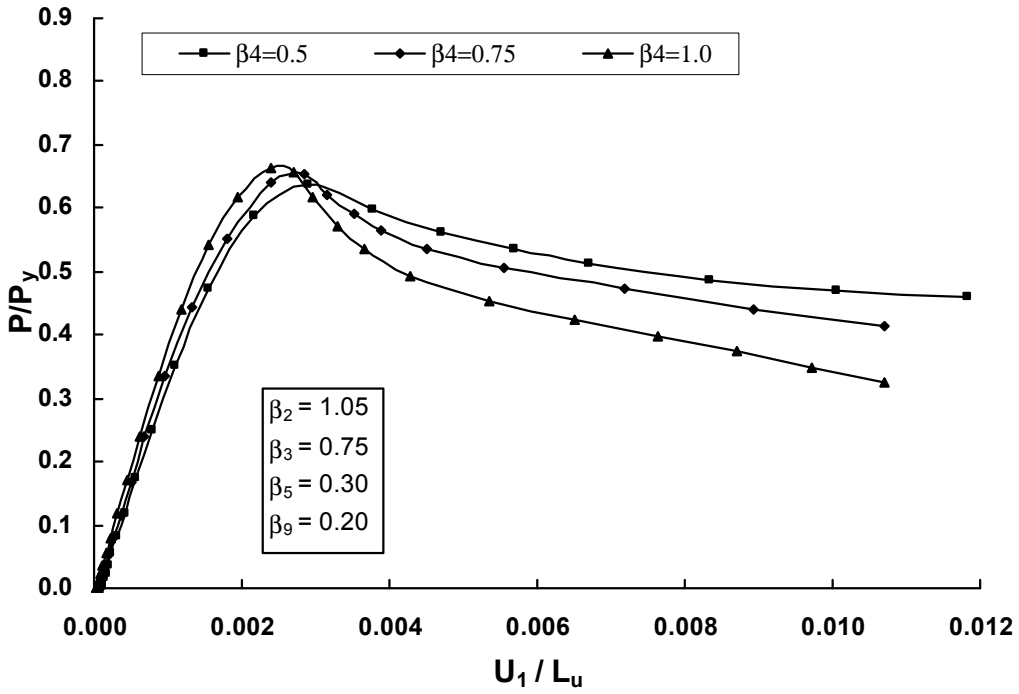

Figure 5.41 Effect of β_4 on the behaviour of plates failing by plate buckling ($\beta_1 = 2.25$)

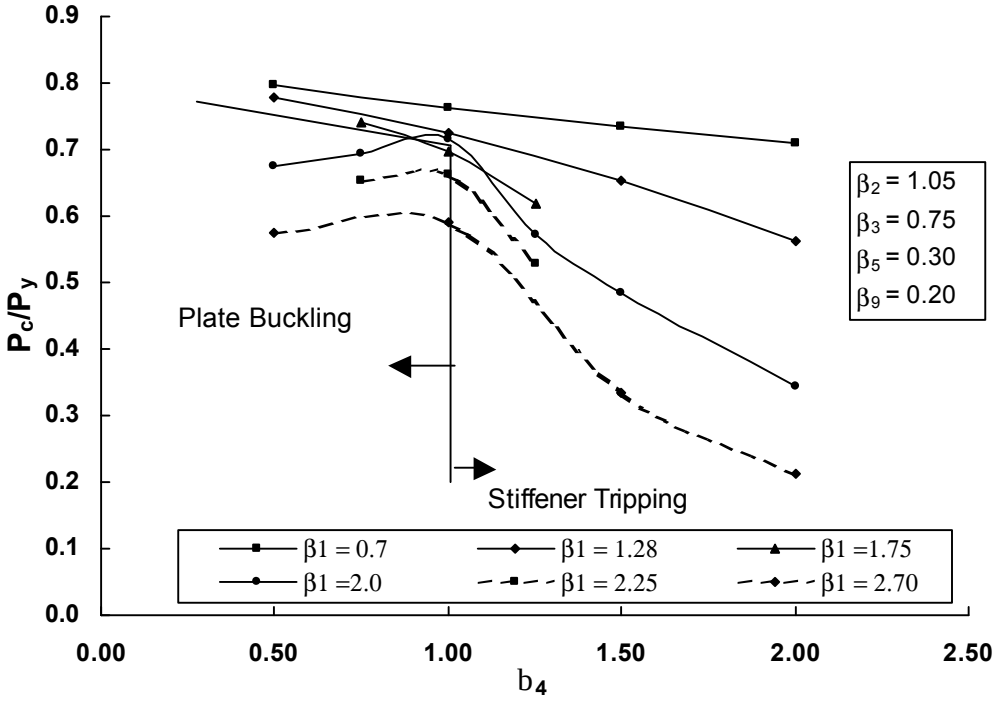

Figure 5.42 Effect of β_4 on the strength of stiffened plates

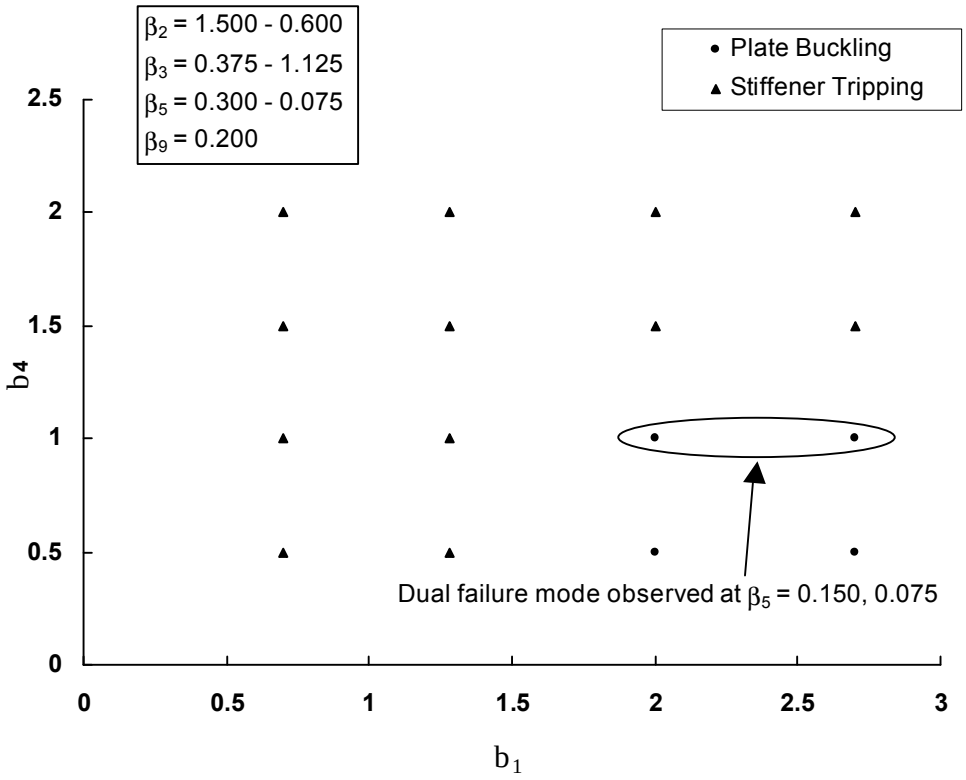

Figure 5.43 Observed failure modes under combined compression and bending

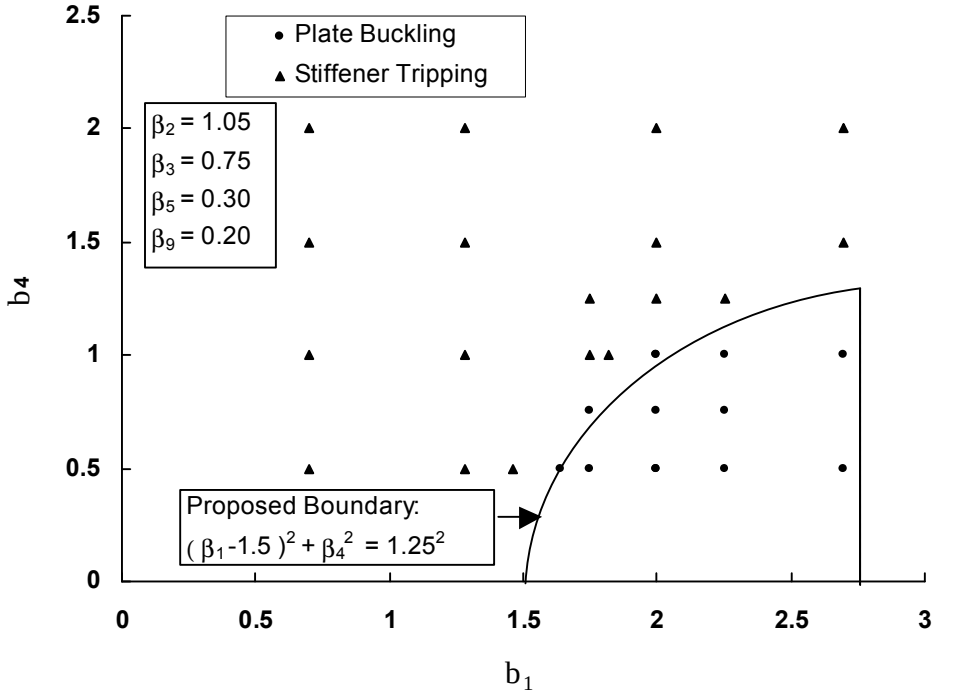

Figure 5.44 Proposed boundary between stiffener tripping and plate buckling for combined compression and bending

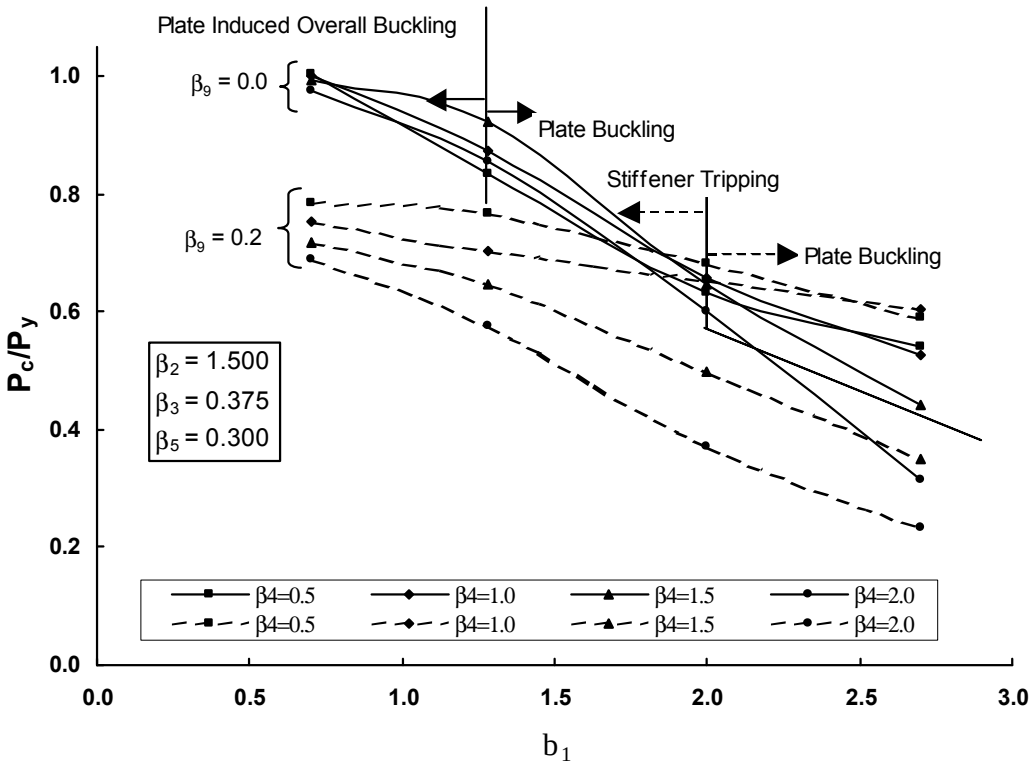

Figure 5.45 Effect of β_1 and β_9 on the strength of stiffened plates

CHAPTER 6

EVALUATION OF EXISTING DESIGN GUIDELINES

6.1 INTRODUCTION

The parameters characterising the behaviour and strength of stiffened steel plates were established in chapter 4. Chapter 5 presented a parametric study conducted using the geometric parameters proposed in chapter 4 for the uniaxial compression and combined compression and bending load cases. The objective of this chapter is to evaluate the existing design guidelines (DnV, 1995; and API, 1987) using the results of the parametric study presented in Chapter 5.

6.2 DESIGN GUIDELINES

The design guidelines proposed by Det Norske Veritas (DnV, 1995) and the American Petroleum Institute (API, 1987) were selected for this phase of the research program because they both provide a comprehensive procedure for computation of the buckling strength of stiffened steel plates. Only a brief summary of the part of the guidelines related to uniaxial compression and combined compression and bending case is presented in the following.

6.2.1 Det Norske Veritas CN no. 30.1(1995)

The analysis of stiffened steel plates presented in DnV classification notes no. 30.1 (1995) is based on the Perry-Robertson column approach. The approach makes use of an effective width concept whereby a single stiffener with an effective width of plate replaces a multiply stiffened plate. The Perry-Robertson column equation is based on first-yield criterion, i.e. the sum of applied axial stress and bending stress, amplified to account for initial imperfections, at the extreme fibre should not exceed the yield stress of the material. The resulting column equation for an imperfect column under axial load, in its simplest form, is given by:

$$\frac{P}{A}+\frac{P\Delta_0 y}{I\left[1-\frac{P}{P_{cr}}\right]}=s_0 \qquad (6.1)$$

where P is the applied axial load, A is area I is moment of inertia of the stiffened panel, y is distance of extreme fibre from the centroid of the stiffened panel, P_{cr} is the Euler buckling load of the column, Δ_0 is the magnitude of maximum initial imperfection in the column, and σ_0 is the extreme fibre stress in the stiffened panel.

With reference to the failure modes mentioned in Chapter 4, Perry-Robertson 'column' approach caters directly to plate and stiffener induced overall buckling mode. The effect of plate buckling in predicting plate and stiffener induced overall buckling mode is incorporated by reducing the plate width associated with each stiffener to an effective plate width. The plate panel effective width adopted by DnV (1995) depends on whether the failure of the stiffened plate is induced by the stiffener or by the plate and is given as:

for plate induced overall buckling:

$$\frac{b_{ep}}{b_p}=\frac{1.8}{b}-\frac{0.8}{b^2} \qquad \text{for } b \geq 1 \qquad (6.2)$$

$$\frac{b_{ep}}{b_p}=1 \qquad \text{for } b < 1 \qquad (6.3)$$

for stiffener induced overall buckling:

$$\frac{b_{ep}}{b_p}=1.1-0.1b \qquad \text{for } b \geq 1 \qquad (6.4)$$

$$\frac{b_{ep}}{b_p}=1 \qquad \text{for } b < 1 \qquad (6.5)$$

where b_{ep} is the effective plate width, b_p is the plate width and b is the plate transverse flexural slenderness, same as b_1 for this study.

For stiffener tripping failure, the elastic tripping stress replaces the extreme fibre stress in the stiffener used in Perry-Robertson's formula. The elastic tripping stress is given as:

$$\sigma_{ET} = b\frac{A_w + \left(\frac{t_f}{t_w}\right)^2 A_f}{A_w + 3A_f} G\left(\frac{t_w}{h_w}\right)^2 + \frac{2.6\pi^2 EI_z}{\left(\frac{A_w}{3} + A_f\right)L_u^2} \qquad (6.6)$$

where b is a factor that depends on stiffened panels cross-sectional dimensions and usage factor G is the shear modulus and E is the modulus of elasticity. The usage factor is defined as the ratio between the actual value of the reference stress due to design loading and the critical value of reference stress. It is taken as 1.0 for this study since the buckling condition is sought.

Equation 6.1 can, thus, be re-arranged to solve for the ultimate stress of an axially compressed imperfect column as:

$$\sigma_u = \frac{P_u}{A_e} = \frac{\sigma_{cre}}{2}\left[\left\{1 + w\left(\frac{\sigma_{oe}}{\sigma_{cre}} + \eta\right)\right\} - w\sqrt{\left\{1 + w\left(\frac{\sigma_{oe}}{\sigma_{cre}} + \eta\right)\right\}^2 - 4w\left\{\frac{\sigma_{oe}}{\sigma_{cre}}\right\}}\right] \qquad (6.7)$$

where,

A_e = Area of stiffened panel

σ_{cre} = Euler's elastic buckling stress of the effective column

σ_{oe} = Effective yield stress. It is taken as:

ι) Yield stress of material for stiffener induced and plate induced overall buckling modes

ii) Torsional buckling stress, found by applying Equation 6.7 on stiffener portion of the assembly, using elastic tripping stress (Equation 6.6) in place of Euler's elastic buckling stress, for stiffener tripping failure mode

w = Factor to account for direction of stresses

i) measured at extreme fibres on stiffener side for stiffener induced overall buckling and stiffener tripping failure modes

ii) measured at extreme fibre on plate side for plate induced overall buckling

= 1 (for compression), –1 (for tension)

η = Effective imperfection factor = $y\Delta_{0eff} / r_e^2$

where

Δ_{oeff} = effective imperfection magnitude

= function of (effective imperfection (column mode), loading eccentricity, specified camber or curvature)

r_e = radius of gyration of effective cross-section

y = extreme fibre distance

The plate buckling strength is found by determining the characteristic buckling resistance of the plate panel between stiffeners as:

$$s_{ucr} = \frac{s_k}{\sqrt{1+l^4}} \quad \text{if} \quad \lambda \le 1.0 \tag{6.8}$$

$$s_{ucr} = \frac{s_k}{l\sqrt{2}} \quad \text{if} \quad l < \lambda \le 5.0 \tag{6.9}$$

where

λ = $\sqrt{\frac{s_k}{s_E}}$ = reduced slenderness

where

σ_k = yield strength of the plate

$$\sigma_E = C\frac{p^2 E}{12(1-n^2)}\left(\frac{t_p}{b_p}\right)^2 \tag{6.10}$$

where C depends on the loading condition, aspect ratio of the plate panel and boundary conditions, E is Young's modulus of elasticity, n is Poisson's ratio, t_p is plate thickness and b_p is plate width between stiffeners.

The critical stress for all four failure modes, i.e. plate and stiffener induced overall buckling, plate buckling, and stiffener tripping, is found by the equations described above. The minimum critical stress value obtained from the above equations governs the capacity and the corresponding failure mode is the governing failure mode of stiffened plate.

The effect of applied bending moment is incorporated by adding the extreme fibre stress caused by the applied bending moment to the stress given in the above formulation

based on the section's properties (area, moment of inertia, centroid etc.) calculated for stiffener attached with effective plating (a plate whose width is reduced to take into account the effect of plate buckling, by applying Equations 6.2 through 6.5) and accounting for the P-δ effect.

6.2.2 American Petroleum Institute Bulletin 2V (1987)

API design guidelines for stiffened steel plates are based on the concept of reduced slenderness of the stiffened panel consisting of stiffener acting with plate of reduced width. The reduced plate width formulation is based on experimental results given by Faulkner, 1975. Classical strength of materials formulations (Timoshenko and Gere, 1961) are applied to find the buckling load for stiffened panel failing by plate and stiffener induced overall buckling and stiffener tripping failure modes.

For overall buckling modes (for buckling in the plane of symmetry):

$$P_E = \frac{P_y}{l^2} \tag{6.11}$$

where

$$\lambda = \left(\frac{KL_u}{r_e p}\right)\sqrt{\frac{f_y}{E}}$$

where K is the stiffened plate effective length factor, which is a function of the end boundary conditions, l_u is the length of the stiffened panel, r_e is the radius of gyration about the major axis of the effective stiffened panel (stiffener attached with effective plate width), f_y is the yield stress of the material and E is Young's modulus of elasticity for steel.

For sections containing only one plane of symmetry the ultimate limit state is governed by a combination of twisting and bending. Since these two actions cannot be decoupled, therefore, flexural torsional buckling load for the section is found. The flexural buckling load corresponds to overall buckling load (P_E) of the effective stiffened panel (Equation 6.11) and torsional buckling load (P_T) corresponds to torsional buckling load of the stiffener portion of stiffened panel alone found at stiffener to plate junction and is given as:

$$P_T = \left(\frac{A}{I_s}\right)\left(GJ + p^2 EC_w / L_u^2\right) \quad (6.12)$$

where

A = Area of cross-section of stiffener

I_s = Moment of inertia of stiffener about an axis parallel to plate surface at the base of stiffener

J = Torsion constant of stiffener

C_w = Warping constant of stiffener

Stiffener tripping load is obtained by finding the smallest root of following quadratic equation:

$$\frac{I_c}{I_s}P^2 - P(P_E + P_T) + P_E P_T = 0 \quad (6.13)$$

where

I_c = Polar moment of inertia of stiffener with attached effective plating about its centroid

I_s = Moment of inertia of stiffener about an axis parallel to plate surface at the base of stiffener

P_E = Overall buckling load for buckling parallel to plane of symmetry (Equation 6.11)

P_T = Torsional load of stiffener alone, calculated at the plate to stiffener junction (Equation 6.12)

P = Stiffener tripping load of stiffened panel

Inelastic effects for the stiffened panels whose capacity exceed the proportional limit (0.5 times yield strength set by API (1987)) in Equations 6.11 and 6.13 are incorporated by applying Ostenfeld-Bleich's parabola (Bleich, 1951) given as:

$$P_p = P_y\left[1 - \frac{p_r(1-p_r)}{P/P_y}\right] \quad (6.14)$$

where P_p is the inelastic capacity of the stiffened panel, P_y is the yield capacity of the stiffened panel, p_r is the proportional limit set for stiffened steel plates and P is either the overall buckling load obtained from Equation 6.11 or the stiffener tripping load obtained from Equation 6.13.

API (1987) also suggests dividing Equation 6.11 by a factor (y) to account for strain hardening effects on the overall buckling failure mode. The factor (y) is given as follows:

$$y = 0.165\sqrt{p_r}\,l + 0.835, 0 < l < \frac{1}{\sqrt{p_r}} \tag{6.15}$$

where p_r is proportional limit for the material (0.5) and l is the reduced slenderness of the stiffened panel (same as defined earlier in this section).

Plate buckling stress is found by applying plate effective width formulation based on the work of Faulkner (1975) and is given as:

$$f_u = f_y\left(\frac{2}{b} - \frac{1}{b^2}\right) \quad , \quad \text{for } b \geq 1 \tag{6.16}$$

$$f_u = f_y \quad , \quad \text{for } b < 1 \tag{6.17}$$

Equations 6.15 and 6.16 apply when plate edge stress reaches yield before stiffener fails, otherwise the following formulas should be used:

$$f_u = f_y\frac{1}{b} \quad , \quad \text{for } b \geq 1 \tag{6.18}$$

$$f_u = f_y \quad , \quad \text{for } b < 1 \tag{6.19}$$

where f_u is the plate buckling stress , f_y is yield strength of the material and b is the plate transverse flexural slenderness (same as b_1 for this study).

The failure mode giving the least value is the governing failure mode and the load corresponding to that failure mode is the critical load of the stiffened panel.

The effect of applied bending moment is incorporated for plate and stiffener induced overall buckling and stiffener tripping failure modes by applying beam-column interaction equation, modified to take into account second order effects and the effect of applied moments. For plate buckling failure mode, the stress at centre of plate is found by applying conventional beam theory (Timoshenko and Gere, 1961) and critical load is adjusted to give the plate buckling stress.

6.3 DISCUSSION

The guidelines are evaluated only for the geometric parameters that were found to affect both the behaviour and strength of stiffened plates in Chapter 5, i.e. plate transverse flexural slenderness, β_1, ratio of torsional slenderness of stiffener to plate transverse flexural slenderness, β_4 and stiffener to plate area ratio, β_5. Average values of β_2 (1.05), stiffener web slenderness, and β_3 (0.75), stiffener flange slenderness, are maintained for evaluating the guidelines because these two parameters were found to have negligible effect on stiffened plate behaviour and strength. Since it was found in Chapter 4 that the non-dimensional input parameter set ($\beta_1 - \beta_9$) is independent of scale, material strength and behaviour of stiffened plate, therefore, all the variables involved in stiffened steel plates problem (b_p, t_p, h_w, t_w, b_f, t_f, L_u, f_{yp}, f_{ys}, δ_p, δ_s, f_r, M_a) can be expressed as a function of material strength and the stiffener web tickness, t_w. Figure 6.1 shows a stiffened panel cross-sectional dimensions expressed as a function of the non-dimensional parameters, stiffener web thickness, t_w, and the material yield strength, f_y.

Code evaluation results are presented in Appendix A (Tables A.1 to A.12) with respect to β_1 and β_4, for both DnV (1995) and API (1987). The results are separated on the basis of load cases, i.e. uniaxial compression and combined compression and bending, and further on the basis of stiffener to plate area ratio. Peak strength ratio, predicted using the design guidelines (DnV, 1995; API, 1987) for all four common failure modes, i.e.

plate and stiffener induced overall buckling, plate buckling and stiffener tripping, along with critical load (the one giving minimum peak strength ratio) and governing failure mode (failure mode giving minimum peak strength ratio) is reported in Tables A.1 through A.12. Since both API (1987) and DnV (1995) guidelines give governing failure mode and peak strength ratio of a stiffened panel, therefore, only these two parameters are compared with finite element analysis results for this study.

The results of evaluation of design guidelines with respect to governing failure mode are listed in Appendix B (Tables B.1 to B.6). These tables present the comparison between the peak strength ratios obtained from finite element analysis with the peak strength ratios predicted by the design guidelines. The tables also present a comparison between the failure modes predicted by finite element analysis and the failure modes predicted by the design guidelines.

A summary of comparison of failure modes predicted by finite element analysis with the guidelines predicted failure modes is presented in Table 6.1. The table suggests that both design guidelines do not consistently predict finite element analysis failure mode. For uniaxial compression DnV (1995) predicted finite element analysis failure mode correctly at 4 out of 58 observations, whereas API (1987) was only able to predict finite element analysis failure at 2 out of 58 observations. For combined compression and bending case, DnV (1995) predicted finite element analysis failure modes correctly at 40 of 58 observations, whereas API (1987) predicted finite element analysis failure modes correctly at 25 out of 58 observations. Rigo *et al.* (1995) evaluated several stiffened steel plate design guidelines (including DnV (1987) and API (1987)) against available experimental results and made a similar observation.

Since both API (1987) and DnV (1995) do not consistently predict finite element analysis failure modes, the guidelines peak strength ratio for the finite element analysis failure mode was compared with finite element analysis predicted peak strength (Appendix C, Table C.1 to C.5). These tables are first sorted on the basis of load cases, i.e. uniaxial compression and combined compression and bending, and then on the basis of observed failure modes. A summary of this evaluation is presented in Table 6.2 (for

uniaxial compression case) and Table 6.3 (for combined compression and bending case). Since both guidelines do not predict any dual failure mode (failure mode characterised by plate induced overall buckling taking over plate buckling in the post-buckling range (Chapter 5)) the strength corresponding to the governing failure mode (the one giving the minimum strength ratio) for each guideline is used for cases for which finite element analysis predicted dual failure mode. A test to predicted ratio greater than 1.0 indicates the guideline predicts the strength conservatively and a value less than 1.0 indicates that it predicts the strength unconservatively. The mean and standard deviation of finite element analysis to predicted ratio was also calculated as a measure of the accuracy of the guidelines (DnV, 1995; API, 1987) for the strength prediction over the full range of parameters investigated. The results of this evaluation are discussed in detail in the following.

6.3.1 Uniaxial Compression

A finite element analysis of stiffened steel plates indicated that stiffened plates loaded in uniaxial compression can fail in one of three modes (Chapter 5): plate induced overall buckling, plate buckling, and a failure mode characterized by the interaction between plate buckling and overall buckling. A summary of the comparison of finite element analysis peak strength with the strength predicted by current guidelines (API, 1987; DnV, 1995) is presented in Table 6.2.

The mean and standard deviation of finite element analysis to predicted strength ratio, for the uniaxial compression case, indicate that DnV predicts the capacity for plate induced overall buckling accurately (mean ratio of finite element prediction to guideline prediction of 1.01 and standard deviation of 0.02), whereas API (1987) is unconservative, with a mean ratio of finite element prediction to guideline prediction of 0.88 and standard deviation of 0.02.

Table 6.2 indicates that the prediction of the plate buckling capacity, using DnV (1995), is not as accurate as it was observed for the plate induced overall buckling mode and it errs on the unconservative side (mean ratio of 0.89 and standard deviation of 0.08). API (1987) gives mainly conservative predictions for plate buckling failure mode.

The predictions are significantly variable (mean ratio of finite element prediction to guideline prediction of 1.13 and standard deviation of 0.12).

Both guidelines are not able to predict accurately the capacity of stiffened steel plates that failed by the dual failure mode. The mean and standard deviation of finite element analysis to predicted strength, for uniaxial compression case, for dual failure mode was found to be 1.75 and 0.48 for DnV (1995) and 1.72 and 0.58 for API (1987) respectively. Both guidelines, (DnV, 1995; API, 1987) are very conservative in predicting the strength of dual failure mode. Moreover they are not able to predict the dual mode failure strength with any degree of accuracy.

6.3.2 Combined Compression and Bending

Finite element analysis indicated that stiffened steel plates loaded in combined compression and bending can fail in one of three modes (Chapter 5), for the range of parameters investigated: stiffener tripping, plate buckling and dual failure mode. A summary of the comparison of finite element analysis peak strength with the strength predicted by current guidelines (API, 1987; DnV, 1995), for finite element analysis failure mode, is presented in Table 6.3 and is discussed in the following:

The mean and standard deviation of finite element analysis to predicted strength ratio, for stiffener tripping failure mode was found to be 1.23 and 0.25, respectively, for DnV (1995) and 0.98 and 0.29, respectively, for API (1987). DnV (1995) is conservative and inconsistent in predicting the strength of the stiffener tripping failure mode, whereas API seems to be more accurate on average (with a mean ratio of 0.98), but the large standard deviation (0.29) indicates that it is unreliable. This suggests that both design guidelines need to be revisited for the stiffener tripping failure mode.

The mean and standard deviation of finite element analysis to predicted strength ratio for plate buckling failure mode, for the combined compression and bending case, was found to be 0.75 and 0.05 for DnV (1995) and 1.17 and 0.03 for API (1987). DnV (1995) is unconservative in predicting the strength whereas API (1987) is

conservative. Both guidelines, however, show a relative low standard deviation of strength ratio.

The ability of both guidelines to predict dual failure mode capacity under combined compression and bending is again poor as shown by the large mean strength value (2.05 and 2.21 for DnV and API, respectively) and the large standard deviation (0.45 and 0.10 for DnV and API, respectively). Since, both guidelines are very conservative in predicting the strength of dual failure mode, therefore, new design guidelines that specifically addresses the dual failure mode needs to be formulated for both the uniaxial compression and combined compression and bending cases.

Table 6.1 Summary of observed (finite element analysis) and correctly predicted failure modes

Failure mode*	FEA	DnV (1995)	API (1987)
Uniaxial Compression			
Total number of observations = 58			
PI	10	0	0
SI	0	0	0
PB	23	4	2
ST	0	0	0
DFM	25	0	0
Combined Compression and Bending			
Total number of observations = 58			
PI	0	0	0
SI	0	0	0
PB	14	0	3
ST	40	40	22
DFM	4	0	0

* SI : Stiffener induced overall buckling
PI : Plate induced overall buckling
PB : Plate buckling
ST : Stiffener tripping
DFM : Dual failure mode

Table 6.2 Summary of evaluation of existing guidelines for uniaxial compression

	$P_{c\ FEA} / P_{c\ code}$	
	DnV (1995)	**API (1987)**
Plate induced overall buckling; Number of observations = 10		
Mean	1.01	0.88
Standard deviation	0.02	0.02
Plate buckling; Number of observations = 23		
Mean	0.89	1.13
Standard deviation	0.08	0.12
Dual mode failure; Number of observations = 25		
Mean	1.75	1.72
Standard deviation	0.48	0.58
Overall summary for uniaxial compression; Number of observations = 58		
Mean	**1.25**	**1.37**
Standard deviation	**0.46**	**0.47**

Table 6.3 Summary of evaluation of existing guidelines for combined compression and bending

	$P_{c\ FEA} / P_{c\ code}$	
	DnV (1995)	**API (1987)**
Stiffener tripping; Number of observations = 40		
Mean	1.23	0.98
Standard deviation	0.25	0.29
Plate buckling; Number of observations = 14		
Mean	0.75	1.17
Standard deviation	0.05	0.03
Dual failure mode; Number of observations = 4		
Mean	2.05	2.21
Standard deviation	0.45	0.10
Overall summary for combined compression and bending; Number of observations = 58		
Mean	**1.17**	**1.11**
Standard deviation	**0.34**	**0.34**

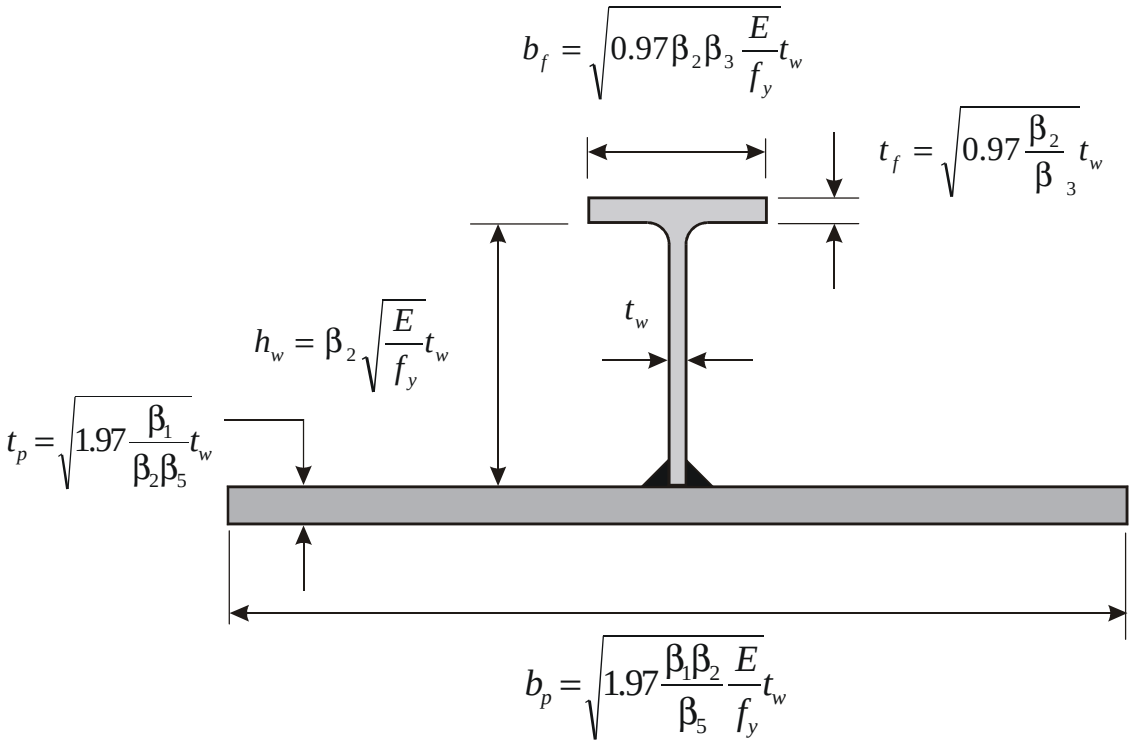

Figure 6.1 Stiffened plate dimensions expressed as a function of β-parameters, yield strength and stiffener web thickness

CHAPTER 7

SUMMARY, CONCLUSIONS AND RECOMMENDATIONS

7.1 SUMMARY

Thin steel plates that are stabilised in one direction by stiffeners form an integral part of many structural systems in which a high strength-to-weight ratio is important. This type of structural system has to resist in-plane compression and combined compression and bending loads. Under the action of compressive axial forces and bending moments, stiffened panels are susceptible to failure by instability. Instability of stiffened plates under uniaxial compression or under combined bending and compression can take one of four forms: plate induced overall buckling (PI), stiffener induced overall buckling (SI), plate buckling (PB) and stiffener tripping (ST). Test results (Grondin et al., 1998; Murray, 1973) have indicated that stiffener tripping failure mode is more critical than the plate buckling failure mode because it is associated with a sudden drop in capacity. Current design guidelines do not adequately address the stiffener tripping failure mode because they are based on certain simplified assumption not applicable over the full practical range of parameters that govern stiffened plates behaviour. The intent of the study presented in this report has been to determine the parameters that will trigger the stiffener tripping failure mode.

As a first step towards achieving this goal, a dimensional analysis was performed to identify the parameters that characterise the behaviour and strength of the stiffened steel plates. The analysis was performed using a finite element model developed earlier and validated by comparison with full-scale test results. The parameters were divided into geometric, material properties, loading and deformation parameters. The dimensionless parameters were selected from the literature and were investigated for all ranges of material response and all possible failure modes of stiffened steel plates under uniaxial compression and combined compression and bending. The parameters selected were: plate transverse flexural slenderness, stiffener web slenderness, stiffener flange slenderness, ratio of stiffener torsional slenderness to plate transverse flexural

slenderness, stiffener to plate area ratio, initial plate imperfection, initial stiffener imperfection, plate compressive residual stress, applied to plastic moment ratio, peak to yield load ratio and axial shortening to unsupported length ratio. The validity of the parameters was then established by conducting a series of analysis where the scale of the specimen were changed without changing the value of the dimensionless parameters. The selected parameter set was found to be able to predict the behaviour and strength of the stiffened steel plates for different scales of the model.

A practical range of selected parameter set was then established from a literature review. The selected parameters set was then analysed under uniaxial compression for "average" (Smith et al., 1991) magnitude of plate and stiffener initial imperfections, "severe" (Smith et al., 1991) magnitude of plate compressive residual stresses and least stable stiffener's geometric configuration, i.e. slender web and a stocky flange. The effect of plate transverse flexural slenderness, ratio of torsional slenderness of stiffener to plate transverse flexural slenderness and stiffener to plate area ratio on behaviour and strength of stiffened steel plates under uniaxial compression was found.

Three types of failure were observed for stiffened plates under uniaxial compression, namely, plate induced overall buckling, plate buckling, and a dual failure mode characterised by plate induced overall buckling taking over the plate buckling failure mode in the post-buckling range. This type of failure mode resulted in a loss of peak strength as well as an abrupt drop in the post-buckling response of the stiffened steel plates.

The plate transverse flexural slenderness, β_1, was found to be the most influential parameter affecting the strength and behaviour of stiffened steel plates for all the failure modes observed for uniaxial compression case. The ratio of stiffener torsional slenderness to plate transverse flexural slenderness, β_4, and stiffener to plate area ratio, β_5, showed no effect on the strength of stiffened plates failing by either plate buckling or plate induced overall buckling. The dual failure mode was, however, affected by β_4 and β_5. A decrease in strength as well as post-buckling response was observed with an increase in β_4 and a decrease in β_5.

Three types of failure modes were observed for plates under combined compression and bending, namely, stiffener tripping, plate buckling, and, for a very limited number of cases, dual failure mode. The plate transverse flexural slenderness, β_1, was found to be the most influential parameter affecting both the strength and behaviour of stiffened steel plate for all the failure modes observed under combined compression and bending. An increase in β_1 results in a decrease in strength for all the failure modes observed.

The stiffener web and flange slenderness showed no effect on the strength of stiffened steel plates. It only affected the post-buckling strength of stiffened steel plates failing by stiffener tripping failure mode. A decrease in post-buckling strength was observed with an increase in stiffener web or flange slenderness.

The ratio of stiffener torsional slenderness to plate transverse flexural slenderness, β_4, affected both the strength and behaviour of stiffened plates failing by stiffener tripping. A decrease in peak strength and post-buckling response was observed with an increase in β_4 for stiffened plates failing by stiffener tripping.

The stiffener to plate area ratio, β_5, affected neither the strength nor the behaviour of stocky plates stiffened with stocky stiffeners for both the stiffener tripping and plate buckling failure modes. A decrease in both the peak strength and post-buckling response for stiffener tripping was observed with the decrease in β_5, for slender plates stiffened with slender stiffeners.

Design guidelines that provide the most comprehensive approach for the design of stiffened steel plates (API, 1987; DnV, 1995) were compared with the finite element analysis results. The guidelines were not able to predict the failure modes predicted by the finite element analysis with any degree of consistency for both uniaxial compression and combined compression and bending cases.

The design guidelines (API, 1987; DnV 1995) were able to predict the strength of stiffened plates failing by plate induced overall buckling and plate buckling modes reasonably accurately. The mean and standard deviation of finite element analysis to

predicted strength ratio, for the uniaxial compression case, indicates that DnV predicts the capacity for plate induced failure very accurately (mean ratio of 1.01 and standard deviation of 0.02) whereas the API guideline is unconservative, with a mean ratio of 0.88 and standard deviation of 0.02.

The prediction of the plate buckling capacity for uniaxial compression case, using DnV (1995), was not as accurate as it was observed for the plate induced overall buckling mode and it erred on the unconservative side (mean of 0.89 and standard deviation of 0.08). API (1987) gives mainly conservative predictions for plate buckling failure mode, the predictions are significantly variable (mean ratio of finite element prediction to guideline prediction of 1.13 and standard deviation of 0.12). The mean and standard deviation of finite element analysis to predicted strength ratio for plate buckling failure mode, for the combined compression and bending case, was found to be 0.75 and 0.05 respectively, for DnV (1995), and 1.17 and 0.03 respectively, for API (1987).

Both guidelines were not able to predict accurately the capacity of stiffened steel plates that failed by the dual failure mode. The mean and standard deviation of finite element analysis to predicted strength, for uniaxial compression case, for dual failure mode was found to be 1.75 and 0.48 respectively, for DnV (1995), and 1.72 and 0.58 respectively, for API (1987). The ability of both guidelines to predict dual failure mode capacity under combined compression and bending was found to be poor as shown by large mean strength value (2.05 for DnV (1995) and 2.21 for API (1987)) and large standard deviation (0.45 for DnV (1995) and 0.10 for API (1987)).

The mean and standard deviation of the finite element analysis to predicted strength ratio, for stiffener tripping failure mode, for combined compression and bending case, was found to be 1.23 and 0.25 respectively, for DnV (1995), and 0.98 and 0.29 respectively, for API (1987). DnV (1995) is unconservative and inconsistent in predicting the strength of the stiffener tripping failure mode, whereas API (1987) seems to be more accurate on average (with a mean ratio of 0.98), but the large standard deviation (0.29) indicates that it is unreliable. This suggests that both design guidelines need to be revisited for the stiffener tripping failure mode.

7.2 CONCLUSIONS

Considerable progress has been made towards the understanding of various buckling modes in stiffened steel plate. The following conclusions can be drawn from the numerical investigation carried out:

1. The behaviour of stiffened steel plates can be uniquely characterised by the plate transverse flexural slenderness, stiffener web slenderness, stiffener flange slenderness, ratio of stiffener torsional slenderness to plate transverse flexural slenderness, stiffener to plate area ratio, initial plate imperfections, initial stiffener imperfections, plate compressive residual stresses, applied to plastic moment ratio, peak to yield load ratio and axial shortening to unsupported panel length ratio.

2. The strength of stiffened steel plates failing by plate buckling and plate induced overall buckling failure modes is mainly governed by the plate transverse flexural slenderness ratio.

3. A dual failure mode, characterised by plate induced overall buckling following plate buckling in the post-buckling range, was identified in this study. This failure mode is a potentially severe failure mode, which results in a decrease of peak strength and an abrupt loss of capacity of stiffened plate structures. Dual failure mode takes place depending on the plate transverse flexural slenderness, stiffener to plate area ratio and, to some extent, on the ratio of stiffener torsional slenderness to plate transverse flexural slenderness.

4. Stiffener tripping failure mode is only triggered when a bending moment is applied to place the stiffener flange in compression. Stiffener tripping failure mode primarily depends on the ratio of stiffener torsional slenderness to plate transverse flexural slenderness,β_4 and plate transverse flexural slenerness, β_1. The boundary between stiffener tripping to plate buckling can be defined as:

   Stiffener tripping if $(\beta_1 - 2.75)^2 + \beta_4^2 > 1.25^2$

   Plate buckling if $(\beta_1 - 2.75)^2 + \beta_4^2 < 1.25^2$

5. Stiffener flange slenderness and stiffener web slenderness only affect the post-buckling strength of stiffened plates failing by stiffener tripping failure mode.

6. The stiffener to plate area ratio affects only the strength of stiffened steel plate failing by stiffener tripping and dual failure mode.

7. The current DnV (1995) and API (1987) design guidelines for stiffened steel plates are not able to predict the behaviour (failure mode) and strength of stiffened steel plates with reasonable degree of accuracy. Furthermore, these guidelines do not provide any formulation for dual failure mode.

7.3 RECOMMENDATIONS

This study concentrated only on the geometric parameters alone, the scope of the current study needs to be broadened to include the effect of other parameters affecting the behaviour and strength of stiffened steel plates, i.e. deformation and loading parameters. Only one set of deformation parameters, i.e. initial plate ("average", Smith et al., 1991) and stiffener ("average", Smith et al., 1991) imperfection, was investigated for this study. The other magnitudes, i.e. "slight" and "severe", and their combinations, e.g. "slight" imperfection in plate and "severe" imperfection in stiffener should also be investigated. A wider range of loading parameters, i.e. residual compressive stresses in plate ("slight" and "average") and applied bending moment should be investigated. The effect of other loading conditions, i.e. transverse and biaxial compression, shear, and combinations of shear and uniaxial or biaxial compression, need to be investigated.

Although the finite element model used for this investigation had been validated by comparison with full-scale test specimens, some of the results obtained herein should be investigated experimentally. The behaviours that should be investigated experimentally are:

- The dual failure mode;

- The effect of the ratio of stiffener torsional slenderness to plate transverse flexural slenderness on the stiffener tripping failure mode;
- The proposed parameter set (β_1 to β_{11}) should be tested experimentally for scale effects.

Based on the numerical study, backed by experimental results, design guidelines that are able to predict the behaviour and strength for stiffened steel plates need to be formulated.

REFERENCES

American Petroleum Institute (1987). Bulletin on Design of Flat Plate Structures, API Bulletin 2V, First Edition, May 1, 1987, Washington, D.C.

Balaz, I. and Murray, N.W. (1992). A Comparison of Some Design Rules with Results from Tests on Longitudinally Stiffened Deck Plates of Box Girders, Journal of Constructional Steel Research, Vol. 23, pp. 31 – 54.

Bedair, O.K. and Sherbourne, A.N. (1993). Plate Stiffener Assemblies in Uniform Compression. Part I: Buckling, Journal of Engineering Mechanics, ASCE, Vol. 119, No. 10, pp. 1937 – 1972.

Bleich, F. (1951). Buckling Strength of Metal Structures, McGraw Hill, N.Y.

Bonello, M.A. ,Chryssanthopouls, M.K., and Dowling, P.J. (1993). Ultimate Strength Design of Stiffened Plates under Axial Compression and Bending, Marine Structures, Vol. 6, pp. 533 – 552.

Brosowski, B. and Ghavami, K. (1997). Multi-Criteria Optimal Design of Stiffened Plates Part II, Mathematical Modelling of the Optimal Design of Longitudinally Stiffened Plates, Thin-Walled Structures, Vol. 28, No. 2, pp. 179 – 198.

Brosowski, B. and Ghavami, K. (1996). Multi-Criteria Optimal Design of Stiffened Plates. Part 1. Choice of the Formula for the Buckling Load, Thin-Walled Structures, Vol. 24, No. 4, pp. 353 – 369.

Canadian Standards Association (1994). CAN/CSA – S16.1- 94 – Limit State Design of Steel Structures, Canadian Standards Association, Toronto, Ontario.

Caridas, P.A. and Frieze, P.A. (1988). Flexural-Torsional Elastic-Plastic Buckling in Flat Stiffened Plating using Dynamic Relaxation. Part I: Theory, Thin-Walled Structures, Vol. 6, No.6, pp. 458 – 481.

Carlsen, C.A. (1980). A Parametric Study of Collapse of Stiffened Plates in Compression, The Structural Engineer, Vol. 58B, No. 2, pp. 33 – 40.

Carlsen, C.A. and Czujko, J. (1978). The Specification of Post Welding Distortion Tolerances for Stiffened Plates in Compression, The Structural Engineer, Vol. 56A, No. 5, pp. 133 – 141.

Carlsen, C.A. (1977). Simplified Collapse Analysis of Stiffened Plates, Norwegian Maritime Research, No. 4, pp. 20 – 36.

Chapman, J.C., Smith, C.S., Davidson, P.C., Dowling, P.J. (1991). Recent Developments in the Design of Stiffened Plate Structures, Advances in Marine Structures-2, pp. 529 – 548.

Chen, Q., Kulak, G.L., Elwi, A.E. and Cheng, J.J.R. (1993). Bending Strength of Longitudinally Stiffened Steel Cylinders, University of Alberta, Department of Civil Engineering, Structural Engineering Report No. 192.

Danielson, D.A., Kihl, D.P., and Hodges, D.H. (1990). Tripping of Thin-Walled Plating Stiffeners in Axial Compression, Thin-Walled Structures, Vol. 10, pp. 121 – 142.

Davidson, P.C., Chapman, J.C., Smith, C.S. and Dowling, P.J. (1989). The Design of Flat Plate Panels Subject to In-Plane Shear and Biaxial Compression, The Royal Institute of Naval Architecture, pp. 267 – 286.

Det Norske Veritas (1995). Classification Notes No. 30.1, Buckling Strength Analysis, Det Norske Veritas, Hovik, Norway.

Faulkner, D. (1975). A Review of Effective Plating for use in the Analysis of Stiffened Plating in Bending and Compression, Journal of Ship Research, Vol. 19, No. 1, pp. 1 – 17.

Faulkner, D., Adamchak, J. and Snyder, G.J. and Vetter, M.F. (1973). Synthesis of Welded Grillages to withstand Compression and Normal Loads, Computers and Structures, Vol. 3, pp. 221 – 246.

Fujikobo, M. and Yao, T. (1999). Elastic Local Buckling Strength Stiffened Plates Considering Plate/Stiffener Interaction and Welding Residual Stress, Marine Structures, Vol. 12, pp. 543 – 564.

Ghavami, K. (1994). Experimental Study of Stiffened Plates in Compression up to Collapse, Journal of Constructional Steel Research, Vol. 28, pp. 197 – 221.

Ghoneim, G. A. and Tadros, G. (1992). Finite Element Analysis of Damaged Ship Hull Structures, OMAE - Offshore Technology, Vol. 1-B, pp. 611 – 620.

Glambos, T.V. (1998). Guide to Stability Design Criteria for Metal Structures, 4th Ed., John Wiley & Sons, N.Y.

Grondin, G.Y., Elwi, A.E. and Cheng, J.J.R. (1999), Buckling of Stiffened Steel Plates – A Parametric Study, Journal of Constructional Steel Research, Vol. 50, No. 2, pp. 151 – 175.

Grondin, G.Y., Chen, Q., Elwi, A.E and Cheng, J.J.R. (1998). Buckling of Stiffened Steel Plates – Validation of a Numerical Model, Journal of Constructional Steel Research, Vol. 45, No. 2, pp. 125 – 148.

Hibbet, Karlsson & Sorenson, Inc. (HKS) (1997a). ABAQUS/Standard, Version 5.7-1 (computer software). Hibbet, Karlsson & Sorenson Inc., Pawtucket, Rhode Island.

Hibbet, Karlsson & Sorenson, Inc. (HKS) (1997b). ABAQUS/Standard Theory Manual, Version 5.7. Hibbet, Karlsson & Sorenson Inc., Pawtucket, Rhode Island.

Hibbet, Karlsson & Sorenson, Inc. (HKS) (1997c). ABAQUS/Standard User's Manual, Version 5.7. Hibbet, Karlsson & Sorenson Inc., Pawtucket, Rhode Island.

Horne, M.R. and Narayanan, R. (1976). The Strength of Straightened Welded Steel Stiffened Plates, The Structural Engineer, Vol. 54, No. 11, pp. 437 – 443.

Hu, S.Z., Chen, Q., Pegg, N. and Zimmerman, T.J.E. (1997). Ultimate Collapse Tests of Stiffened-Plate Ship Structural Units, Marine Structures, Vol. 10, pp. 587 – 610.

Hu, S.Z. (1993). A Finite Element Assessment of the Buckling of Strength Equations of Stiffened Plates, Second Canadian Marine Dynamics Conference, Vancouver, British Columbia, Aug. 9 -11, pp. J1 - J 10.

Hu, Y. and Sun, J. (1999). An Approximate Method to Generate Average Stress-Strain curve with the Residual Stress for Rectangular Plates under Uniaxial Compression in Ship Structures, Marine Structures, Vol. 12, pp. 585 – 603.

Hughes, O.F. and Ma, M. (1996). Elastic Tripping Analysis of Asymmetrical Stiffeners, Computers and Structures, Vol. 60, No. 3, pp. 369 – 389.

Hughes, O.F. and Ma, M. (1996). In-Elastic Analysis of Panel Collapse by Stiffeners Buckling, Computers and Structures, Vol. 61, No. 1, pp. 107 – 117.

Kármán, von T. (1924). Die mittragende Breite, August-Föpp1 – Festschrift (Beiträge zur technischen Physik), Springer – Verlag, Berlin.

Langhaar, H.L. (1951). Dimensional Analysis and Theory of Models, John Wiley and Sons, N.Y.

Leheta, H.W. and Mansour, A.E. (1997). Reliability-Based Method for Optimal Design of Stiffened Panels, Marine Structures, Vol. 10, pp. 323 – 352.

Mansour, A.E. (1992). Behaviour of Plates under Combined Loads, Proceedings of the Second International Offshore and Polar Engineering Conference, Jun. 14-19, San Francisco, USA, pp. 468 – 474.

Mansour, A., Yang J.M. and Thayamballi, A.K. (1990). An Experimental Investigation of Ship Hull Ultimate Strength, SNAME Transactions, Vol. 98, pp. 411 – 439.

Mansour, A.E., de Oliveria, J.G. and Kinara, R.K. (1987). Design of Flat Plate Structures for Offshore Applications, Proceedings of the Offshore Marine and Arctic Engineering Conference, Sept. 14-19, Houston, USA, pp. 413 – 421.

Maquoi, R. and Skaloud, M. (2000). Stability of Plates and Plated Structures – General Report, Journal of Construction Steel and Research, Vol. 55, pp. 45 – 68.

Murray, N.W. (1975). Analysis and Design of Stiffened Plates for Collapse Load, The Structural Engineer, Vol. 53, No. 3, pp. 153 – 158.

Murray, N.W. (1973). Buckling of Stiffened Panels Loaded Axially and in Bending, The Structural Engineer, Vol. 51, No. 8, pp. 285 – 301.

Niwa, Y., Watanabe, E. and Isami, H.A. (1985). New Approach to Predict the Strength of Compressed Steel Stiffened Plates, Proceedings of JSCE Structural Engineering/ Earthquake Engineering, Vol. 2, No. 2, pp. 281s - 290s.

Paik, J. K., Thayamballi, A.K. and Kim, D.H. (1999). An Analytical Method for the Ultimate Compressive Strength and Effective Plating of Stiffened Panels, Journal of Construction Steel Research, Vol. 49, pp. 43 – 68.

Paik, J. K., Thayamballi, A.K and Lee, W.H. (1998). A Numerical Investigation of Tripping, Marine Structures, Vol. 11, pp. 159 – 183.

Pan, Y. and Louca, L.A. (1999). Experimental and Numerical Studies on the Response of Stiffened Plates Subjected to Gas Explosions, Journal of Construction Steel Research, Vol. 52, pp. 171 – 193.

Pangiotopoulus, G.D. (1992). Ultimate Torsional Strength of Flat-Bar Stiffeners Attached to Plating under Axial Compression, Marine Structures, Vol. 5, pp. 535 – 557.

Ricks, E. (1979). An Incremental Approach to the Solution of Snapping and Buckling Problems. International Journal of Solids and Structures, Vol. 15, pp. 529 – 551.

Rigo, P.A.D.A., Moan, T., Frieze, P.A. and Chryssanthopoulos, M. (1995). Benchmarking of Ultimate Strength Prediction for Longitudinally Stiffened Panels, The Sixth International Symposium on Practical Design of Ships and Mobile Units, Journal of Structural Division, ASCE, Sept. 17-22, Seoul, Korea, pp. 2.869 - 2.882.

Rogers, N.A. and Dwight, J.B. (1976). Outstand Strength, Proceeding of the Conference on the Steel Plated Structures, 6 – 9 July, London, England.

Roman, V.G. and Elwi, A.E. (1987). Post-Buckling Behaviour of Thin Steel Cylinders under Transverse Shear, Structural Engineering Report No. 146, Department of Civil and Environmental Engineering, University of Alberta, Edmonton, Alberta.

Rondal, J. and Maquoi, R. (1979). Single Equation for SSRC Column-Strength Curves, Journal of the Structural Division, ASCE, Vol. 105, ST1, pp. 247 – 250.

Rutherford, S.E. and Caldwell, J.B. (1990). Ultimate Longitudinal Strength of Ships: A Case Study, SNAME Transactions, Vol. 98, pp. 441 – 471.

Smith, C.S., Anderson, N., Chapman, J.C., Davidson, P.C. and Dowling, P.J. (1991). Strength of Stiffened Plating under Combined Compression and Lateral Pressure, the Royal Institute of Naval Architecture, Vol. 133, pp. 131 – 147.

Smith, C.S., Davidson, P.C., Chapman, J.C. and Dowling, P.J. (1988). Strength and Stiffness of Ships Plating under In-Plane Compression and Tension, the Royal Institute of Naval Architects, Vol. 130, pp. 277 – 296.

Soares, C.G. and Gordo, J.M. (1997). Design Methods for Stiffened Panels under Predominantly Uniaxial Compression, Marine Structures, Vol. 10, pp. 465 – 497.

Timoshenko, S.P. and Gere, J.M. (1961). Theory of Elastic Stability, Second Edition, Engineering Societies Monographs, McGraw Hill, N.Y.

Winter, G. (1948). Performance of Thin Steel Compression Flanges, Proceeding of the Third Congress of Association of Bridge and Structural Engineering, Liege, Belgium.

Appendix A

Code Evaluation Results

Table A.1 DnV (1995) evaluation for uniaxial compression

b_1	b_4	P_c / P_y				Governing	
		PI	**SI**	**PB**	**ST**	P_c / P_y	**Failure mode***
0.25	**0.5**	1.00	0.99	1.00	0.99	0.99	ST
0.40	**0.5**	1.00	0.99	1.00	1.00	0.99	ST
0.55	**0.5**	1.00	0.99	1.00	1.00	0.99	ST
0.70	**0.5**	0.99	0.98	1.00	0.98	0.98	ST
1.28	**0.5**	0.99	0.97	0.97	0.97	0.97	ST
2.00	**0.5**	0.96	0.96	0.85	0.96	0.85	PB
2.70	**0.5**	0.93	0.95	0.66	0.95	0.66	PB
0.55	**1.0**	0.99	0.98	1.00	0.98	0.98	ST
0.70	**1.0**	0.99	0.97	1.00	1.00	0.97	ST
1.28	**1.0**	0.98	0.94	0.97	0.94	0.94	ST
2.00	**1.0**	0.94	0.81	0.85	0.63	0.63	ST
2.70	**1.0**	0.90	0.75	0.66	0.50	0.50	ST
0.70	**1.5**	0.99	0.95	1.00	0.95	0.95	ST
0.85	**1.5**	0.99	0.94	0.99	0.94	0.94	ST
1.00	**1.5**	0.98	0.93	0.99	0.93	0.93	ST
1.14	**1.5**	0.98	0.92	0.98	0.92	0.92	ST
1.28	**1.5**	0.97	0.81	0.97	0.63	0.63	ST
2.00	**1.5**	0.91	0.70	0.85	0.42	0.42	ST
2.70	**1.5**	0.83	0.64	0.66	0.30	0.30	ST
0.70	**2.0**	0.99	0.94	1.00	0.94	0.94	ST
0.85	**2.0**	0.98	0.92	0.99	0.92	0.92	ST
1.00	**2.0**	0.98	0.80	0.99	0.61	0.69	ST
1.15	**2.0**	0.97	0.77	0.98	0.55	0.55	ST
1.28	**2.0**	0.96	0.74	0.97	0.49	0.49	ST
2.00	**2.0**	0.85	0.62	0.85	0.29	0.29	ST
2.70	**2.0**	0.66	0.56	0.66	0.20	0.20	ST

at $\beta_2 = 1.05$; $\beta_3 = 0.75$; $\beta_5 = 0.30$; $\beta_9 = 0.0$

* SI : Stiffener induced overall buckling

PI : Plate induced overall buckling

PB : Plate buckling

ST : Stiffener tripping

Table A.2 DnV (1995) evaluation for uniaxial compression

b_1	b_4	P_c / P_y				Governing	
		PI	**SI**	**PB**	**ST**	P_c / P_y	**Failure mode ***
0.70	**0.5**	1.00	0.97	1.00	0.97	0.97	ST
1.28	**0.5**	0.99	0.95	0.97	0.95	0.95	ST
2.00	**0.5**	0.97	0.93	0.85	0.93	0.85	PB
2.70	**0.5**	0.95	0.90	0.66	0.90	0.66	PB
0.70	**1.0**	0.99	0.95	1.00	0.95	0.95	ST
1.28	**1.0**	0.98	0.90	0.97	0.90	0.90	ST
2.00	**1.0**	0.95	0.69	0.85	0.46	0.46	ST
2.70	**1.0**	0.91	0.60	0.66	0.34	0.34	ST
0.70	**1.5**	0.99	0.92	1.00	0.92	0.92	ST
1.28	**1.5**	0.97	0.69	0.97	0.46	0.46	ST
2.00	**1.5**	0.90	0.54	0.85	0.27	0.27	ST
2.70	**1.5**	0.76	0.47	0.66	0.19	0.19	ST
0.70	**2.0**	0.99	0.88	1.00	0.88	0.88	ST
1.28	**2.0**	0.95	0.58	0.97	0.33	0.33	ST
2.00	**2.0**	0.74	0.45	0.85	0.18	0.18	ST
2.70	**2.0**	0.51	0.39	0.66	0.12	0.12	ST

at $\beta_2 = 1.05$; $\beta_3 = 0.75$; $\beta_5 = 0.15$; $\beta_9 = 0.0$

* SI : Stiffener induced overall buckling

PI : Plate induced overall buckling

PB : Plate buckling

ST : Stiffener tripping

Table A.3 DnV (1995) evaluation for uniaxial compression

b_1	b_4	P_c / P_y				Governing	
		PI	**SI**	**PB**	**ST**	P_c / P_y	**Failure mode***
0.70	**0.5**	1.00	0.95	1.00	0.95	0.95	ST
1.28	**0.5**	0.99	0.91	0.97	0.91	0.91	ST
2.00	**0.5**	0.98	0.86	0.85	0.86	0.85	PB
2.70	**0.5**	0.96	0.82	0.66	0.82	0.66	PB
0.70	**1.0**	0.99	0.90	1.00	0.90	0.90	ST
1.28	**1.0**	0.98	0.81	0.97	0.81	0.81	ST
2.00	**1.0**	0.95	0.95	0.52	0.28	0.28	ST
2.70	**1.0**	0.89	0.42	0.66	0.19	0.19	ST
0.70	**1.5**	0.99	0.85	1.00	0.85	0.85	ST
1.28	**1.5**	0.96	0.52	0.97	0.28	0.28	ST
2.00	**1.5**	0.79	0.36	0.85	0.14	0.14	ST
2.70	**1.5**	0.56	0.30	0.66	0.09	0.09	ST
0.70	**2.0**	0.98	0.79	1.00	0.79	0.79	ST
1.28	**2.0**	0.87	0.40	0.97	0.18	0.18	ST
2.00	**2.0**	0.49	0.29	0.85	0.09	0.09	ST
2.70	**2.0**	0.34	0.25	0.66	0.06	0.06	ST

at $\beta_2 = 1.05$; $\beta_3 = 0.75$; $\beta_5 = 0.075$; $\beta_9 = 0.0$

* SI : Stiffener induced overall buckling

PI : Plate induced overall buckling

PB : Plate buckling

ST : Stiffener tripping

Table A.4 DnV (1995) evaluation for combined compression and bending

b_1	b_4	P_c / P_y				Governing	
		PI	**SI**	**PB**	**ST**	P_c / P_y	**Failure mode***
0.70	**0.50**	1.03	0.83	1.01	0.83	0.83	ST
1.28	**0.50**	1.03	0.83	0.98	0.83	0.83	ST
1.46	**0.50**	1.01	0.83	0.96	0.83	0.83	ST
1.75	**0.50**	1.00	0.82	0.98	0.82	0.82	ST
2.00	**0.50**	0.99	0.82	0.88	0.82	0.82	ST
2.25	**0.50**	0.98	0.81	0.82	0.81	0.81	ST
2.70	**0.50**	0.97	0.81	0.76	0.81	0.81	ST
1.75	**0.75**	1.00	0.81	0.92	0.81	0.81	ST
2.00	**0.75**	0.99	0.80	0.88	0.80	0.80	ST
2.25	**0.75**	0.98	0.79	0.82	0.79	0.79	ST
0.70	**1.00**	1.03	0.82	1.01	0.82	0.82	ST
1.28	**1.00**	1.02	0.80	0.98	0.80	0.80	ST
1.75	**1.00**	0.99	0.71	0.92	0.57	0.57	ST
2.00	**1.00**	0.98	0.69	0.88	0.54	0.54	ST
2.25	**1.00**	0.96	0.68	0.82	0.50	0.50	ST
2.70	**1.00**	0.93	0.64	0.76	0.43	0.43	ST
1.75	**1.25**	0.98	0.67	0.92	0.50	0.50	ST
2.00	**1.25**	0.96	0.65	0.88	0.45	0.45	ST
2.25	**1.25**	0.94	0.62	0.82	0.40	0.40	ST
0.70	**1.50**	1.02	0.80	1.01	0.80	0.80	ST
1.28	**1.50**	1.00	0.69	0.98	0.53	0.53	ST
2.00	**1.50**	0.94	0.60	0.88	0.36	0.36	ST
2.70	**1.50**	0.85	0.55	0.76	0.26	0.26	ST
0.70	**2.00**	1.02	0.79	1.01	0.79	0.79	ST
1.28	**2.00**	0.99	0.63	0.98	0.42	0.42	ST
2.00	**2.00**	0.87	0.53	0.88	0.25	0.25	ST
2.70	**2.00**	0.68	0.48	0.76	0.17	0.17	ST

at $\beta_2 = 1.05$; $\beta_3 = 0.75$; $\beta_5 = 0.30$; $\beta_9 = 0.2$

* SI : Stiffener induced overall buckling

PI : Plate induced overall buckling

PB : Plate buckling

ST : Stiffener tripping

Table A.5 DnV (1995) evaluation for combined compression and bending

b_1	b_4	P_c / P_y				Governing	
		PI	**SI**	**PB**	**ST**	P_c / P_y	**Failure mode***
0.70	**0.5**	1.02	0.78	1.00	0.78	0.78	ST
1.28	**0.5**	1.01	0.78	0.97	0.78	0.78	ST
2.00	**0.5**	0.99	0.77	0.86	0.77	0.77	ST
2.70	**0.5**	0.97	0.75	0.85	0.75	0.75	ST
0.70	**1.0**	1.02	0.75	1.00	0.75	0.75	ST
1.28	**1.0**	1.00	0.73	0.97	0.73	0.73	ST
2.00	**1.0**	0.97	0.57	0.86	0.38	0.38	ST
2.70	**1.0**	0.93	0.50	0.85	0.28	0.28	ST
0.70	**1.5**	1.01	0.73	1.00	0.73	0.73	ST
1.28	**1.5**	0.99	0.56	0.97	0.38	0.38	ST
2.00	**1.5**	0.92	0.44	0.86	0.23	0.23	ST
2.70	**1.5**	0.78	0.39	0.85	0.16	0.16	ST
0.70	**2.0**	1.01	0.71	1.00	0.71	0.71	ST
1.28	**2.0**	0.97	0.48	0.97	0.27	0.27	ST
2.00	**2.0**	0.75	0.38	0.86	0.15	0.15	ST
2.70	**2.0**	0.52	0.33	0.85	0.10	0.10	ST

at $\beta_2 = 1.05$; $\beta_3 = 0.75$; $\beta_5 = 0.15$; $\beta_9 = 0.2$

* SI : Stiffener induced overall buckling

PI : Plate induced overall buckling

PB : Plate buckling

ST : Stiffener tripping

Table A.6 DnV (1995) evaluation for combined compression and bending

b_1	b_4	P_c / P_y				Governing	
		PI	**SI**	**PB**	**ST**	P_c / P_y	**Failure mode***
1.28	**0.5**	1.00	0.66	0.97	0.66	0.66	ST
2.00	**0.5**	0.99	0.66	0.85	0.66	0.66	ST
2.70	**0.5**	0.98	0.64	0.86	0.64	0.64	ST
0.70	**1.0**	1.01	0.62	1.00	0.62	0.62	ST
1.28	**1.0**	1.00	0.59	0.97	0.59	0.59	ST
2.00	**1.0**	0.96	0.40	0.85	0.21	0.21	ST
2.70	**1.0**	0.90	0.32	0.86	0.15	0.15	ST
0.70	**1.5**	1.00	0.59	1.00	0.59	0.59	ST
1.28	**1.5**	0.98	0.38	0.97	0.21	0.21	ST
2.00	**1.5**	0.80	0.27	0.85	0.11	0.11	ST
2.70	**1.5**	0.57	0.23	0.86	0.07	0.07	ST
0.70	**2.0**	1.00	0.54	1.00	0.54	0.54	ST
1.28	**2.0**	0.88	0.30	0.97	0.13	0.13	ST
2.00	**2.0**	0.50	0.22	0.85	0.07	0.07	ST
2.70	**2.0**	0.33	0.20	0.86	0.05	0.05	ST

at $\beta_2 = 1.05$; $\beta_3 = 0.75$; $\beta_5 = 0.075$; $\beta_9 = 0.2$

* SI : Stiffener induced overall buckling

PI : Plate induced overall buckling

PB : Plate buckling

ST : Stiffener tripping

Table A.7 API (1987) evaluation for uniaxial compression

b_1	b_4	P_c / P_y				Governing	
		PI	**SI**	**PB**	**ST**	P_c / P_y	**Failure mode***
0.25	**0.5**	1.19	1.19	1.00	1.00	1.00	ST
0.4	**0.5**	1.19	1.19	1.00	0.99	0.99	ST
0.55	**0.5**	1.18	1.18	1.00	0.98	0.98	ST
0.7	**0.5**	1.18	1.18	1.00	0.96	0.96	ST
1.28	**0.5**	1.16	1.16	0.78	0.82	0.78	PB
2	**0.5**	1.13	1.14	0.50	0.52	0.50	PB
2.7	**0.5**	1.10	1.12	0.37	0.31	0.31	ST
0.55	**1**	1.16	1.16	1.00	0.95	0.95	ST
0.7	**1**	1.15	1.15	1.00	0.91	0.91	ST
1.28	**1**	1.10	1.11	0.78	0.66	0.66	ST
2	**1**	1.03	1.06	0.50	0.29	0.29	ST
2.7	**1**	0.95	1.00	0.37	0.18	0.18	ST
0.7	**1.5**	1.12	1.12	1.00	0.89	0.89	ST
0.85	**1.5**	1.10	1.10	1.00	0.84	0.84	ST
1	**1.5**	1.07	1.07	1.00	0.79	0.79	ST
1.14	**1.5**	1.05	1.06	0.88	0.69	0.69	ST
1.28	**1.5**	1.02	1.04	0.78	0.58	0.58	ST
2	**1.5**	0.89	0.94	0.50	0.24	0.24	ST
2.7	**1.5**	0.74	0.83	0.37	0.15	0.15	ST
0.7	**2**	1.09	1.09	1.00	0.87	0.87	ST
0.85	**2**	1.05	1.05	1.00	0.83	0.83	ST
1	**2**	1.01	1.01	0.99	0.77	0.77	ST
1.15	**2**	0.97	0.98	0.87	0.66	0.66	ST
1.28	**2**	0.93	0.96	0.78	0.54	0.54	ST
2	**2**	0.72	0.81	0.50	0.22	0.22	ST
2.7	**2**	0.48	0.63	0.37	0.14	0.14	ST

at $\beta_2 = 1.05$; $\beta_3 = 0.75$; $\beta_5 = 0.30$; $\beta_9 = 0.0$

* SI : Stiffener induced overall buckling

PI : Plate induced overall buckling

PB : Plate buckling

ST : Stiffener tripping

Table A.8 API (1987) evaluation for uniaxial compression

b_1	b_4	P_c / P_y				Governing	
		PI	**SI**	**PB**	**ST**	P_c / P_y	**Failure mode***
0.70	**0.5**	1.17	1.17	1.00	0.94	0.94	ST
1.28	**0.5**	1.14	1.15	0.78	0.73	0.73	ST
2.00	**0.5**	1.11	1.13	0.50	0.34	0.34	ST
2.70	**0.5**	1.08	1.11	0.37	0.21	0.21	ST
0.70	**1.0**	1.14	1.14	1.00	0.92	0.92	ST
1.28	**1.0**	1.06	1.08	0.78	0.64	0.64	ST
2.00	**1.0**	0.97	1.02	0.50	0.26	0.26	ST
2.70	**1.0**	0.88	0.95	0.37	0.16	0.16	ST
0.70	**1.5**	1.10	1.10	1.00	0.91	0.91	ST
1.28	**1.5**	0.96	0.99	0.78	0.61	0.61	ST
2.00	**1.5**	0.78	0.87	0.50	0.24	0.24	ST
2.70	**1.5**	0.60	0.75	0.37	0.15	0.15	ST
0.70	**2.0**	1.05	1.05	1.00	0.90	0.90	ST
1.28	**2.0**	0.83	0.88	0.78	0.60	0.60	ST
2.00	**2.0**	0.55	0.70	0.50	0.23	0.23	ST
2.70	**2.0**	0.34	0.50	0.37	0.14	0.14	ST

at $\beta_2 = 1.05$; $\beta_3 = 0.75$; $\beta_5 = 0.15$; $\beta_9 = 0.0$

* SI : Stiffener induced overall buckling

PI : Plate induced overall buckling

PB : Plate buckling

ST : Stiffener tripping

Table A.9 API (1987) evaluation for uniaxial compression

b_1	b_4	P_c / P_y				Governing	
		PI	**SI**	**PB**	**ST**	P_c / P_y	**Failure mode***
0.70	**0.5**	1.16	1.16	1.00	0.93	0.93	ST
1.28	**0.5**	1.13	1.13	0.78	0.66	0.66	ST
2.00	**0.5**	1.08	1.10	0.50	0.27	0.27	ST
2.70	**0.5**	1.03	1.08	0.37	0.16	0.16	ST
0.70	**1.0**	1.12	1.12	1.00	0.92	0.92	ST
1.28	**1.0**	1.01	1.03	0.78	0.63	0.63	ST
2.00	**1.0**	0.87	0.95	0.50	0.24	0.24	ST
2.70	**1.0**	0.74	0.87	0.37	0.15	0.15	ST
0.70	**1.5**	1.06	1.06	1.00	0.92	0.92	ST
1.28	**1.5**	0.86	0.90	0.78	0.62	0.62	ST
2.00	**1.5**	0.60	0.74	0.50	0.24	0.24	ST
2.70	**1.5**	0.39	0.59	0.37	0.14	0.14	ST
0.70	**2.0**	0.99	0.99	1.00	0.90	0.90	ST
1.28	**2.0**	0.67	0.74	0.78	0.61	0.61	ST
2.00	**2.0**	0.34	0.49	0.50	0.23	0.23	ST
2.70	**2.0**	0.22	0.33	0.37	0.14	0.14	ST

at $\beta_2 = 1.05$; $\beta_3 = 0.75$; $\beta_5 = 0.075$; $\beta_9 = 0.0$

* SI : Stiffener induced overall buckling

PI : Plate induced overall buckling

PB : Plate buckling

ST : Stiffener tripping

Table A.10 API (1987) evaluation for combined compression and bending

b_1	b_4	P_c / P_y				Governing	
		PI	**SI**	**PB**	**ST**	P_c / P_y	**Failure mode***
0.70	**0.50**	0.94	0.94	1.06	0.98	0.94	PI
1.28	**0.50**	0.91	0.92	0.85	0.89	0.85	PB
1.46	**0.50**	0.90	0.91	0.76	0.84	0.76	PB
1.75	**0.50**	0.89	0.90	0.66	0.76	0.66	PB
2.00	**0.50**	0.88	0.89	0.59	0.69	0.59	PB
2.25	**0.50**	0.87	0.89	0.55	0.61	0.55	PB
2.70	**0.50**	0.84	0.87	0.49	0.46	0.46	ST
1.75	**0.75**	0.84	0.86	0.66	0.60	0.60	ST
2.00	**0.75**	0.82	0.84	0.59	0.48	0.48	ST
2.25	**0.75**	0.79	0.83	0.55	0.39	0.39	ST
0.70	**1.00**	0.91	0.91	1.06	0.94	0.91	PI
1.28	**1.00**	0.84	0.85	0.85	0.74	0.74	ST
1.75	**1.00**	0.77	0.81	0.66	0.48	0.48	ST
2.00	**1.00**	0.74	0.78	0.59	0.37	0.37	ST
2.25	**1.00**	0.70	0.75	0.55	0.30	0.30	ST
2.70	**1.00**	0.63	0.70	0.49	0.23	0.23	ST
1.75	**1.25**	0.70	0.74	0.66	0.40	0.40	ST
2.00	**1.25**	0.65	0.70	0.59	0.32	0.32	ST
2.25	**1.25**	0.60	0.67	0.55	0.26	0.26	ST
0.70	**1.50**	0.87	0.87	1.06	0.92	0.87	PI
1.28	**1.50**	0.73	0.76	0.85	0.66	0.66	ST
2.00	**1.50**	0.55	0.62	0.59	0.29	0.29	ST
2.70	**1.50**	0.40	0.49	0.49	0.18	0.18	ST
0.70	**2.00**	0.82	0.82	1.06	0.90	0.82	PI
1.28	**2.00**	0.61	0.65	0.85	0.61	0.61	ST
2.00	**2.00**	0.38	0.46	0.59	0.25	0.25	ST
2.70	**2.00**	0.24	0.32	0.49	0.15	0.15	ST

at $\beta_2 = 1.05$; $\beta_3 = 0.75$; $\beta_5 = 0.30$; $\beta_9 = 0.2$

* SI : Stiffener induced overall buckling

PI : Plate induced overall buckling

PB : Plate buckling

ST : Stiffener tripping

Table A.10 API (1987) evaluation for combined compression and bending

b_1	b_4	P_c / P_y				Governing	
		PI	**SI**	**PB**	**ST**	P_c / P_y	**Failure mode***
0.70	**0.5**	0.93	0.93	1.04	0.96	0.93	SI
1.28	**0.5**	0.90	0.90	0.82	0.79	0.79	ST
2.00	**0.5**	0.85	0.87	0.56	0.44	0.44	ST
2.70	**0.5**	0.80	0.84	0.45	0.27	0.27	ST
0.70	**1.0**	0.89	0.89	1.04	0.93	0.89	PI
1.28	**1.0**	0.78	0.80	0.82	0.68	0.68	ST
2.00	**1.0**	0.64	0.71	0.56	0.30	0.30	ST
2.70	**1.0**	0.51	0.61	0.45	0.19	0.19	ST
0.70	**1.5**	0.83	0.83	1.04	0.92	0.83	SI
1.28	**1.5**	0.63	0.67	0.82	0.65	0.63	PI
2.00	**1.5**	0.41	0.51	0.56	0.27	0.27	ST
2.70	**1.5**	0.70	0.37	0.45	0.17	0.17	ST
0.70	**2.0**	0.76	0.76	1.04	0.91	0.76	SI
1.28	**2.0**	0.47	0.52	0.82	0.63	0.47	PI
2.00	**2.0**	0.64	0.33	0.56	0.26	0.26	ST
2.70	**2.0**	0.39	0.22	0.45	0.15	0.15	ST

at $\beta_2 = 1.05$; $\beta_3 = 0.75$; $\beta_5 = 0.15$; $\beta_9 = 0.2$

* SI : Stiffener induced overall buckling

PI : Plate induced overall buckling

PB : Plate buckling

ST : Stiffener tripping

Table A.12 API (1987) evaluation for combined compression and bending

b_1	b_4	P_c / P_y				Governing	
		PI	**SI**	**PB**	**ST**	P_c / P_y	**Failure mode***
1.28	**0.5**	0.87	0.88	0.81	0.69	0.69	ST
2.00	**0.5**	0.80	0.84	0.54	0.29	0.29	ST
2.70	**0.5**	0.74	0.80	0.42	0.18	0.18	ST
0.70	**1.0**	0.87	0.87	1.03	0.92	0.87	SI
1.28	**1.0**	0.71	0.74	0.81	0.65	0.65	ST
2.00	**1.0**	0.52	0.62	0.54	0.26	0.26	ST
2.70	**1.0**	0.38	0.51	0.42	0.15	0.15	ST
0.70	**1.5**	0.79	0.79	1.03	0.92	0.79	SI
1.28	**1.5**	0.89	0.39	0.81	0.63	0.39	SI
2.00	**1.5**	0.73	0.39	0.54	0.25	0.25	ST
2.70	**1.5**	0.46	0.27	0.42	0.15	0.15	ST
0.70	**2.0**	0.70	0.70	1.03	0.89	0.70	PI
1.28	**2.0**	0.89	0.39	0.81	0.56	0.39	SI
2.00	**2.0**	0.41	0.23	0.54	0.25	0.23	SI
2.70	**2.0**	0.26	0.15	0.42	0.11	0.11	ST

at $\beta_2 = 1.05$; $\beta_3 = 0.75$; $\beta_5 = 0.075$; $\beta_9 = 0.2$

* SI : Stiffener induced overall buckling

PI : Plate induced overall buckling

PB : Plate buckling

ST : Stiffener tripping

Appendix B

Evaluation of existing guidelines for the governing failure mode

Table B.1 Evaluation for uniaxial compression

b_1	b_4	FEA (P_c/P_y)	$P_{c\,FEA} / P_{c\,code}$		Failure mode*		
			DnV	API	FEA	DnV	API
0.25	**0.5**	1.02	1.03	1.03	PI	ST	ST
0.40	**0.5**	1.02	1.03	1.03	PI	ST	ST
0.55	**0.5**	1.01	1.02	1.04	PB	ST	ST
0.70	**0.5**	1.00	1.02	1.04	PB	ST	ST
1.28	**0.5**	0.83	0.86	1.07	PB	ST	PB
2.00	**0.5**	0.63	0.75	1.26	PB	PB	PB
2.70	**0.5**	0.54	0.82	1.75	PB	PB	ST
0.55	**1.0**	1.01	1.05	1.07	PI	ST	ST
0.70	**1.0**	1.00	1.03	1.10	PB	ST	ST
1.28	**1.0**	0.87	0.93	1.33	PB	ST	ST
2.00	**1.0**	0.66	1.05	2.28	PB	ST	ST
2.70	**1.0**	0.53	1.05	2.91	PB	ST	ST
0.70	**1.5**	0.99	1.04	1.12	PI	ST	ST
0.85	**1.5**	0.98	1.04	1.16	PB	ST	ST
1.00	**1.5**	0.96	1.04	1.22	PB	ST	ST
1.14	**1.5**	0.94	1.03	1.36	PB	ST	ST
1.28	**1.5**	0.92	1.46	1.58	PB	ST	ST
2.00	**1.5**	0.65	1.52	2.67	PB	ST	ST
2.70	**1.5**	0.44	1.48	2.86	DFM	ST	ST
0.70	**2.0**	0.97	1.04	1.12	PI	ST	ST
0.85	**2.0**	0.95	1.04	1.15	PI	ST	ST
1.00	**2.0**	0.93	1.35	1.20	PB	ST	ST
1.15	**2.0**	0.89	1.64	1.36	PB	ST	ST
1.28	**2.0**	0.86	1.73	1.57	PB	ST	ST
2.00	**2.0**	0.60	2.07	2.71	DFM	ST	ST
2.70	**2.0**	0.31	1.61	2.26	DFM	ST	ST

at $\beta_2 = 1.05$; $\beta_3 = 0.75$; $\beta_5 = 0.30$; $\beta_9 = 0.0$

* SI : Stiffener induced overall buckling
PI : Plate induced overall buckling
PB : Plate buckling
ST : Stiffener tripping
DFM : Dual failure mode

Table B.2 Evaluation for uniaxial compression

b_1	b_4	FEA (P_c/P_y)	$P_{c\,FEA} / P_{c\,code}$		Failure mode*		
			DnV	API	FEA	DnV	API
0.70	**0.5**	1.00	1.03	1.06	PI	ST	ST
1.28	**0.5**	0.83	0.88	1.14	PB	ST	ST
2.00	**0.5**	0.59	0.70	1.73	PB	PB	ST
2.70	**0.5**	0.49	0.75	2.38	PB	PB	ST
0.70	**1.0**	1.00	1.05	1.09	PI	ST	ST
1.28	**1.0**	0.83	0.93	1.30	PB	ST	ST
2.00	**1.0**	0.60	1.30	2.30	DFM	ST	ST
2.70	**1.0**	0.46	1.37	2.90	DFM	ST	ST
0.70	**1.5**	0.99	1.08	1.09	DFM	ST	ST
1.28	**1.5**	0.84	1.83	1.37	DFM	ST	ST
2.00	**1.5**	0.52	1.92	2.15	DFM	ST	ST
2.70	**1.5**	0.31	1.67	2.09	DFM	ST	ST
0.70	**2.0**	0.97	1.10	1.08	PI	ST	ST
1.28	**2.0**	0.78	2.37	1.30	DFM	ST	ST
2.00	**2.0**	0.40	2.25	1.70	DFM	ST	ST
2.70	**2.0**	0.21	1.79	1.51	DFM	ST	ST

at $\beta_2 = 1.05$; $\beta_3 = 0.75$; $\beta_5 = 0.15$; $\beta_9 = 0.0$

* SI : Stiffener induced overall buckling

PI : Plate induced overall buckling

PB : Plate buckling

ST : Stiffener tripping

DFM : Dual failure mode

Table B.3 Evaluation for uniaxial compression

b_1	b_4	FEA (P_c/P_y)	$P_{c\,FEA} / P_{c\,code}$		Failure mode*		
			DnV	API	FEA	DnV	API
0.70	**0.5**	1.02	1.07	1.10	PI	ST	ST
1.28	**0.5**	0.85	0.94	1.29	PB	ST	ST
2.00	**0.5**	0.63	0.74	2.34	DFM	ST	ST
2.70	**0.5**	0.46	0.70	2.89	DFM	ST	ST
0.70	**1.0**	0.99	1.10	1.08	PB	ST	ST
1.28	**1.0**	0.81	1.00	1.28	DFM	ST	ST
2.00	**1.0**	0.52	1.85	2.13	DFM	ST	ST
2.70	**1.0**	0.32	1.73	2.21	DFM	ST	ST
0.70	**1.5**	0.98	1.16	1.07	DFM	ST	ST
1.28	**1.5**	0.75	2.68	1.20	DFM	ST	ST
2.00	**1.5**	0.33	2.34	1.39	DFM	ST	ST
2.70	**1.5**	0.18	1.90	1.25	DFM	ST	ST
0.70	**2.0**	0.96	1.22	1.06	DFM	ST	ST
1.28	**2.0**	0.59	3.30	0.97	DFM	ST	ST
2.00	**2.0**	0.22	2.49	0.95	DFM	ST	ST
2.70	**2.0**	0.12	2.03	0.86	DFM	ST	ST

at $\beta_2 = 1.05$; $\beta_3 = 0.75$; $\beta_5 = 0.075$; $\beta_9 = 0.0$

* SI : Stiffener induced overall buckling

PI : Plate induced overall buckling

PB : Plate buckling

ST : Stiffener tripping

DFM : Dual failure mode

Table B.4 Evaluation for combined compression and bending

b_1	b_4	FEA (P_c/P_y)	$P_{c\ FEA} / P_{c\ code}$		Failure mode*		
			DnV	API	FEA	DnV	API
0.70	**0.50**	0.80	0.96	0.85	ST	ST	PI
1.28	**0.50**	0.78	0.94	0.92	ST	ST	PB
1.46	**0.50**	0.78	0.95	0.99	ST	ST	PB
1.75	**0.50**	0.73	0.88	1.11	PB	ST	PB
2.00	**0.50**	0.68	0.82	1.14	PB	ST	PB
2.25	**0.50**	0.64	0.78	1.17	PB	ST	PB
2.70	**0.50**	0.58	0.71	1.24	PB	ST	ST
1.75	**0.75**	0.74	0.92	1.23	PB	ST	ST
2.00	**0.75**	0.69	0.87	1.43	PB	ST	ST
2.25	**0.75**	0.65	0.83	1.68	PB	ST	ST
0.70	**1.00**	0.76	0.93	0.84	ST	ST	PI
1.28	**1.00**	0.73	0.91	0.98	ST	ST	ST
1.75	**1.00**	0.70	1.21	1.47	ST	ST	ST
2.00	**1.00**	0.71	1.33	1.94	PB	ST	ST
2.25	**1.00**	0.66	1.34	2.21	PB	ST	ST
2.70	**1.00**	0.59	1.38	2.62	PB	ST	ST
1.75	**1.25**	0.62	1.24	1.53	ST	ST	ST
2.00	**1.25**	0.57	1.28	1.82	ST	ST	ST
2.25	**1.25**	0.53	1.33	2.04	ST	ST	ST
0.70	**1.50**	0.73	0.91	0.84	ST	ST	PI
1.28	**1.50**	0.65	1.22	0.99	ST	ST	ST
2.00	**1.50**	0.49	1.34	1.70	ST	ST	ST
2.70	**1.50**	0.33	1.31	1.88	ST	ST	ST
0.70	**2.00**	0.71	0.90	0.86	ST	ST	PI
1.28	**2.00**	0.56	1.34	0.93	ST	ST	ST
2.00	**2.00**	0.34	1.38	1.37	ST	ST	ST
2.70	**2.00**	0.21	1.27	1.39	ST	ST	ST

at $\beta_2 = 1.05$; $\beta_3 = 0.75$; $\beta_5 = 0.30$; $\beta_9 = 0.20$

* SI : Stiffener induced overall buckling
PI : Plate induced overall buckling
PB : Plate buckling
ST : Stiffener tripping

Table B.5 Evaluation for combined compression and bending

b_1	b_4	FEA (P_c/P_y)	$P_{c\,FEA}$ / $P_{c\,code}$		Failure mode*		
			DnV	API	FEA	DnV	API
0.70	**0.5**	0.78	0.99	0.83	ST	ST	SI
1.28	**0.5**	0.73	0.94	0.93	ST	ST	ST
2.00	**0.5**	0.64	0.84	1.47	PB	ST	ST
2.70	**0.5**	0.51	0.68	1.91	PB	ST	ST
0.70	**1.0**	0.71	0.95	0.80	ST	ST	PI
1.28	**1.0**	0.65	0.89	0.95	ST	ST	ST
2.00	**1.0**	0.61	1.60	2.03	DFM	ST	ST
2.70	**1.0**	0.45	1.59	2.38	DFM	ST	ST
0.70	**1.5**	0.67	0.92	0.81	ST	ST	SI
1.28	**1.5**	0.54	1.43	0.87	ST	ST	PI
2.00	**1.5**	0.35	1.51	1.26	ST	ST	ST
2.70	**1.5**	0.23	1.43	1.33	ST	ST	ST
0.70	**2.0**	0.63	0.89	0.83	ST	ST	SI
1.28	**2.0**	0.41	1.53	0.88	ST	ST	PI
2.00	**2.0**	0.21	1.38	0.80	ST	ST	ST
2.70	**2.0**	0.13	1.31	0.88	ST	ST	ST

at $\beta_2 = 1.05$; $\beta_3 = 0.75$; $\beta_5 = 0.15$; $\beta_9 = 0.20$

* SI : Stiffener induced overall buckling

PI : Plate induced overall buckling

PB : Plate buckling

ST : Stiffener tripping

DFM : Dual failure mode

Table B.6 Evaluation for combined compression and bending

b_1	b_4	FEM (P_c/P_y)	$P_{c\,FEA}$ / $P_{c\,code}$		Failure mode*		
			DnV	API	FEA	DnV	API
1.28	**0.5**	0.687	1.04	0.99	ST	ST	ST
2.00	**0.5**	0.65	0.98	2.21	PB	ST	ST
2.70	**0.5**	0.48	0.76	2.75	PB	ST	ST
0.70	**1.0**	0.68	1.10	0.79	ST	ST	SI
1.28	**1.0**	0.50	0.85	0.78	ST	ST	ST
2.00	**1.0**	0.56	2.61	2.18	DFM	ST	ST
2.70	**1.0**	0.35	2.38	2.23	DFM	ST	ST
0.70	**1.5**	0.57	0.97	0.72	ST	ST	SI
1.28	**1.5**	0.37	1.79	0.94	ST	ST	SI
2.00	**1.5**	0.21	1.90	0.83	ST	ST	ST
2.70	**1.5**	0.14	1.86	0.91	ST	ST	ST
0.70	**2.0**	0.49	0.90	0.70	ST	ST	PI
1.28	**2.0**	0.25	1.92	0.64	ST	ST	SI
2.00	**2.0**	0.12	1.73	0.54	ST	ST	SI
2.70	**2.0**	0.07	1.45	0.68	ST	ST	ST

at $\beta_2 = 1.05$; $\beta_3 = 0.75$; $\beta_5 = 0.075$; $\beta_9 = 0.20$

* SI : Stiffener induced overall buckling

PI : Plate induced overall buckling

PB : Plate buckling

ST : Stiffener tripping

DFM : Dual failure mode

Appendix C

Evaluation of existing guidelines based on finite element analysis's failure mode

Table C.1 Plate Induced overall buckling for uniaxial compression

b_1	b_4	b_5	**FEA** (P_c/P_y)	$P_{c\ FEA}$ / $P_{c\ code}$	
				DnV	**API**
0.25	**0.5**	**0.300**	1.02	1.03	0.86
0.40	**0.5**	**0.300**	1.02	1.02	0.86
0.55	**1.0**	**0.300**	1.01	1.02	0.87
0.70	**1.5**	**0.300**	0.99	1.00	0.89
0.70	**2.0**	**0.300**	0.97	0.99	0.90
0.70	**0.5**	**0.150**	1.00	1.01	0.85
0.70	**1.0**	**0.150**	1.00	1.00	0.87
0.70	**1.5**	**0.150**	0.99	1.00	0.90
0.70	**0.5**	**0.075**	1.02	1.02	0.88
0.85	**2.0**	**0.300**	0.95	0.97	0.91
Mean				**1.01**	**0.88**
Standard Deviation				**0.02**	**0.02**

at $\beta_2 = 1.05$; $\beta_3 = 0.75$; $\beta_9 = 0.0$

Table C.2 Plate buckling failure mode for uniaxial compression

b_1	b_4	b_5	**FEA** (P_c/P_y)	$P_{c\ FEA} / P_{c\ code}$	
				DnV	**API**
0.55	**0.5**	**0.300**	1.01	1.01	1.01
0.70	**0.5**	**0.300**	1.00	1.01	1.00
0.70	**1.0**	**0.300**	1.00	1.01	1.00
0.70	**1.0**	**0.075**	0.99	0.99	0.99
0.85	**1.5**	**0.300**	0.98	0.99	0.98
1.00	**1.5**	**0.300**	0.96	0.98	0.97
1.00	**2.0**	**0.300**	0.93	0.94	0.93
1.14	**1.5**	**0.300**	0.94	0.96	1.08
1.15	**2.0**	**0.300**	0.89	0.91	1.03
1.28	**0.5**	**0.300**	0.83	0.86	1.07
1.28	**1.0**	**0.300**	0.87	0.90	1.12
1.28	**1.5**	**0.300**	0.92	0.95	1.18
1.28	**2.0**	**0.300**	0.86	0.88	1.10
1.28	**0.5**	**0.150**	0.83	0.86	1.07
1.28	**1.0**	**0.150**	0.83	0.86	1.06
1.28	**0.5**	**0.075**	0.85	0.88	1.09
2.00	**0.5**	**0.300**	0.63	0.75	1.26
2.00	**1.0**	**0.300**	0.66	0.78	1.31
2.00	**1.5**	**0.300**	0.65	0.76	1.29
2.00	**0.5**	**0.150**	0.59	0.70	1.18
2.70	**0.5**	**0.300**	0.54	0.82	1.46
2.70	**1.0**	**0.300**	0.53	0.80	1.42
2.70	**0.5**	**0.150**	0.49	0.75	1.33
Mean				**0.89**	**1.13**
Standard deviation				**0.08**	**0.12**

at $\beta_2 = 1.05$; $\beta_3 = 0.75$; $\beta_9 = 0.0$

Table C.3 Dual failure mode for uniaxial compression

b_1	b_4	b_5	**FEA** (P_c/P_y)	$P_{c\ FEA}$ / $P_{c\ code}$	
				DnV	**API**
0.70	**2.0**	**0.150**	0.97	1.10	0.93
0.70	**1.5**	**0.075**	0.98	1.02	1.07
0.70	**2.0**	**0.075**	0.96	1.22	1.06
1.28	**1.5**	**0.150**	0.84	1.83	1.37
1.28	**2.0**	**0.150**	0.78	2.37	1.30
1.28	**1.0**	**0.075**	0.81	1.00	1.28
1.28	**1.5**	**0.075**	0.75	2.68	1.20
1.28	**2.0**	**0.075**	0.59	3.30	0.97
2.00	**2.0**	**0.300**	0.60	2.07	2.30
2.00	**1.0**	**0.150**	0.60	1.30	2.15
2.00	**1.5**	**0.150**	0.52	1.92	2.09
2.00	**2.0**	**0.150**	0.40	2.25	1.70
2.00	**0.5**	**0.075**	0.63	0.74	2.34
2.00	**1.0**	**0.075**	0.52	1.85	2.13
2.00	**1.5**	**0.075**	0.33	2.34	1.39
2.00	**2.0**	**0.075**	0.22	2.49	0.95
2.70	**1.5**	**0.300**	0.44	1.48	2.86
2.70	**2.0**	**0.300**	0.31	1.61	2.26
2.70	**1.0**	**0.150**	0.46	1.37	2.90
2.70	**1.5**	**0.150**	0.31	1.67	2.09
2.70	**2.0**	**0.150**	0.21	1.79	1.51
2.70	**0.5**	**0.075**	0.46	0.74	2.89
2.70	**1.0**	**0.075**	0.32	1.73	2.21
2.70	**1.5**	**0.075**	0.18	1.90	1.25
2.70	**2.0**	**0.075**	0.12	2.03	0.86
Mean				**1.75**	**1.72**
Standard deviation				**0.48**	**0.58**

at $\beta_2 = 1.05$; $\beta_3 = 0.75$; $\beta_9 = 0.0$

Table C.4 Stiffener tripping failure mode for combined compression and bending

b_1	b_4	b_5	FEA (P_c/P_y)	$P_{c\ FEA} / P_{c\ code}$	
				DnV	API
0.70	**0.50**	**0.300**	0.80	0.96	0.81
0.70	**1.00**	**0.300**	0.76	0.93	0.81
0.70	**1.50**	**0.300**	0.73	0.91	0.80
0.70	**2.00**	**0.300**	0.71	0.90	0.79
0.70	**0.50**	**0.150**	0.78	0.99	0.81
0.70	**1.00**	**0.150**	0.71	0.95	0.77
0.70	**1.50**	**0.150**	0.67	0.92	0.72
0.70	**2.00**	**0.150**	0.63	0.89	0.69
0.70	**1.00**	**0.075**	0.68	1.10	0.74
0.70	**1.50**	**0.075**	0.57	0.97	0.62
0.70	**2.00**	**0.075**	0.49	0.90	0.55
1.28	**0.50**	**0.300**	0.78	0.94	0.87
1.28	**1.00**	**0.300**	0.73	0.91	0.98
1.28	**1.50**	**0.300**	0.65	1.22	0.99
1.28	**2.00**	**0.300**	0.56	1.34	0.93
1.28	**0.50**	**0.150**	0.73	0.94	0.93
1.28	**1.00**	**0.150**	0.65	0.89	0.95
1.28	**1.50**	**0.150**	0.54	1.43	0.87
1.28	**2.00**	**0.150**	0.41	1.53	0.65
1.28	**0.50**	**0.075**	0.62	0.94	0.89
1.28	**1.00**	**0.075**	0.50	0.85	0.78
1.28	**1.50**	**0.075**	0.37	1.79	0.58
1.28	**2.00**	**0.075**	0.25	1.92	0.45
1.46	**2.00**	**0.300**	0.785	0.95	0.99
1.75	**1.00**	**0.300**	0.70	1.21	1.47
1.75	**1.25**	**0.300**	0.62	1.24	1.53
2.00	**1.25**	**0.300**	0.57	1.28	1.82
2.00	**1.50**	**0.300**	0.49	1.34	1.70
2.00	**2.00**	**0.300**	0.34	1.38	1.37
2.00	**1.50**	**0.150**	0.35	1.51	1.26
2.00	**2.00**	**0.150**	0.21	1.38	0.80
2.00	**1.50**	**0.075**	0.21	1.90	0.83
2.00	**2.00**	**0.075**	0.12	1.73	0.49
2.25	**1.25**	**0.300**	0.53	1.33	2.04
2.70	**1.50**	**0.300**	0.33	1.31	1.88

‘contd on page 163

b_1	b_4	b_5	FEA (P_c/P_y)	$P_{c\,FEA} / P_{c\,code}$	
				DnV	API
2.70	**2.00**	**0.300**	0.21	1.27	1.39
2.70	**1.50**	**0.150**	0.23	1.43	1.33
2.70	**2.00**	**0.150**	0.13	1.31	0.88
2.70	**1.50**	**0.075**	0.14	1.86	0.91
2.70	**2.00**	**0.075**	0.07	1.45	0.68
Mean				**1.23**	**0.98**
Standard Deviation				**0.25**	**0.29**

at $\beta_2 = 1.05$; $\beta_3 = 0.75$; $\beta_9 = 0.20$

Table C.5 Plate buckling failure mode for combined compression and bending

b_1	b_4	b_5	FEA (P_c/P_y)	$P_{c\,FEA} / P_{c\,code}$	
				DnV	API
1.75	**0.50**	**0.300**	0.73	0.74	1.11
1.75	**0.75**	**0.300**	0.74	0.80	1.13
2.00	**0.50**	**0.300**	0.68	0.77	1.14
2.00	**0.75**	**0.300**	0.69	0.79	1.17
2.00	**1.00**	**0.300**	0.71	0.82	1.21
2.00	**0.50**	**0.075**	0.65	0.76	1.19
2.25	**0.50**	**0.300**	0.64	0.77	1.17
2.25	**0.75**	**0.300**	0.65	0.80	1.20
2.25	**1.00**	**0.300**	0.66	0.81	1.22
2.70	**0.50**	**0.300**	0.58	0.76	1.19
2.70	**1.00**	**0.300**	0.59	0.78	1.21
2.00	**0.50**	**0.150**	0.64	0.75	1.15
2.70	**0.50**	**0.150**	0.51	0.61	1.16
2.70	**0.50**	**0.075**	0.48	0.56	1.14
Mean				**0.75**	**1.17**
Standard deviation				**0.05**	**0.03**

at $\beta_2 = 1.05$; $\beta_3 = 0.75$; $\beta_9 = 0.20$

Table C.6 Dual failure mode for combined compression and bending

b_1	b_4	b_5	**FEA** (P_c/P_y)	$P_{c\ FEA} / P_{c\ code}$	
				DnV	**API**
2.00	**1.00**	**0.150**	0.61	1.60	2.03
2.00	**1.00**	**0.075**	0.56	2.61	2.18
2.70	**1.00**	**0.150**	0.45	1.59	2.38
2.70	**1.00**	**0.075**	0.35	2.38	2.23
Mean				**2.05**	**2.21**
Standard deviation				**0.45**	**0.10**

at $\beta_2 = 1.05$; $\beta_3 = 0.75$; $\beta_9 = 0.20$